RESULTS AND DISCUSSION

CHAPTER (III)

A—SYNTHESIS AND POLYMERIZATION OF THE MONOMERS

1- Synthesis of p-hydroxy-tri-n-butyltin benzoate :

P-hydroxy-tri-n-butyltin benzoate was prepared through the esterification of p-hydroxybenzonic acid with bis (tri-n-butyltin) oxide according to the method described in page (42).

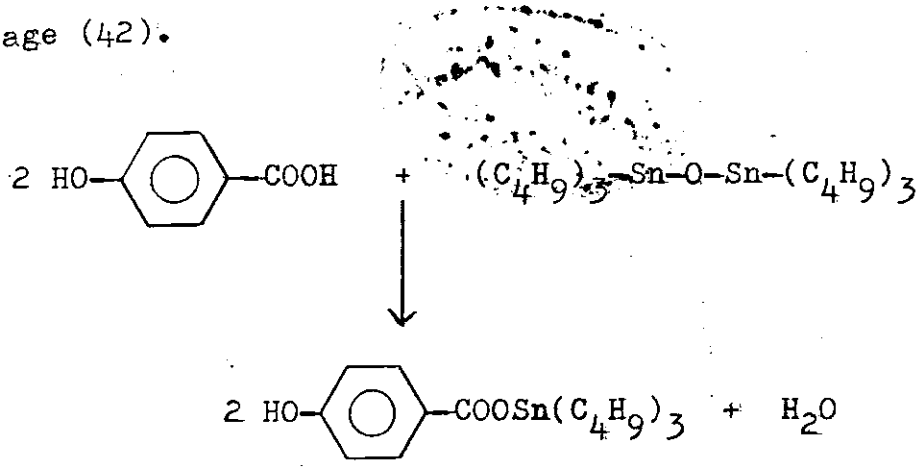

The product was recrystallized from petroleum ether as a colourless needles, m.p. 68°C and the yield was 97.3 %. The tin content of p-hydroxy-tri-n-butyltin benzoate was found to be 27.74 % against a calculated value of 27.87 %. The structure of p-hydroxy-tri-n-butyltin benzoate was established from its IR-spectrum (Fig. 1) which shows the following signals : A broad band at 3200 cm^{-1} due to the O-H stretching vibrations of the -OH group; bands at 2980 — 2960 cm^{-1} due to the C-H

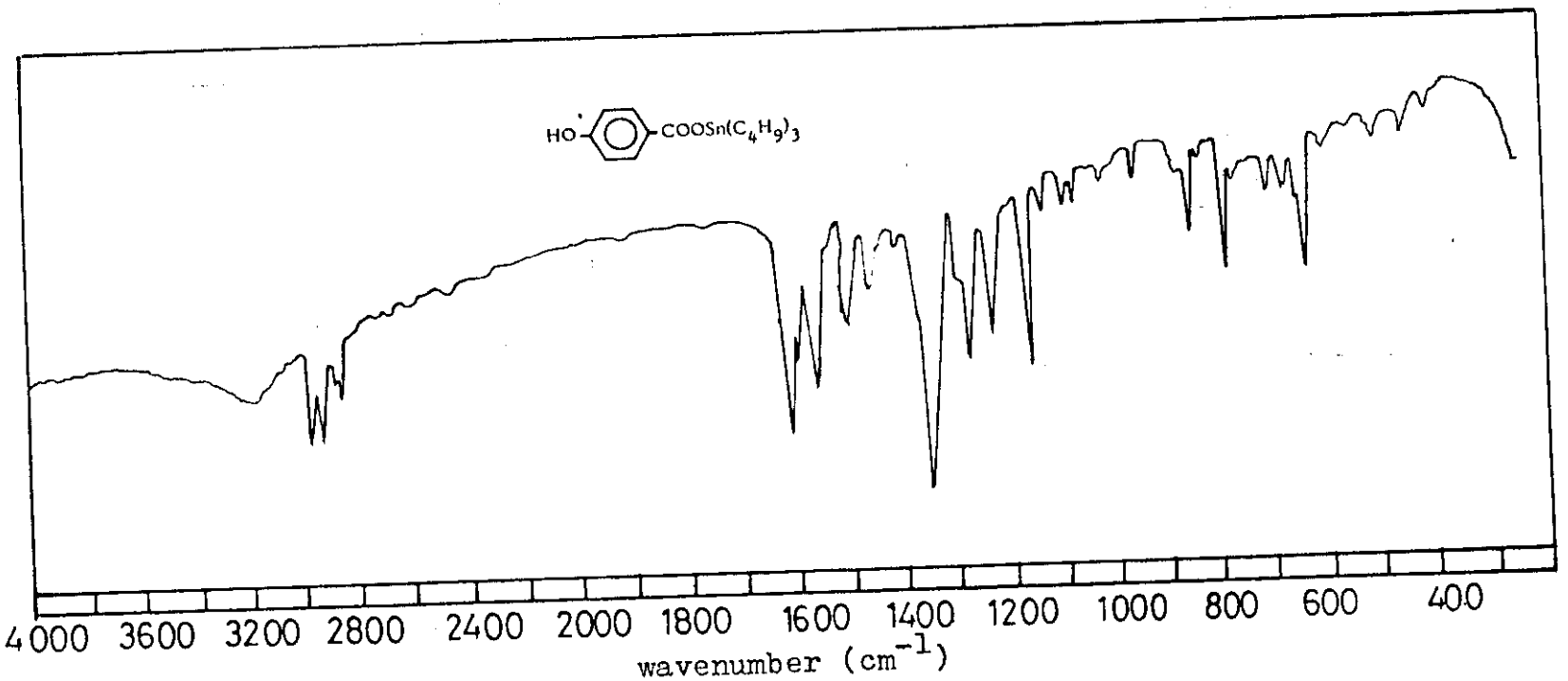

Fig. (1): IR spectrum of p-hydroxy-tri-n-butyltin benzoate .

stretching vibrations of the $-CH_2-$ and $-CH_3$ groups; a strong band at 1565 cm^{-1} due to the $>C=C<$ stretching vibrations of para-substituted benzene; a strong band at 1620 cm^{-1} characteristic for the asymmetric stretching vibrations of the carbonyl group of $-\overset{O}{\overset{\|}{C}}-O-$ conjugated with aromatic ring; and a band at 850 cm^{-1} characteristic for the C-H out-of-plane deformation vibrations of the two adjacent-hydrogen atoms of the para-substituted aromatic compounds .

The ^1H NMR spectrum of p-hydroxy-tri-n-butyltin benzoate Fig.(2) shows signals centered at δ1.0 corresponding to nine protons of $3(CH_3-)$, multiplet at δ1.1 – 2.1 corresponding to eighteen protons of $3(-CH_2-CH_2-CH_2-)$ and two doublets at δ6.85 and δ7.9 corrosponding to four protons of $p-C_6H_4-$ group .

2 – Synthesis of p-acryloyloxybenzoic acid :

p -Acryloyloxybenzoic acid was prepared by the reaction of p-hydroxybenzonic acid with acryloyl chloride in alkaline medium[65] according to the method described in page (42)

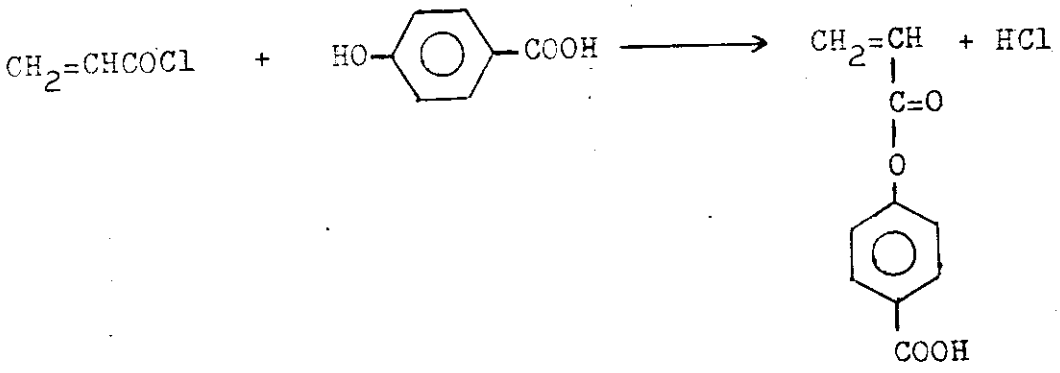

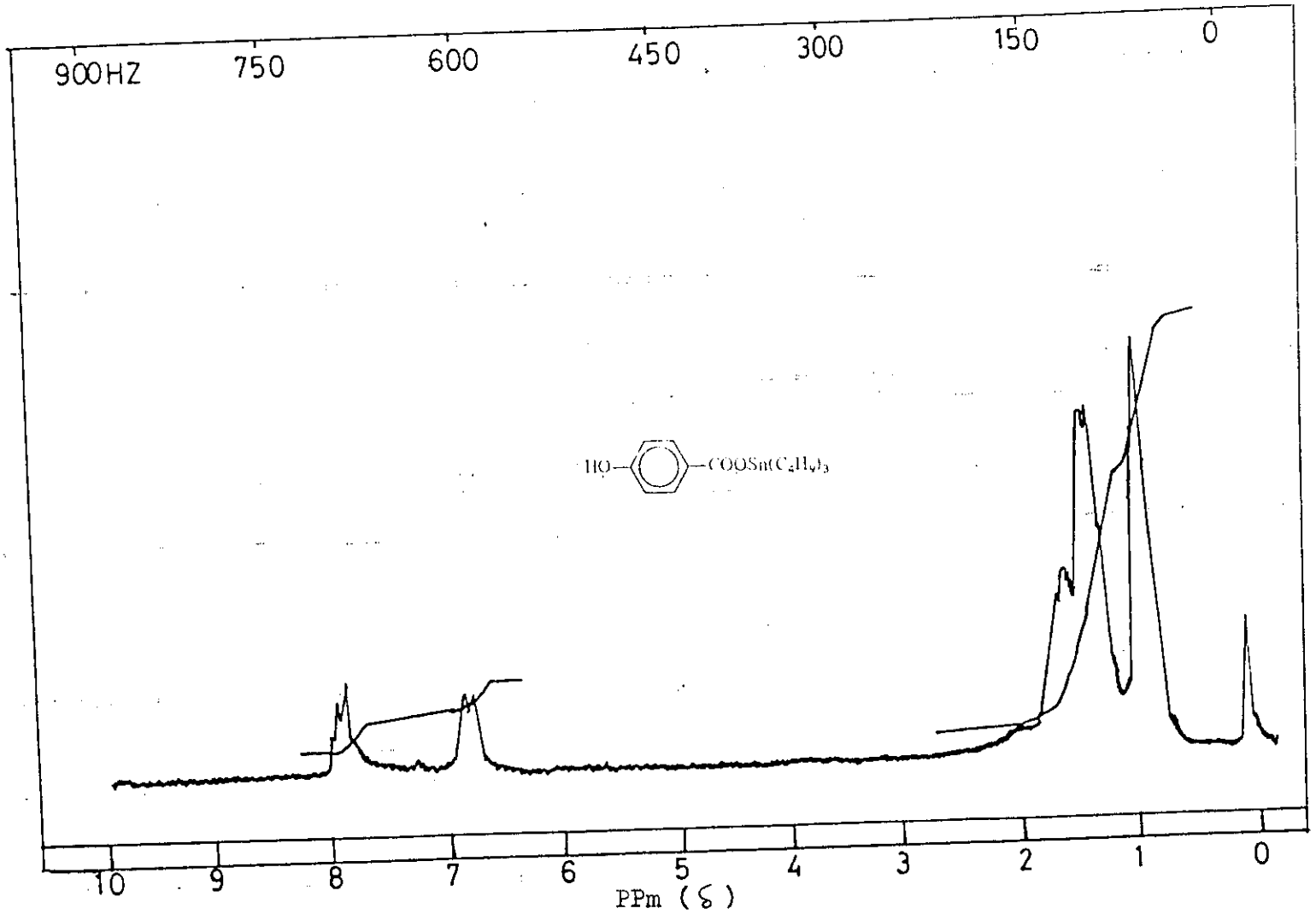

Fig. (2): ^{1}H NMR spectrum of p-hydroxy-tri-n-butyltin benzoate .

The product was recrystallized from water as a white crystals, m.p. 170°C and the yield was 79.52 % .

The structure of p-acryloyloxybenzoic acid was established from the following :

The elemental analysis gave 62.50 % C and 4.17 % H against a calculated value of 62.34 % C and 4.02 % H for $C_{10}H_8O_4$.

The IR spectrum of p-acryloyloxybenzoic acid Fig. (3) show broad bands between 3500-2500 cm^{-1} due to the carboxylic -OH and C-H stretching vibrations; a strong band at 1740 cm^{-1} characteristic for >C=O stretching vibrations of the acrylic ester group; a strong band at 1680 cm^{-1} due to >C=O stretching vibrations of aryl carboxylic acids and a band at 1600 cm^{-1} due to >C=C< stretching vibrations of aromatic compounds.

The ^1H NMR spectrum of p-acryloyloxybenzoic acid Fig. (4) shows a triplet at δ7.5 and a doublet at δ6.5 corresponding to three protons of CH_2=CH- and two multiplets at δ7.9 and δ6.93 corresponding to four protons of C_6H_4- group.

3-Synthesis of p-acryloyloxy-tri-n-butyltin benzoate :

a-N,N-Dicyclohexylcarbodiimide (DCCI) method :

p-Acryloyloxy-tri-n-butyltin benzoate was prepared by the reaction of acrylic acid with p-hydroxy-tri-n-butyltin benzoate in the presence of N,N-dicyclohexylcarbodiimide (DCCI) as a condensing agent according to the method described in page (43) :

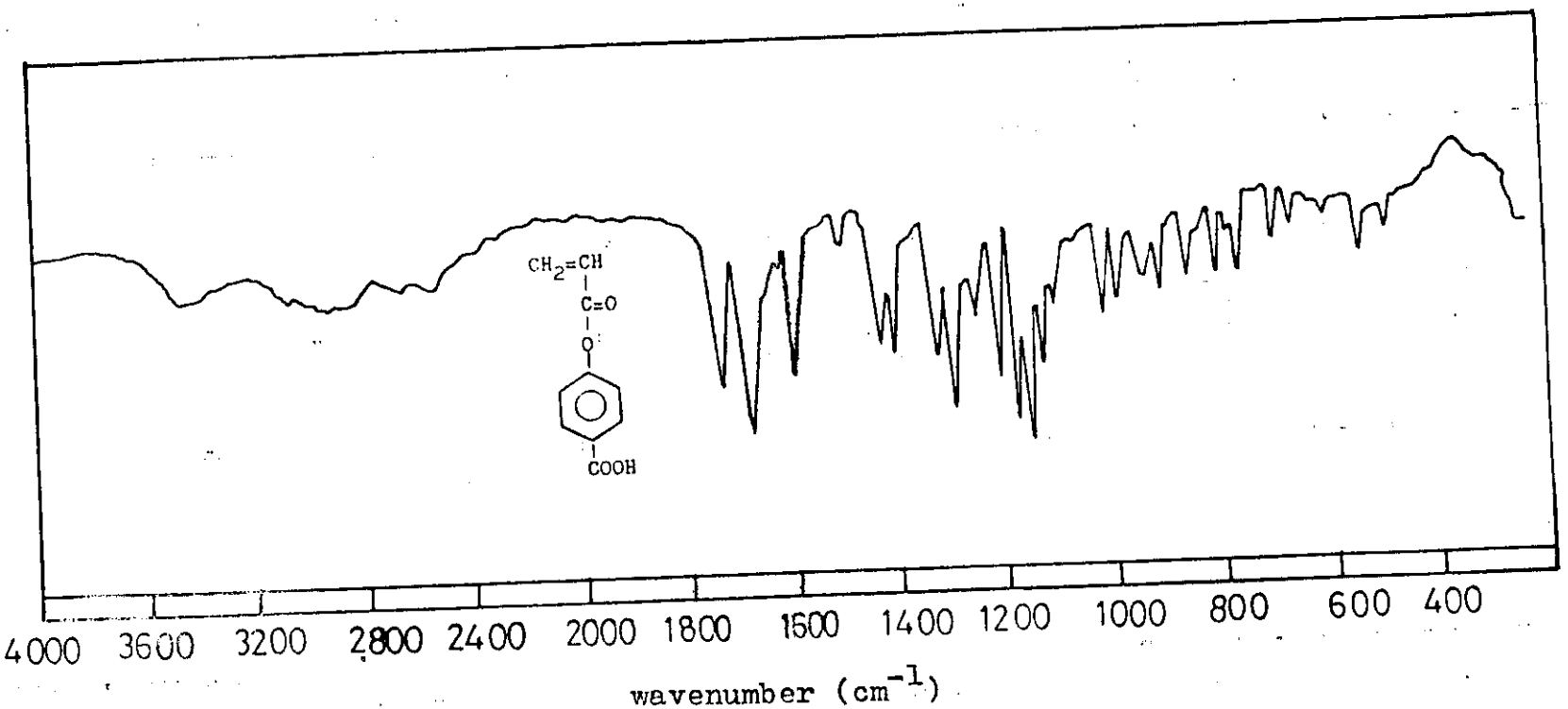

Fig. (3): IR spectrum of p-acryloyloxybenzoic acid.

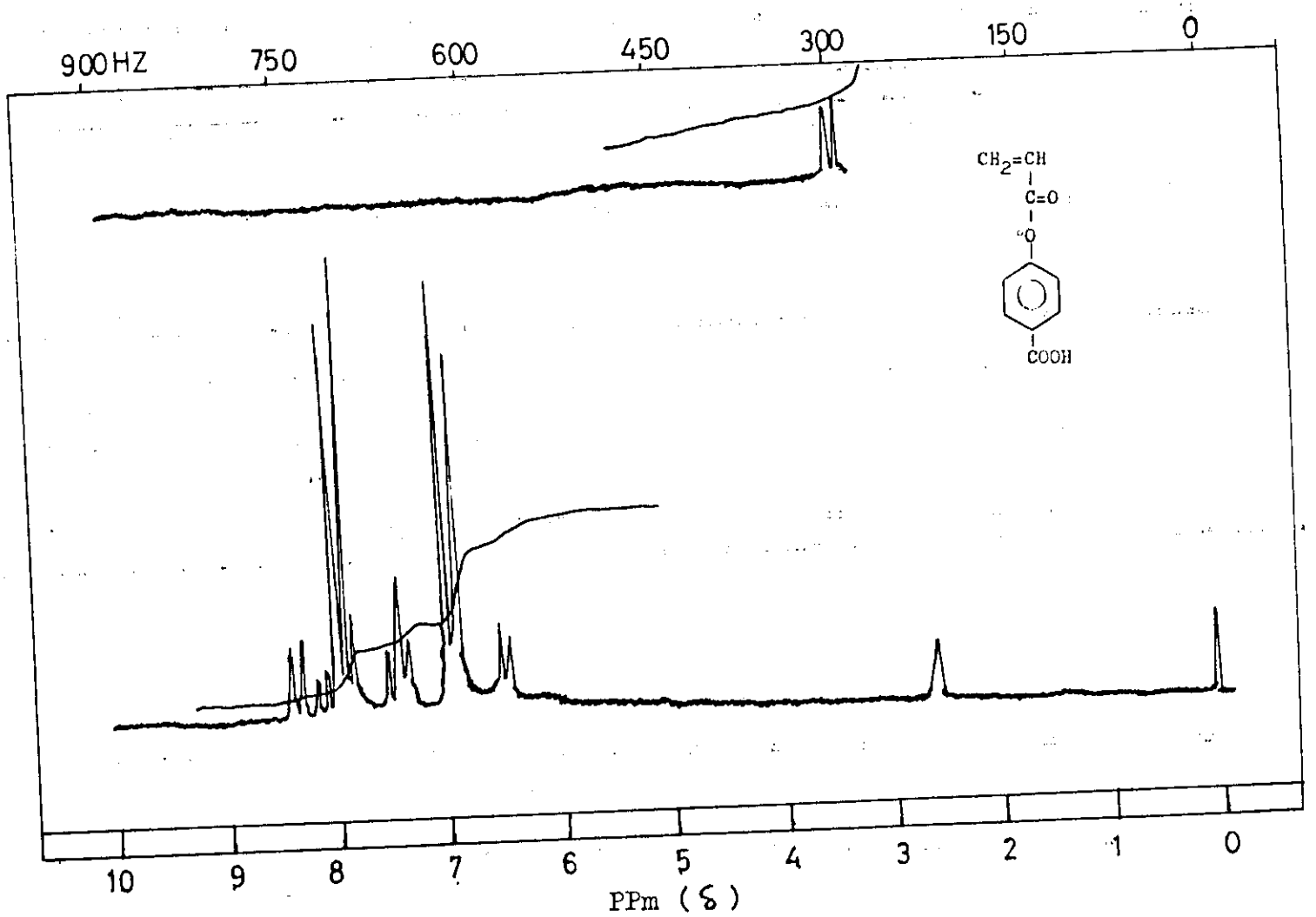

Fig. (4): ^{1}H NMR spectrum of p-acryloyloxybenzoic acid .

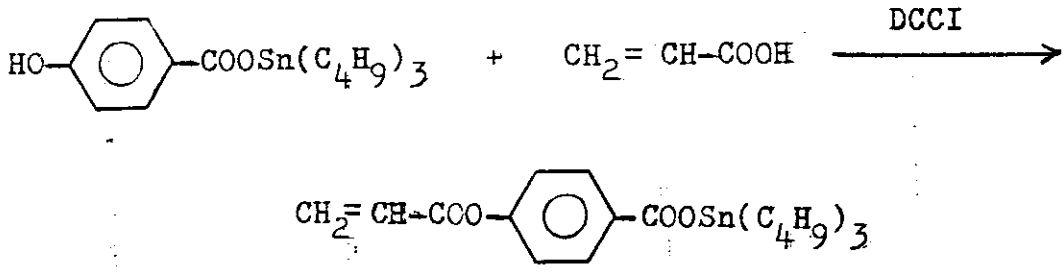

The product was recrystallized from petroleum ether, m.p. 30-32 °C and its tin contant was found to be 24.63 % aginst a calculated value 24.74 % for $C_{22}H_{34}O_4Sn$.

The structure of p-acryloyloxy-tri-n-butyltin benzoate was established from the following :

The ir spectrum of p-acryloyloxy-tri-n-butyltin benzoate Fig. (5) shows the following bands: strong bands between 2950-2850 cm^{-1} due to the C-H stretching vibrations of $-CH_2-$ and $-CH_3$ groups, a strong band at 1740 cm^{-1} corresponding to the $\geq C=O$ stretching vibrations of the carboxylate ester group and a strong band in the region 1570-1640 cm^{-1} due to the carboxylate carbonyl groups of $-COOSn\leqslant$.

The ^1H NMR spectrum of p-acryloyloxy-tri-n-butyltin benzoate Fig. (6) shows signals at 0.80 corresponding to nine protons of $3(CH_3)$, a multiplet at δ 1.15-2.10 due to eighteen protons of $3(-CH_2-CH_2-CH_2-)$ groups and signals between δ 5.5 to δ 8.1 are probably to the seven protons of aromatic and vinyl protons .

b-Esterification method :

p-Acryloyloxy-tri-n-butyltin benzoate was prepared by esterification of p-acryloyloxybenzoic acid with bis (tri-n-butyltin) oxide in the presence of benzene according to the

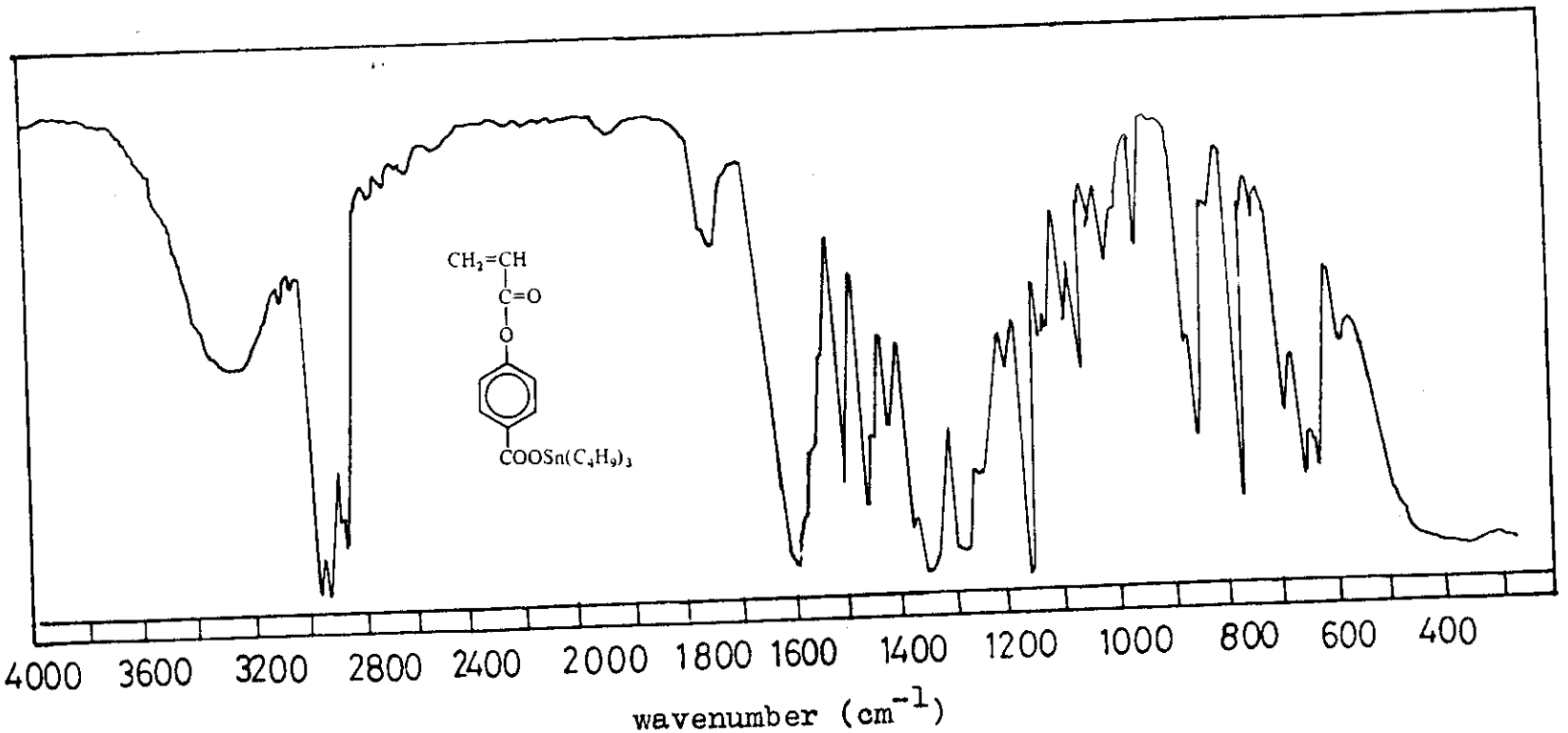

Fig. (5): IR spectrum of p-acryloyloxy-tri-n-butyltin benzoate .

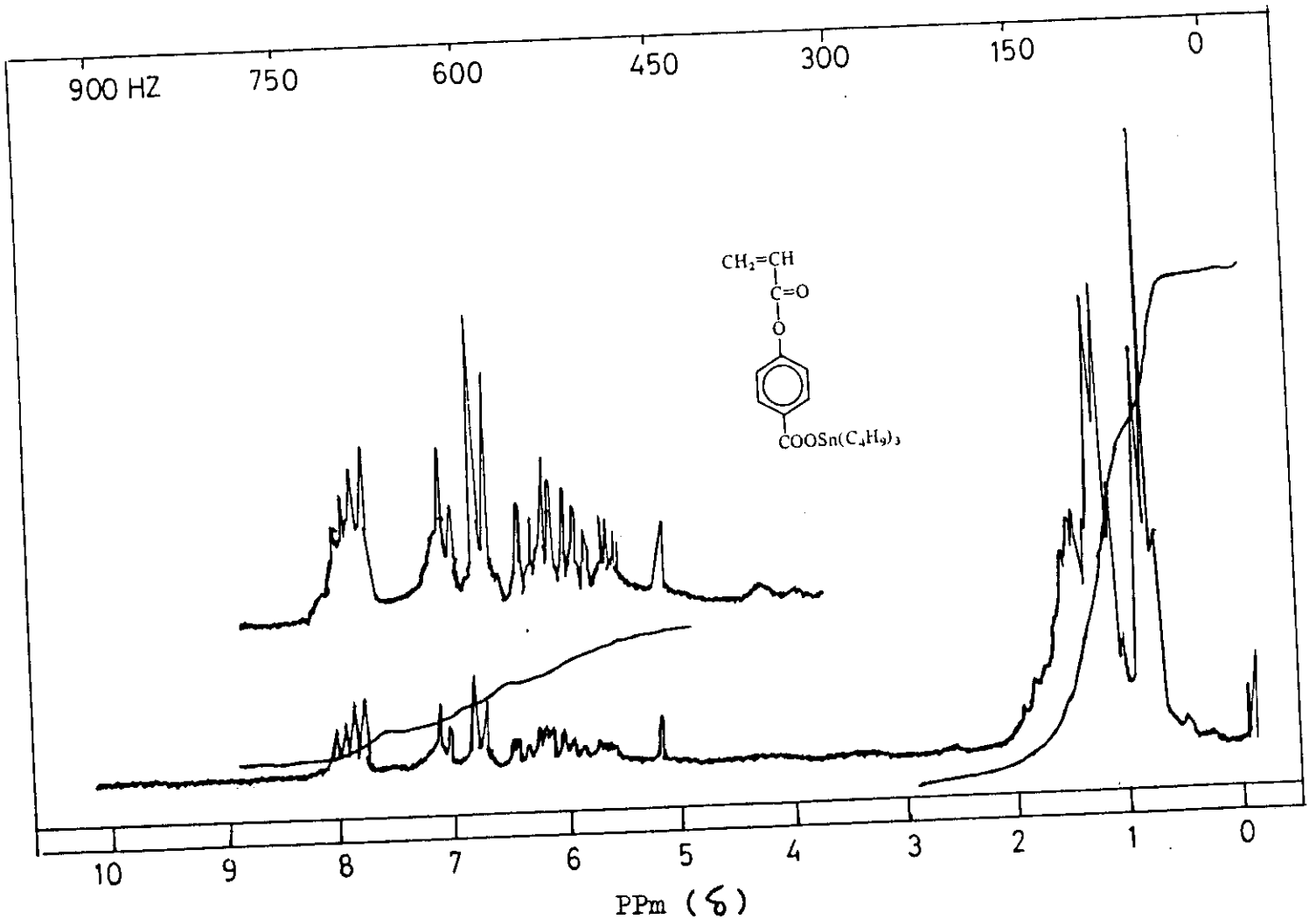

Fig. (6): ^{1}H NMR spectrum of p-acryloyloxy-tri-n-butyltin benzoate .

method described in page (43) .

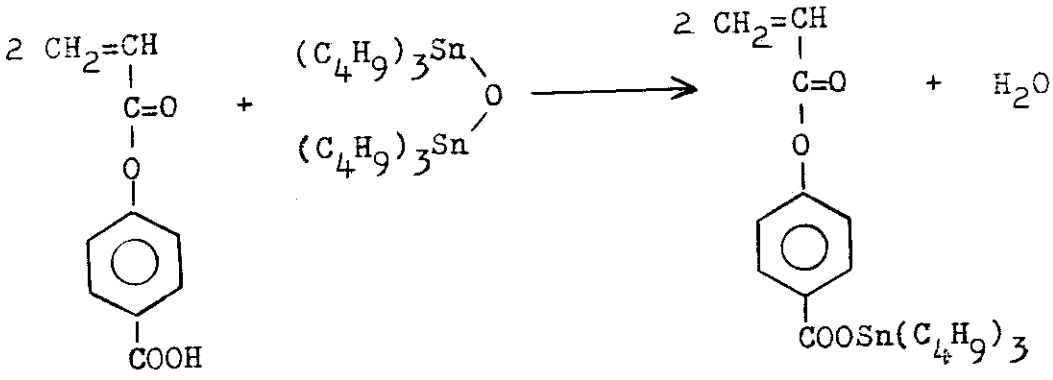

The product was recrystallized from petrolum ether, m.p. and mixed m.p. with the product from the DCCI method was found to be 30-32°C and its tin content was found to be 24.32 % against a calculated value of 24.74 % for $C_{22}H_{34}O_4Sn$.

The IR and ^1H NMR spectra of the product was found to be identical with that prepared by the DCCI method .

4 - Synthesis of N-hydroxytetrabromophthalimide :

N-Hydroxytetrabromophthalimide was prepared by the reaction of tetrabromophthalic anhydride with hydroxylamine hydrochloride in the presence of pyridine[66] according to the method described in page (44)

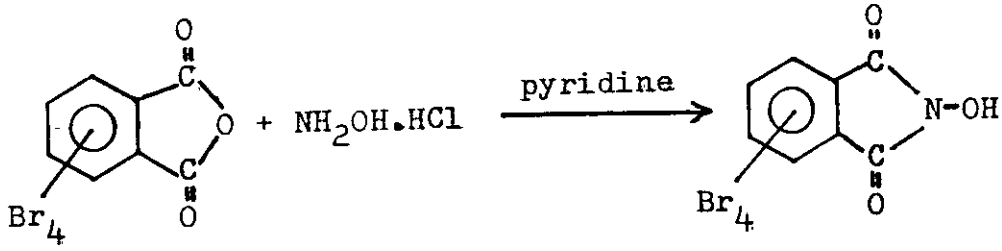

The product was recrystallized from ethanol as yellowish crystals, m.p.>300°C and the yield was 75 % .

The structure of N-hydroxytetrabromophthalimide was investigated from bromine analysis which was found to be 67.3 % aganist a calculated value of 66.81 % .Also, the structure of N-hydroxytetrabromophthalimide was established from its IR spectrum (Fig. 7) which shows the following signals : a broad band at 3550-2400 cm^{-1} due to the -OH and C-Br stretching vibrations and two strong bands at 1780 cm^{-1} and 1730 cm^{-1} characteristic for coupling bands of cyclic imides , a band at 1630 cm^{-1} due to stretching vibrations of aromatic $\rangle C=C\langle$ and a strong band at 660 cm^{-1} for bending vibrations of C-Br bonds .

5 - Synthesis of N-methacryloyloxytetrabromophthalimide :

a - Acid chloride method[67] :

N-Methacryloyloxytetrabromophthalimide monomer was prepared by the reaction of methacryloyl chloride with N-hydroxytetrabromophthalimide in the presence of triethylamine according to method described in page (45)

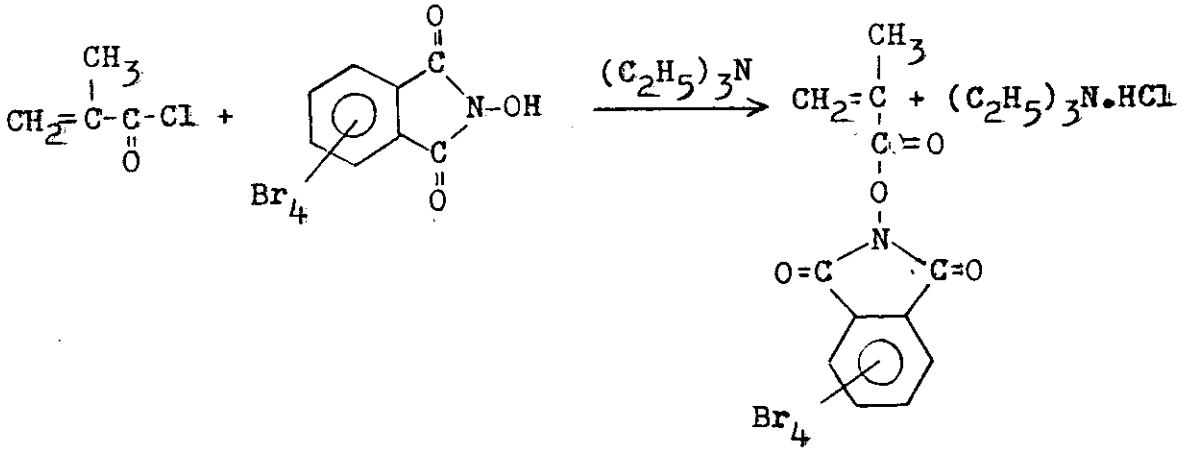

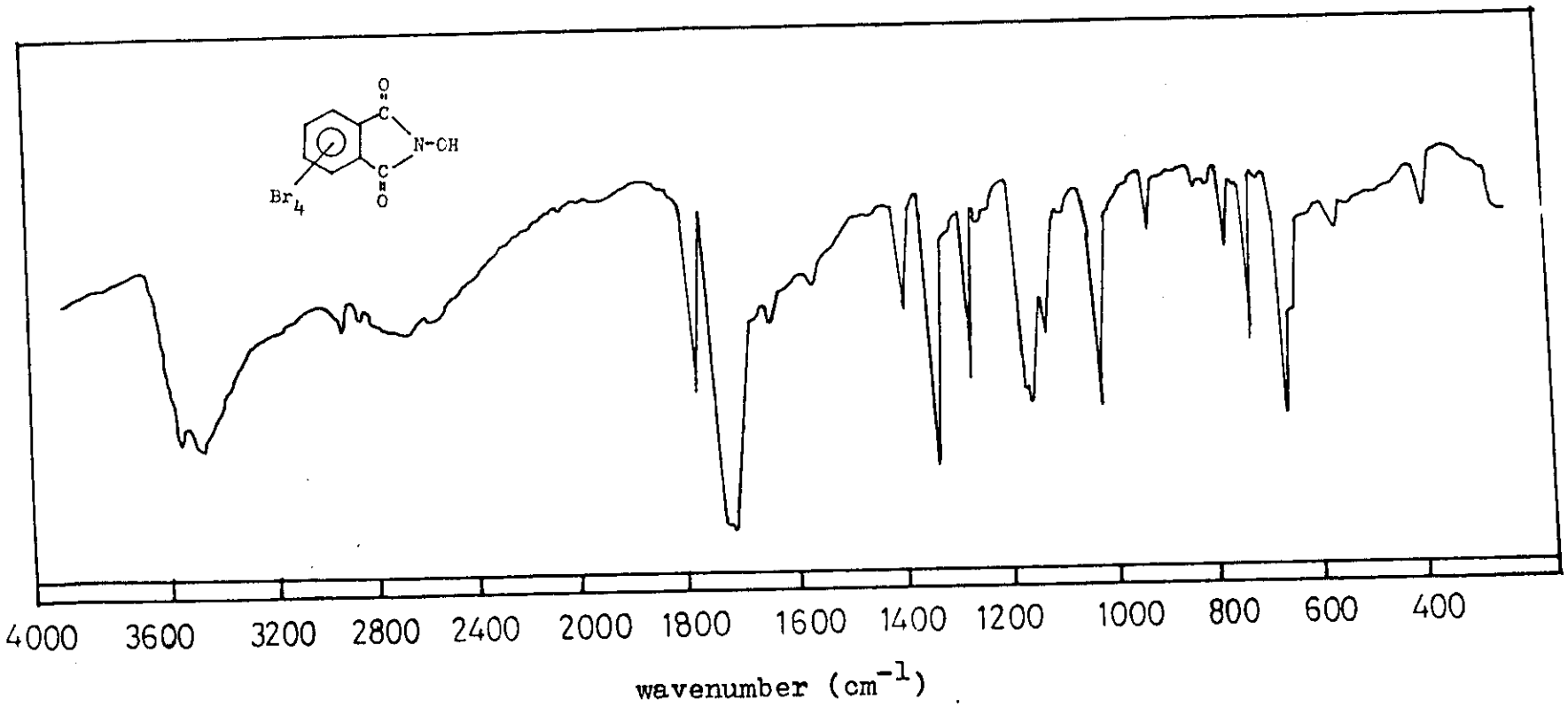

Fig. (7) IR spectrum of N-hydroxytetrabromophthalimide .

The resulting N-methacryloyloxytetrabromophthalimide was obtained as yellowish-white crystals and was recrystalized from benzene/methanol (30 : 70) . The yield of recrystalized product was 87 %, m.p. 184-186 °C .

The structure of N-methacryloyloxytetrabromophthalimide monomer was investigated from bromine analysis which was found to be 58.1 % against a calculated value of 58.5 % for $C_{12}H_5NO_4Br_4$.

The IR spectrum of N-methacryloyloxytetrabromophthalimide Fig.(8) shows the following signals : signals at 2950 cm^{-1} due to the C-H stretching vibrations, at 2870 cm^{-1} due to the C-Br stretching vibrations, a strong band at 1780 cm^{-1} characteristic for the C=O streatching vibrations of phthalimide group, a strong band at 1720 cm^{-1} due to the C=O streatching vibrations of the carboxylate group .The spectrum also shows a strong band at 1640 cm^{-1} which is due to the C=C of vinylidene group and a strong band at 660 cm^{-1} characterstic for the C-Br bending vibrations of bromine compounds .

The structure of N-methacryloyloxytetrabromophthalimide was established from its ^1H NMR spectrum which shows signals at δ 6.3 and δ 5.8 due to the two protons of $CH_2=C$ group and a signal at δ 2.0 corrosponding to three protons of $-CH_3$ group Fig. (9) .

b - N,N-Dicyclohexylcarbodiimide method[68] :

Also, N-methacryloyloxytetrabromophthalimide was

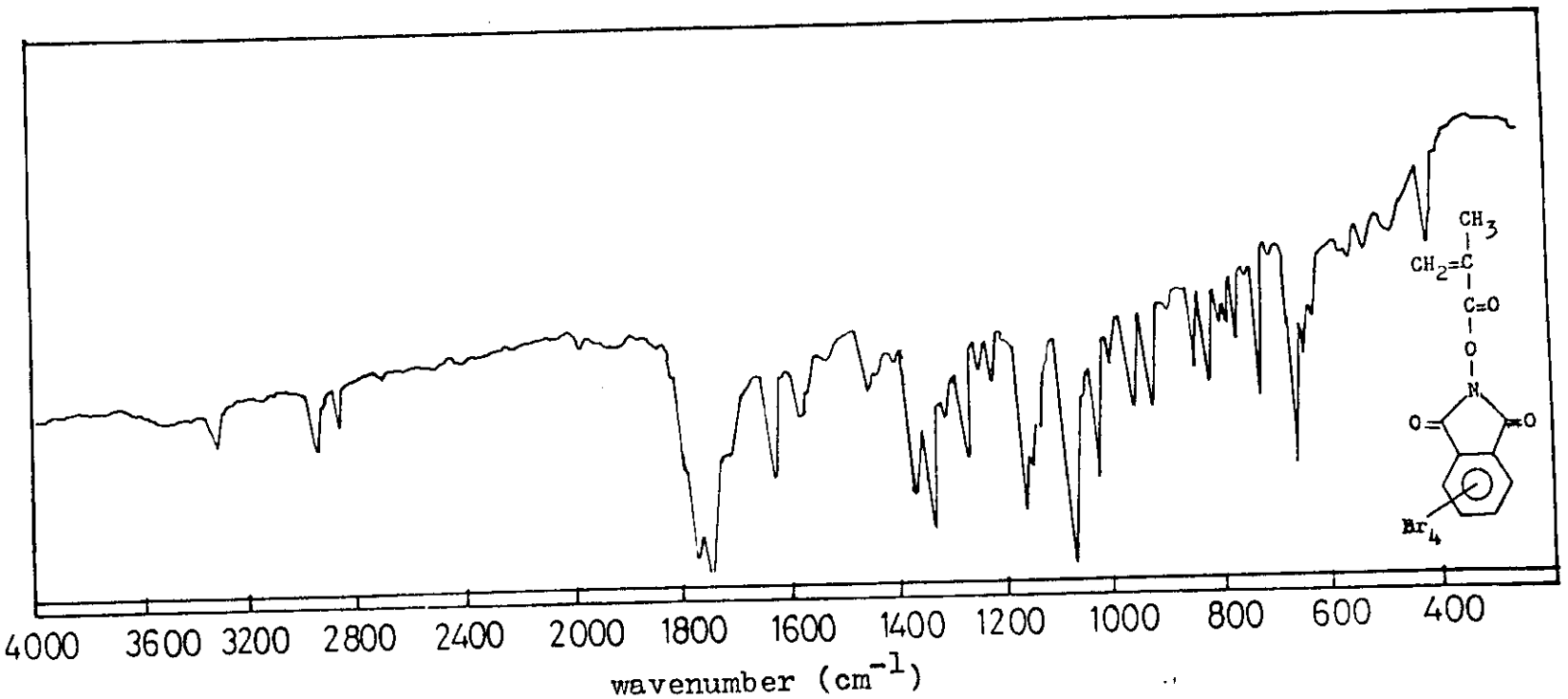

Fig. (8): IR spectrum of N-methacryloyloxytetrabromophthalimide .

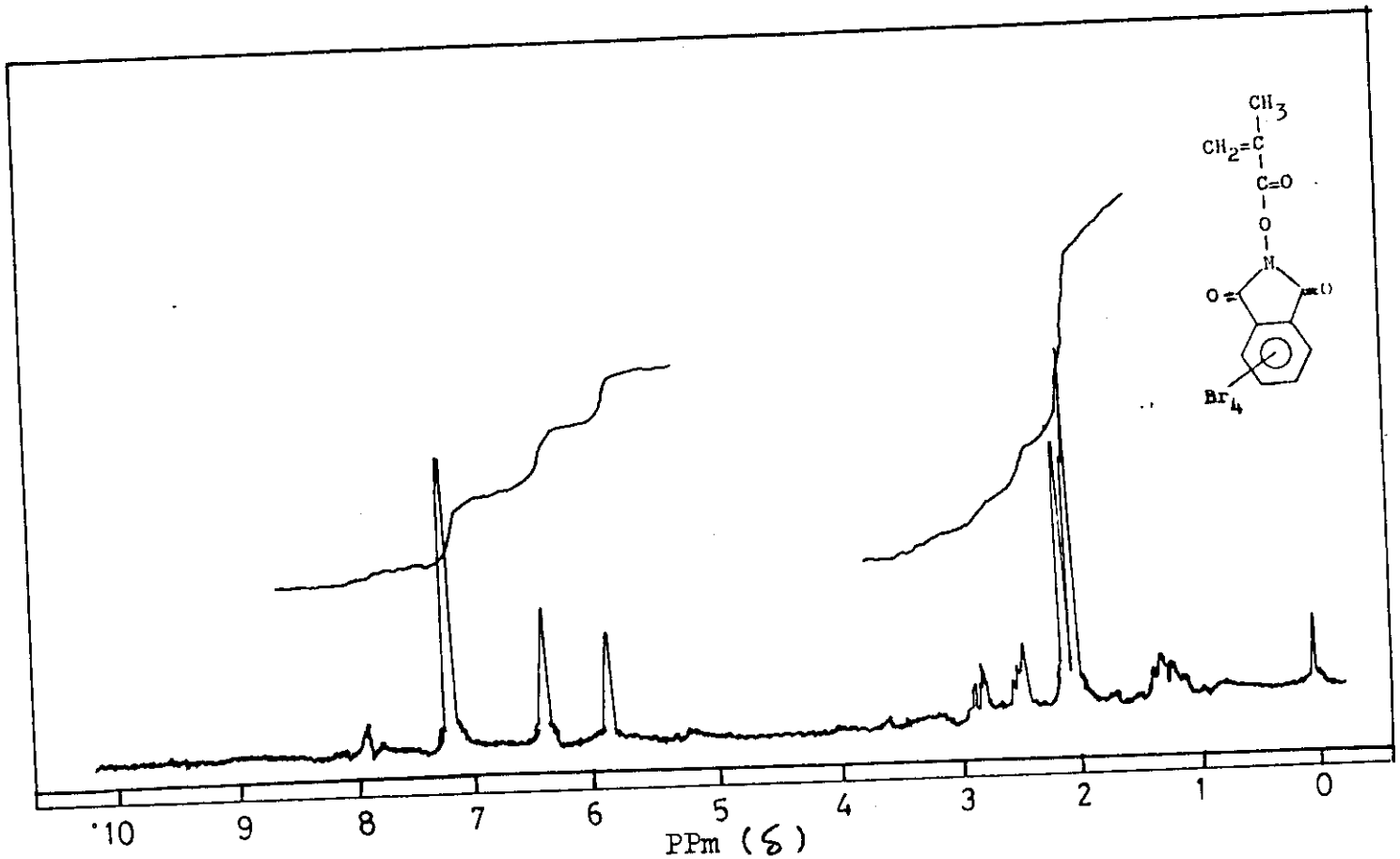

Fig. (9): ^{1}H NMR spectrum of N-methacryloyloxytetrabromophthalimide .

prepared by the reaction of methacrylic acid with N-hydroxy-tetrabromophthalimide in presence of N,N-dicyclohexylcarbodiimide (DCCI) according to method described in page (46)

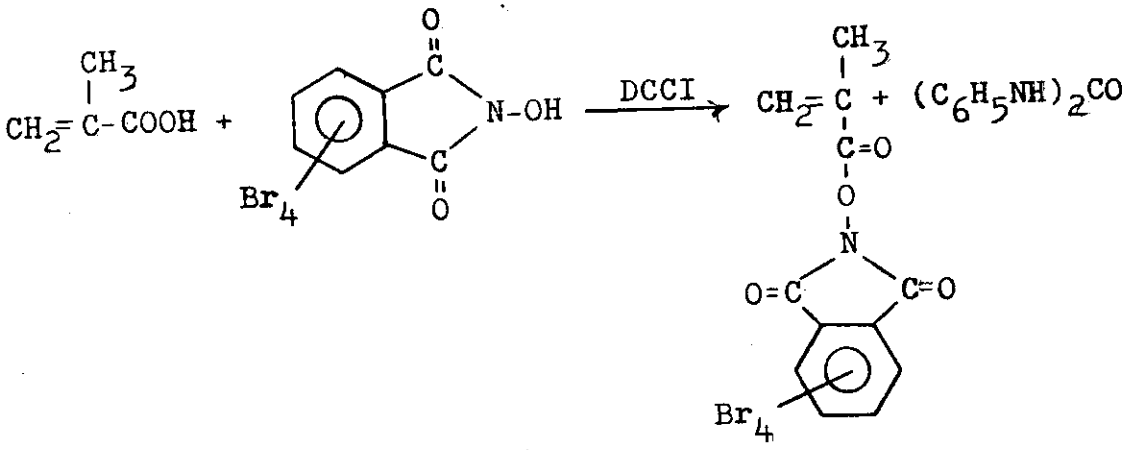

The resulting N-methacryloyloxytetrabromophthalimide was obtained as yellowish-white crystals, recrystallized from benzene/methanol (30 : 70) . The yield of recrystalized product was 72 %, m.p. 185 — 187°C . The yield of the porduct was lower than that prepared by the acid chloride method (87 %)

The structure of the product was established from m.p. and mixed m.p. with an authentic samples prepared by the acid chloride method and was found to be 185-187°C .

6 - Polymerization of p-acryloyloxy-tri-n-butyltin benzoate:

P-Acryloyloxy-tri-n-butyltin benzoate was polymerized in DMF solution at 70°C using AIBN as free radical initiator according to the method described in page (46) to give poly-N-acryloyloxy-tri-n-butyltin benzoate :

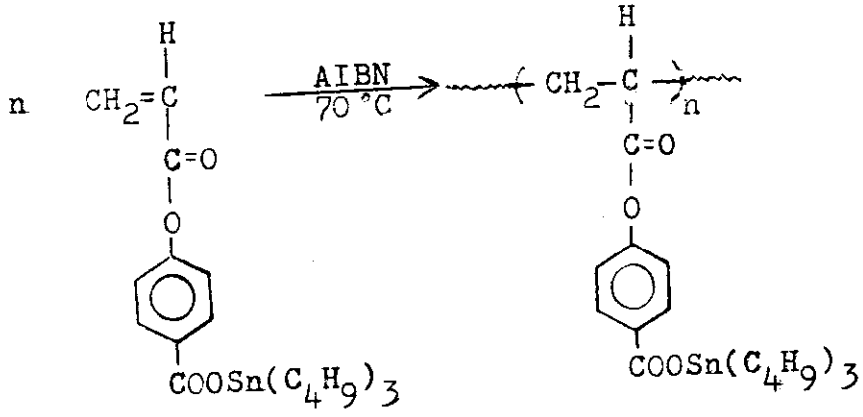

The poly-p-acryloyloxy-tri-n-butyltin benzoate was obtained as viscous material by reprecipitation from methanol. The yield was 88 %.

The structure of the polymer was investigated from tin analysis which was found to be 24.52 % against the calculated value of 24.74 % for $C_{22}H_{34}O_4Sn$.

The IR spectrum of poly-p-acryloyloxy-tri-n-butyltin benzoate (Fig. 10) was found to be similar with that of the monomer (Fig. 5) except that the intensity of the band at 1740 cm^{-1} due to the stretching frequency of the C=O of the acrylate ester is less than that of the monomer.

The ^1H NMR spectrum of poly-p-acryloyloxy-tri-n-butyltin benzoate (Fig. 11) show signals at δ 7.9 and δ 6.7 due to the four aromatic protons and signals between δ 2.1-δ 0.8 are due to the $-CH_2-$ and $-CH_3$ protons.

7- Polymerization of N-methacryloyloxytetrabromophthalimide:

N-Methacryloyloxytetrabromophthalimide was polymerized in dioxan at 70°C, using azo-bis-isobutyronitrile (AIBN) as a free radical initiator, to give poly-N-methacryloyloxy-tetrabromophthalimide :

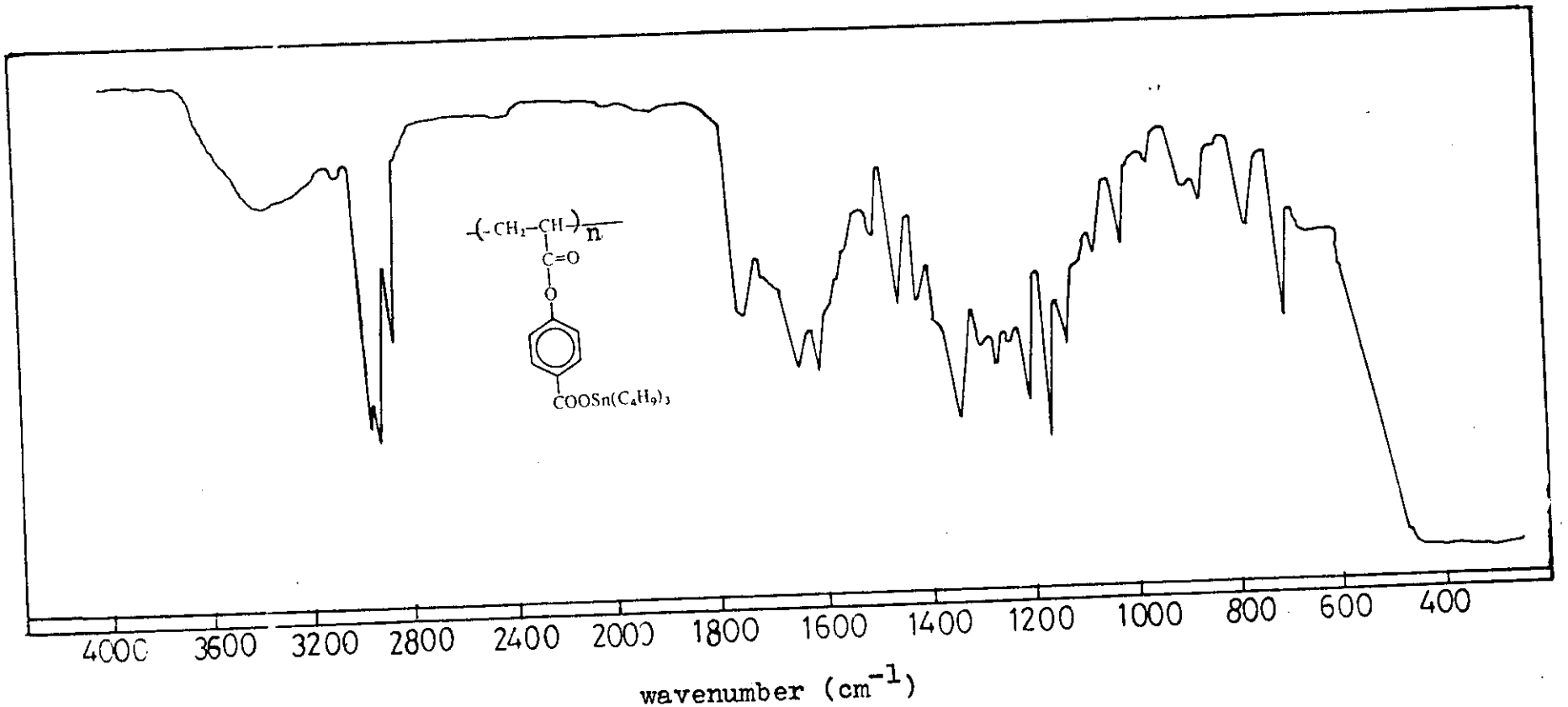

Fig. (10): IR spectrum of poly-(p-acryloyloxy-tri-n-butyltin benzoate).

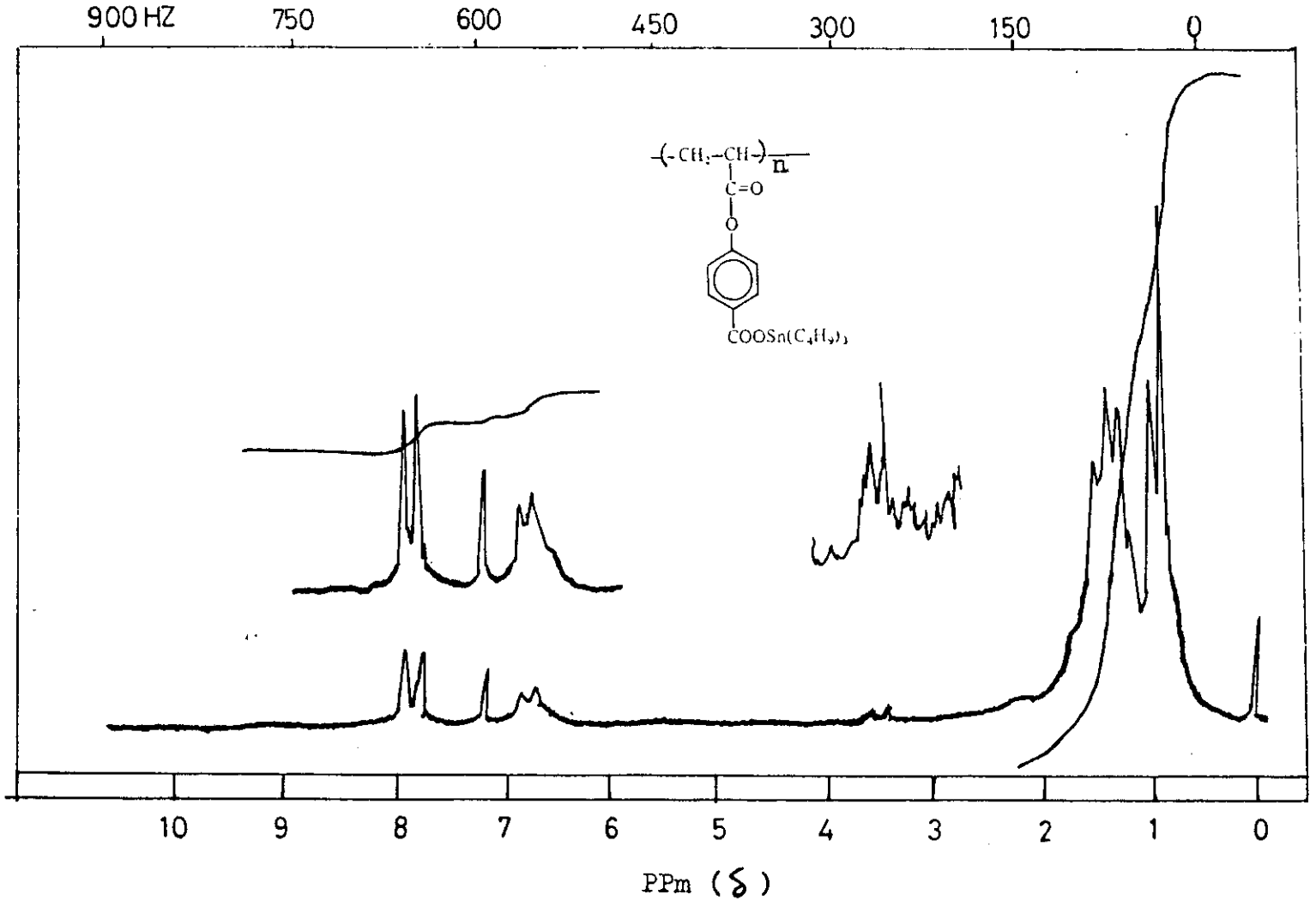

Fig. (11): ^{1}H NMR spectrum of poly-(p-acryloyloxy-tri-n-butyltin benzoate).

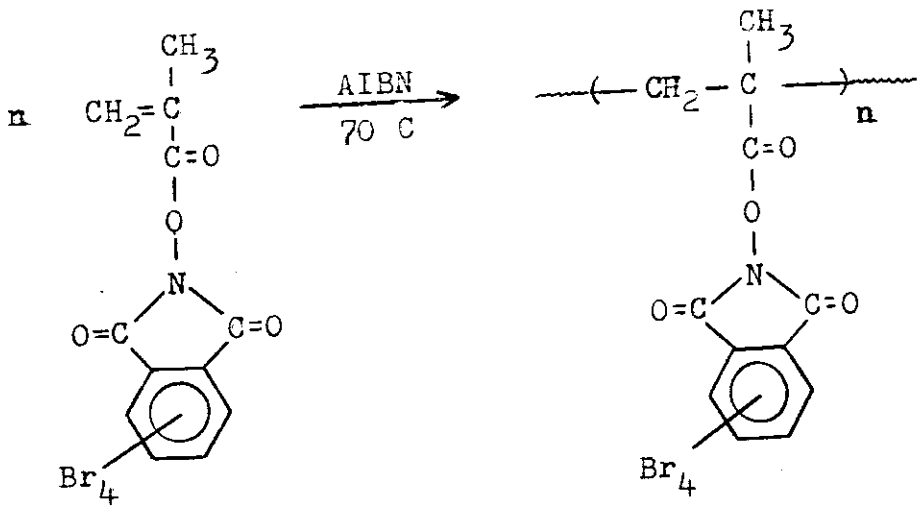

The poly-N-methacryloyloxytetrabromophthalimide was obtained as a solid white substance by repricipitation in methanol and were collected by filtration, washed, dried and weighed . The yield was 94 % . The polymer was solid, soluble in DMF, DMSO and dioxane, but insoluble in most organic solvent .

The structure of the polymer was investigated from bromine analysis which was found to be 58.8 % against a calculated value of 58.5 % for $C_{12}H_5NO_4Br_4$.

The IR spectrum of poly-N-methacryloyloxytetrabromophthalimide (Fig. 12) shows a broad band centered at 3500 cm^{-1} characteristic for the C-H and C-Br stretching vibrations, a strong band at 1780 cm^{-1} characteristic for C=O stretching vibrations of phthalimide group and a strong band at 1720 cm^{-1} due to the C=O vibrations of the carboxylate group .

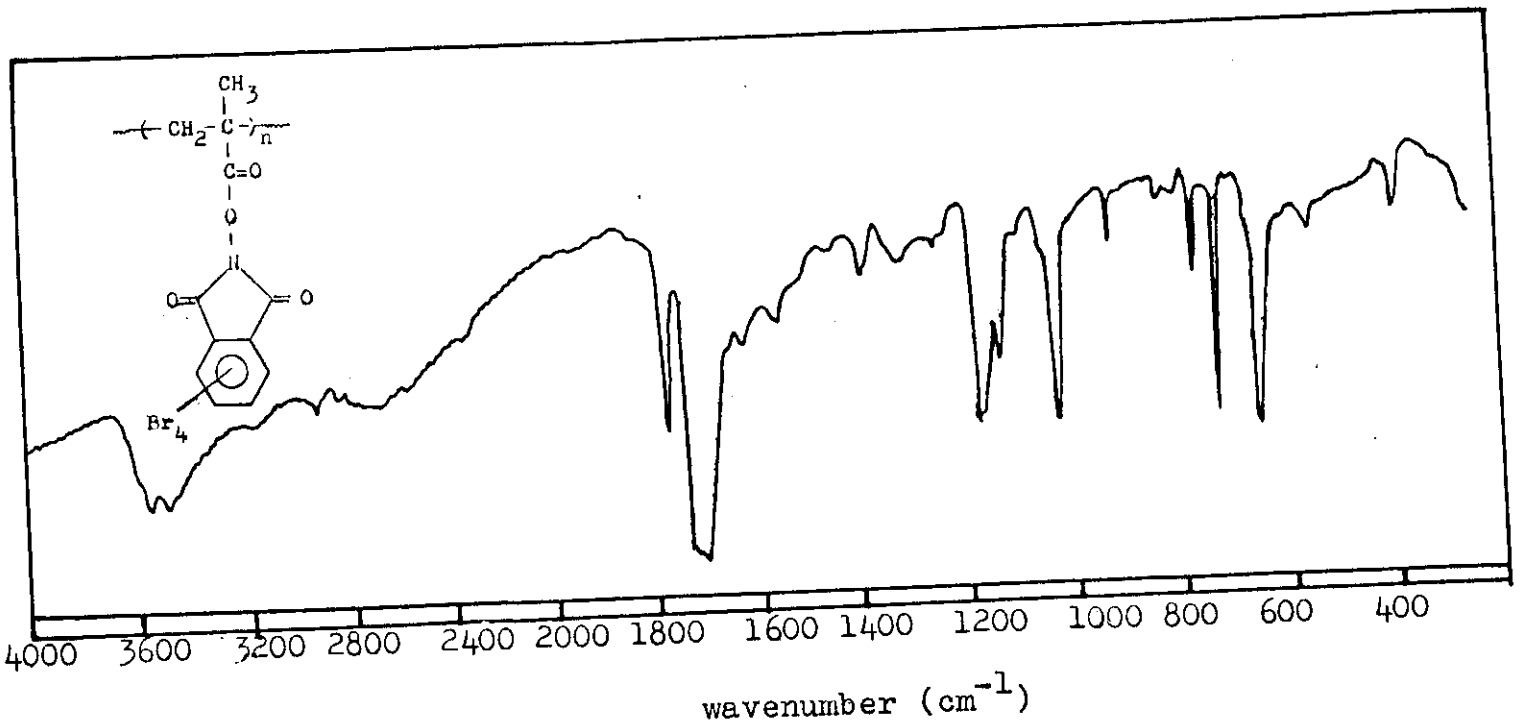

Fig. (12): IR spectrum of poly-(N-methacryloyloxytetrabromophthalimide).

B-BINARY COPOLYMERIZATION REACTIONS

1- Copolymerization Reactions of p-Acryloyloxy-tri-n-butyltin Benzoate (ABTB) with Methyl Acrylate (MA), Ethyl Acrylate (EA), n-Butyl Acrylate (BA), Methyl Methacrylate (MMA), Styrene (ST) and Acrylonitrile (AN).

The copolymerization reactions of ABTB with each of MA, EA, BA, MMA, ST and AN were carried out by the solution copolymerization technique in DMF (1.5 mole/L) at 70 °C in the presence of 1 mole % AIBN, according to the method described in page (46) . The reaction can be represented as :

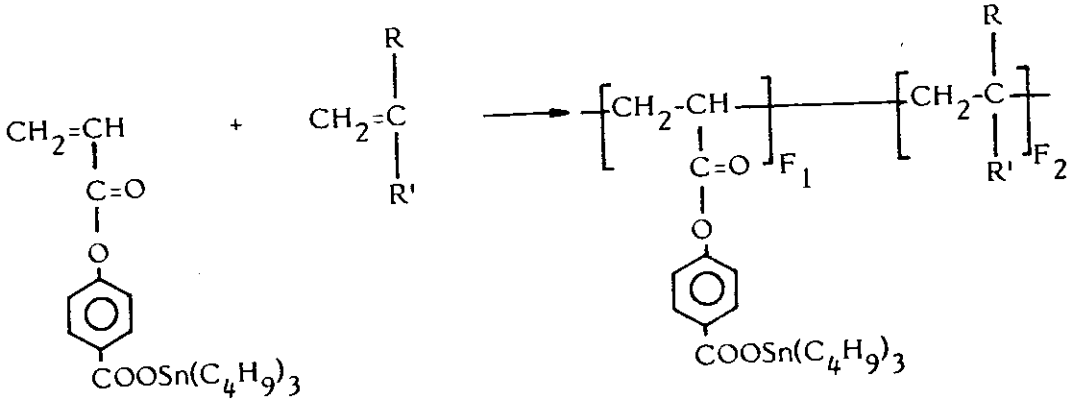

where :

$M_1 - M_2$	R	R'
ABTB – MA	-H	$-COOCH_3$
ABTB – EA	-H	$-COOC_2H_5$
ABTB – BA	-H	$-COOC_4H_9$
ABTB – MMA	$-CH_3$	$-COOCH_3$
ABTB – ST	-H	$-C_6H_5$
ABTB – AN	-H	-C≡N

The prepared copolymers were colourless solids soluble in most organic solvents . The structure of the copolymer systems studied, ABTB-MA, ABTB-EA, ABTB-BA, ABTB-MMA, ABTB-ST and ABTB-AN, was investigated by IR spectroscopy .

Thus, the IR spectra of the prepared copolymers are quite similar and show signals between 3000-2800 cm^{-1} characteristic for the C-H frequencies of $-CH_2-$ and $-CH_3$ groups,a strong band at 1735 cm^{-1} due to the $\rangle C=O$ of the acrylate esters, a strong band at 1640 cm^{-1} characteristic for the $\rangle C=O$ stretching vibrations of the tributyltin carboxylate group, and a signal at 1600 cm^{-1} due to the $\rangle C=C\langle$ of the aromatic ring. Also, the IR spectrum of ABTB-AN copolymer, shows a signal at 2220 cm^{-1} due to the $-C\equiv N$ group of acrylonitrile. Figures (13-15) show the IR spectra of ABTB-MMA, ABTB-ST and ABTB-AN copolymers as examples :

The experimental conditions and results of the copolymerization reactions are illustrated in Tables (1-6) . From the experimental data of the six systems studied (ABTB - MA, ABTB-EA , ABTB-BA , ABTB-MMA , ABTB-ST , and ABTB-AN the monomer reactivity ratios for each system were calculated by both Fineman-Ross[10] and Kelen-Tüdős[13] methods described in pages (19 &20) and the standard deviation of the results were calculated by regression analysis . Fig. (16) illustrate the Kelen-Tüdős plots of the six systems which give r_2 and $-r_2/\alpha$, both as intercepts . The results are summarized in Table (7) which show that there is a good agreement between the values of the reactivity ratios calculated by the two

methods . Also, the range of experimental error in r_1 and r_2 is quite small . Table (7) shows that the monomer reactivity ratio values of ABTB (r_1) for all systems studied are nearly equal to zero, which indicates that the growing radical ending with ABTB unit prefers M_2 monomers than M_1 monomer in the propagation stage . The monomer reactivity ratio values of vinyl monomers M_2 copolymerized with ABTB are greater than unity, which shows that the monomer sequence in these six copolymers consists of large blocks of the comonomer units interrupted by single molecules of ABTB . Fig. (17) illustrate the composition curves of the six binary systems and indicates that all systems studied do not give azeotropic compositions and also show that the copolymers produced have a lower content of F_1 than the comonomer mixtures .

The Q and e values for ABTB were calculated from the determined monomer reactivity ratios as well as Q and e value of vinyl monomers[71] using the Alfrey-Price equation[72]:

$$e_1 = e_2 + (-\mathrm{Ln}\ r_1 r_2)^{\frac{1}{2}}$$

$$Q_1 = (Q_2/r_2)\exp\ -e_2(e_2 - e_1)$$

The Q and e values for ABTB were Q=0.450 and e=1.391 which are in good agreement with the values reported in the literature[71] for the esters of acrylic acid .

Table (1) : Copolymerization of ABTB (M_1) with MA (M_2) .

Initial monomer composition		Conversion%	Sn%	Copolymer composition		Fineman-Ross method		Kelen-Tüdös method	
a^*	f_1^o			b^*	F_1^o	a-a/b	a^2/b	η	ξ
0.6689	0.4008	8.3216	17.4765	0.4302	0.3008	-0.8859	1.0399	-0.6941	0.8148
0.5375	0.3496	7.5185	16.4699	0.3558	0.2625	-0.9719	0.8113	-0.9277	0.7744
0.4279	0.2997	6.7941	15.4788	0.2988	0.2301	-1.0042	0.6128	-1.1825	0.7216
0.3335	0.2501	6.9874	13.9230	0.2301	0.1871	-1.1159	0.4833	-1.5505	0.6715
0.2503	0.2001	5.5648	13.2033	0.2046	0.1699	-0.9731	0.3065	-1.7925	0.5645
0.1763	0.1499	8.3903	11.3407	0.1513	0.1314	-0.9889	0.2056	-2.2377	0.4651
0.1134	0.1019	7.0149	8.6319	0.0958	0.0874	-1.0703	0.1347	-2.8845	0.3629
0.0495	0.0521	7.4186	5.0244	0.0456	0.0436	-1.0360	0.0548	-3.5575	0.1883

* Molar ratio

o Mole fraction

Table (2) : Copolymerization of ABTB (M_1) with EA (M_2) .

Initial monomer composition		Conversion%	Sn%	Copolymer composition		Fineman-Ross method		Kelen-Tüdös method	
a^*	f_1^o			b^*	F_1^o	a-a/b	a^2/b	η	ξ
1.0000	0.5000	6.1237	15.7924	1.0000	0.2687	-1.7218	2.7218	-0.4669	0.7379
0.8183	0.4500	7.2014	15.2015	0.6696	0.2491	-1.6487	2.0187	-0.5523	0.6763
0.6668	0.4000	8.1527	14.3198	0.4446	0.2224	-1.6647	1.5545	-0.6603	0.6167
0.5386	0.3500	5.9148	13.4026	0.2901	0.1975	-1.6499	1.1788	-0.7692	0.5495
0.4286	0.3000	6.8771	12.4125	0.1837	0.1733	-1.6162	0.8764	-0.8771	0.4756
0.3335	0.2500	6.2189	11.1919	0.1112	0.1467	-1.6066	0.6469	-0.9959	0.4009
0.2499	0.1999	7.9126	10.3968	0.0625	0.1311	-1.4062	0.4142	-1.0186	0.3000
0.1765	0.1500	5.8277	9.6018	0.0312	0.0832	-1.7673	0.3436	-1.3492	0.2623

* Molar ratio

o Mole fraction

Table (3) : Copolymerization of ABTB (M_1) with BA (M_2) .

Initial monomer composition		Conversion%	Sn%	Copolymer composition		Fineman-Ross method		Kelen-Tüdős method	
a^*	f_1^o			b^*	F_1^o	a-a/b	a^2/b	η	ξ
1.2219	0.5499	6.3126	14.2168	0.3596	0.2647	-2.1760	4.1524	-0.3642	0.6950
1.0001	0.5000	7.0128	13.6396	0.3274	0.2389	-2.0546	3.0549	-0.4213	0.6263
0.8183	0.4500	7.3246	12.6511	0.2789	0.2112	-2.1157	2.4009	-0.5009	0.5685
0.6667	0.4000	6.4527	11.5918	0.2349	0.1864	-2.1715	1.8923	-0.5846	0.5094
0.5385	0.3500	5.9436	10.7060	0.2033	0.1711	-2.1103	1.4265	-0.6496	0.4391
0.4287	0.3000	6.9828	9.6055	0.1691	0.1501	-2.1065	1.0869	-0.7241	0.3736
0.3333	0.2499	7.2214	8.4783	0.1389	0.1214	-2.0663	0.7999	-0.7880	0.3050

* Molar ratio

o Mole fraction

Table (4) : Copolymerization of ABTB (M_1) with MMA (M_2) .

Initial monomer composition		Conversion%	Sn%	Copolymer composition		Fineman-Ross method		Kelen-Tüdős method	
a^*	f_1°			b^*	F_1°	a-a/b	a^2/b	η	ξ
0.8183	0.4500	7.8203	15.7394	0.3636	0.2666	-1.4323	1.8419	-0.5864	0.7539
0.6650	0.3994	7.1198	14.7737	0.3082	0.2356	-1.4927	1.4348	-0.7332	0.7048
0.5398	0.3506	6.2796	14.0178	0.2718	0.2137	-1.4463	1.0721	-0.8644	0.6408
0.4286	0.3000	7.0355	12.5942	0.2156	0.1773	-1.5529	0.8449	-1.0731	0.5864
0.3333	0.2500	9.1600	10.7417	0.1595	0.1376	-1.7564	0.6966	-1.3529	0.5366
0.2500	0.2000	7.6238	9.7241	0.1346	0.1186	-1.6074	0.4643	-1.5087	0.4358
0.1835	0.1551	7.8500	8.0244	0.0998	0.0907	-1.6554	0.3375	-1.7632	0.3597
0.1100	0.0991	9.2000	5.6608	0.0617	0.0581	-1.6734	0.1962	-2.0989	0.2461

* Molar ratio

° Mole fraction

Table (5) : Copolymerization of ABTB (M_1) with ST (M_2) .

Initial monomer composition		Conversion%	Sn%	Copolymer composition		Fineman-Ross method		Kelen-Tüdös method	
a^*	f_1^o			b^*	F_1^o	a-a/b	a^2/b	η	ξ
0.9999	0.4999	8.2109	17.0816	0.4829	0.3257	-1.0707	2.0704	-0.3814	0.7375
0.8182	0.4501	7.0541	16.2194	0.4122	0.2919	-1.1668	1.6242	-0.4942	0.6879
0.6667	0.4000	7.9628	15.3968	0.3568	0.2629	-1.2019	1.2455	-0.6063	0.6283
0.5386	0.3501	6.8564	14.4061	0.3019	0.2319	-1.2454	0.9609	-0.7336	0.5659
0.4287	0.3001	7.7921	13.3167	0.2524	0.2015	-1.2698	0.7282	-0.8667	0.4971
0.3334	0.2501	5.9903	12.0919	0.2070	0.1715	-1.2772	0.5367	-1.0059	0.4214
0.2500	0.2000	6.2108	10.6150	0.1627	0.1399	-1.2866	0.3841	-1.1477	0.3427
0.1765	0.1500	7.4325	8.7660	0.1188	0.1062	-1.3092	0.2618	-1.3110	0.2621

* Molar ratio

o Mole fraction

Table (6) : Copolymerization of ABTB (M_1) with AN (M_2) .

Initial monomer composition		Conversion%	Sn%	Copolymer composition		Fineman-Ross method		Kelen-Tüdős method	
a^*	f_1^o			b^*	F_1^o	a-a/b	a^2/b	η	ξ
1.5008	0.6001	5.1242	18.6506	0.3379	0.2525	-2.9408	6.6659	-0.3022	0.6849
1.2225	0.5500	5.8871	18.1021	0.3008	0.2313	-2.8417	4.9681	-0.3537	0.6184
0.9998	0.4999	6.1294	17.7063	0.2777	0.2173	-2.6005	3.5996	-0.3902	0.5401
0.8179	0.4499	7.0112	16.5024	0.2209	0.1809	-2.8847	3.0285	-0.4734	0.4969
0.6668	0.4000	5.9914	15.6562	0.1901	0.1598	-2.8408	2.3388	-0.5257	0.4328
0.5386	0.3500	6.0199	14.5832	0.1584	0.1367	-2.8617	1.8314	-0.5844	0.3739
0.4284	0.2999	6.4678	13.3999	0.1303	0.1153	-2.8594	1.4098	-0.6389	0.3150

* Molar ratio

o Mole fraction

Table (7) : Monomer reactivity ratios for copolymerization of ABTB with MA, EA, BA, MMA, ST and AN.

M_1 - M_2	Fineman-Ross Method		Kelen - Tüdős Method			
	r_1	r_2	r_1	r_2	$r_1 r_2$	α
ABTB-MA	0.122±0.065	1.062±0.036	0.080±0.003	1.046±0.024	0.084	0.236
ABTB-EA	0.049±0.048	1.575±0.069	0.039±0.001	1.585±0.087	0.062	0.966
ABTB-BA	0.016±0.016	2.147±0.046	0.019±0.001	2.076±0.024	0.039	1.822
ABTB-MMA	0.160±0.050	1.730±0.050	0.150±0.005	1.710±0.006	0.257	0.357
ABTB-ST	0.123±0.009	1.348±0.011	0.113±0.001	1.339±0.009	0.151	0.737
ABTB-AN	0.009±0.025	2.801±0.098	0.007±0.003	2.853±0.072	0.019	3.066

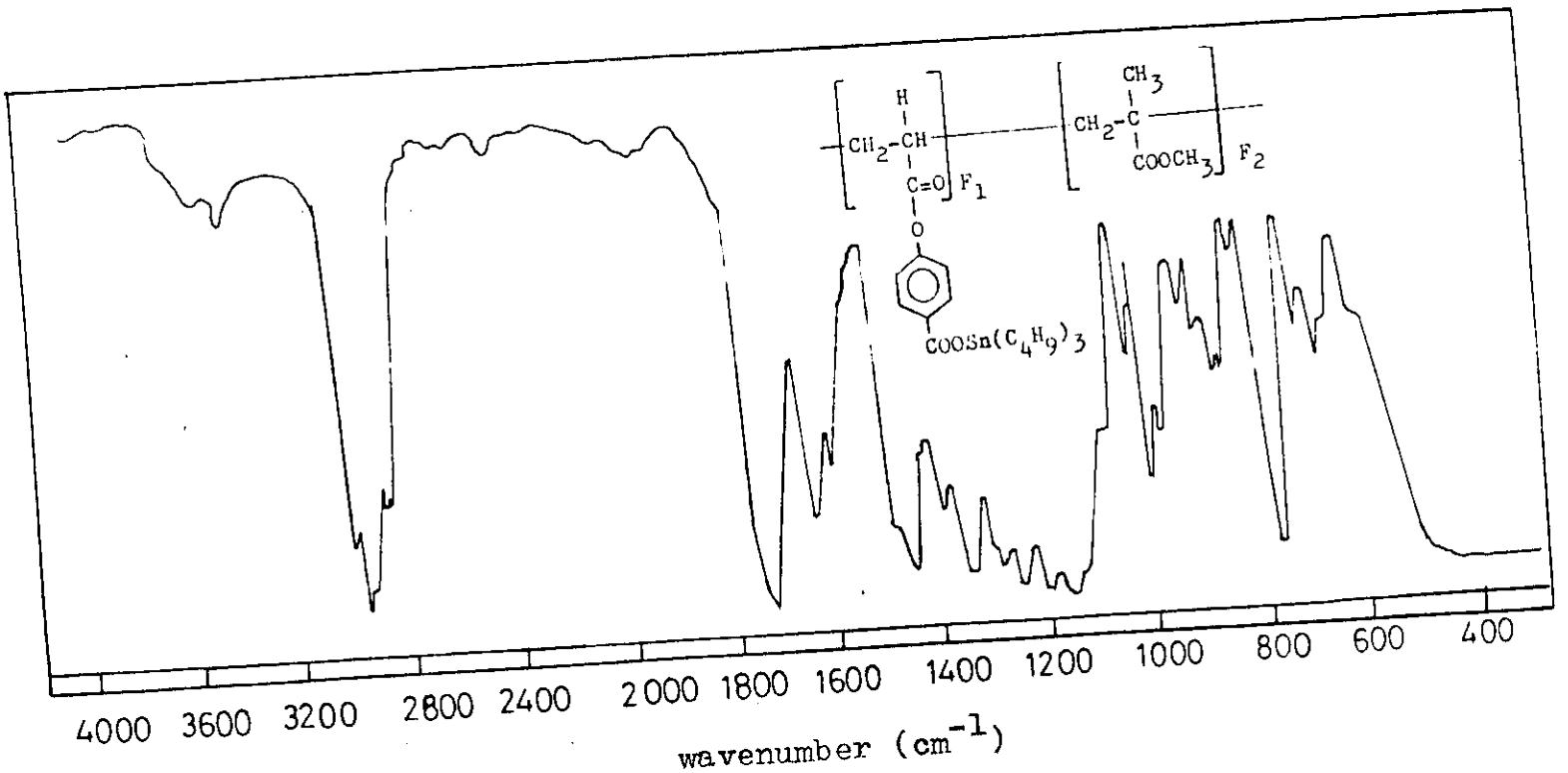

Fig. (13): IR spectrum of ABTB-MMA copolymer

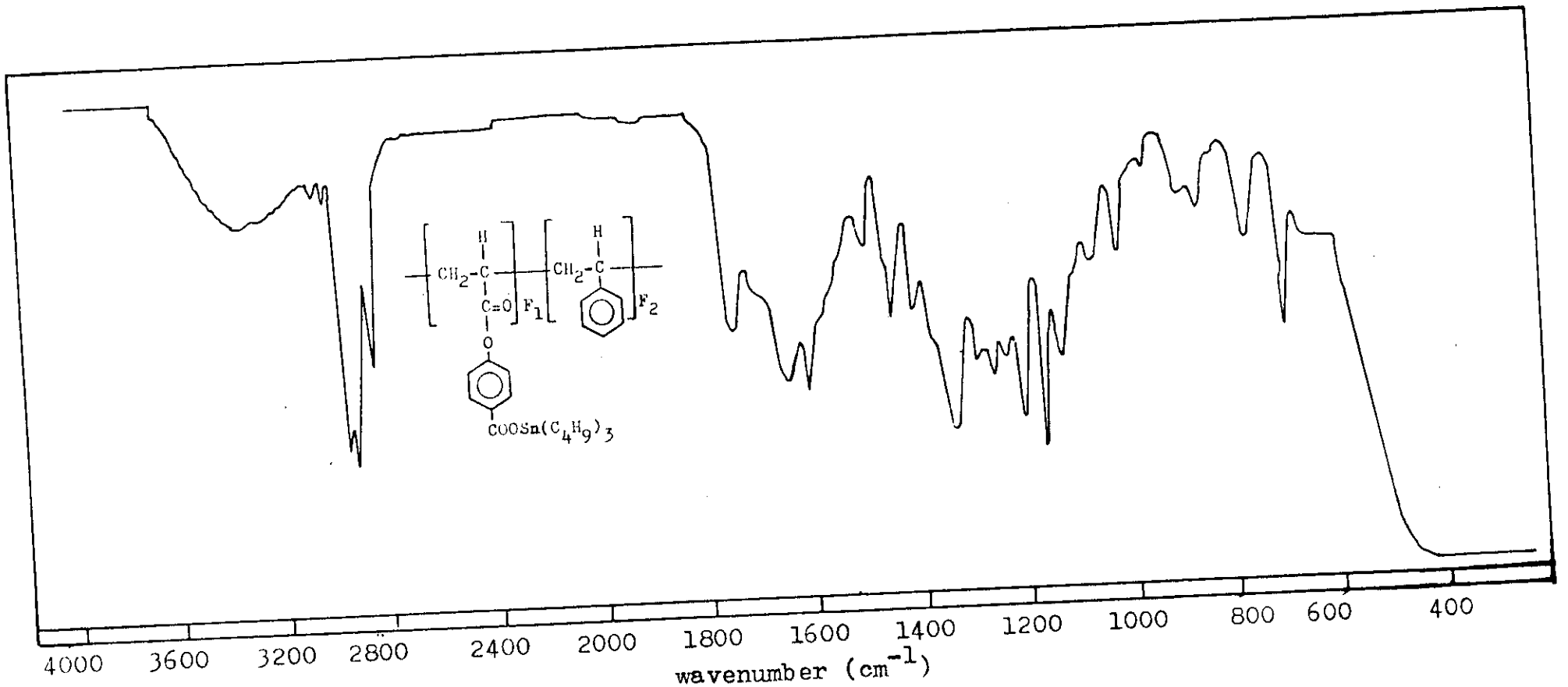

Fig. (14): IR spectrum of ABTB-ST copolymer

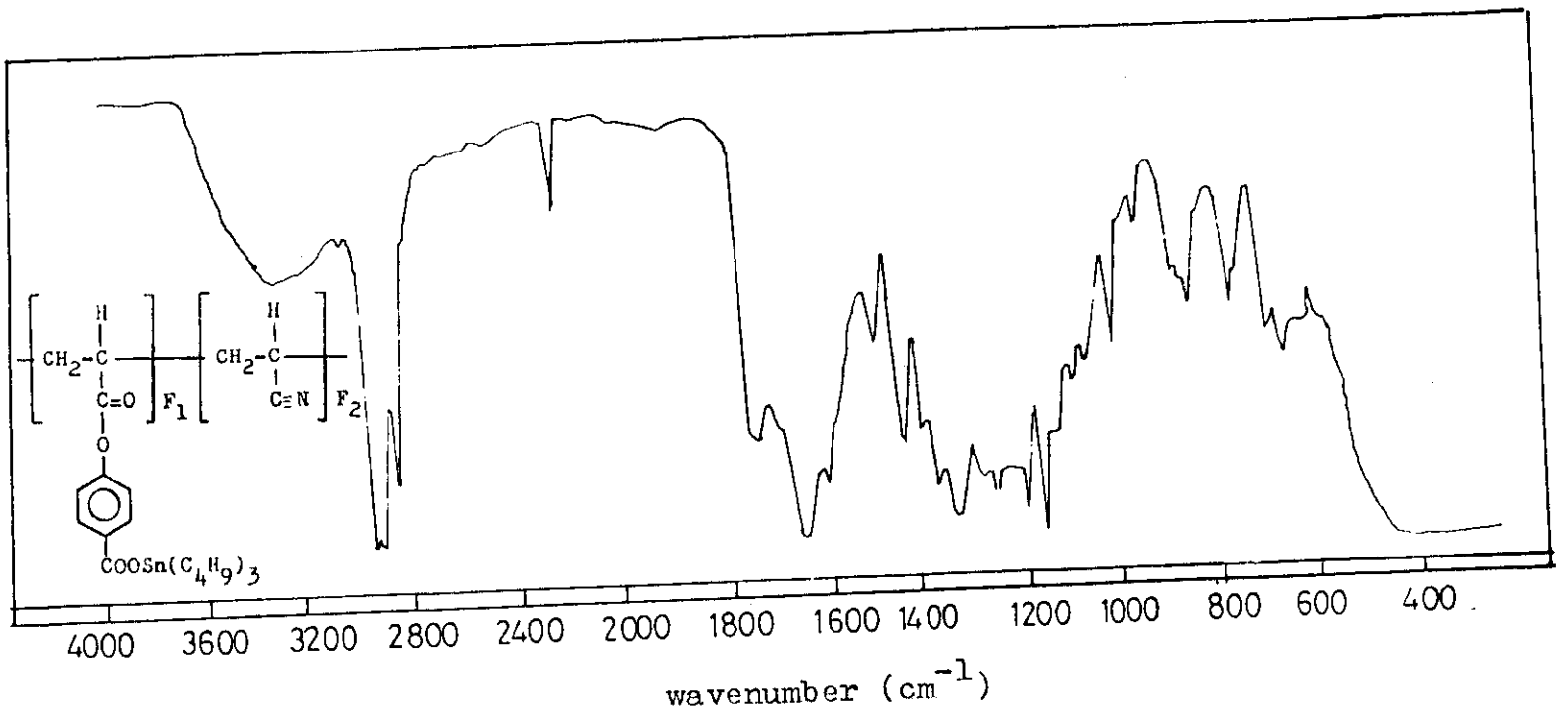

Fig. (15): IR spectrum of ABTB-AN copolymer

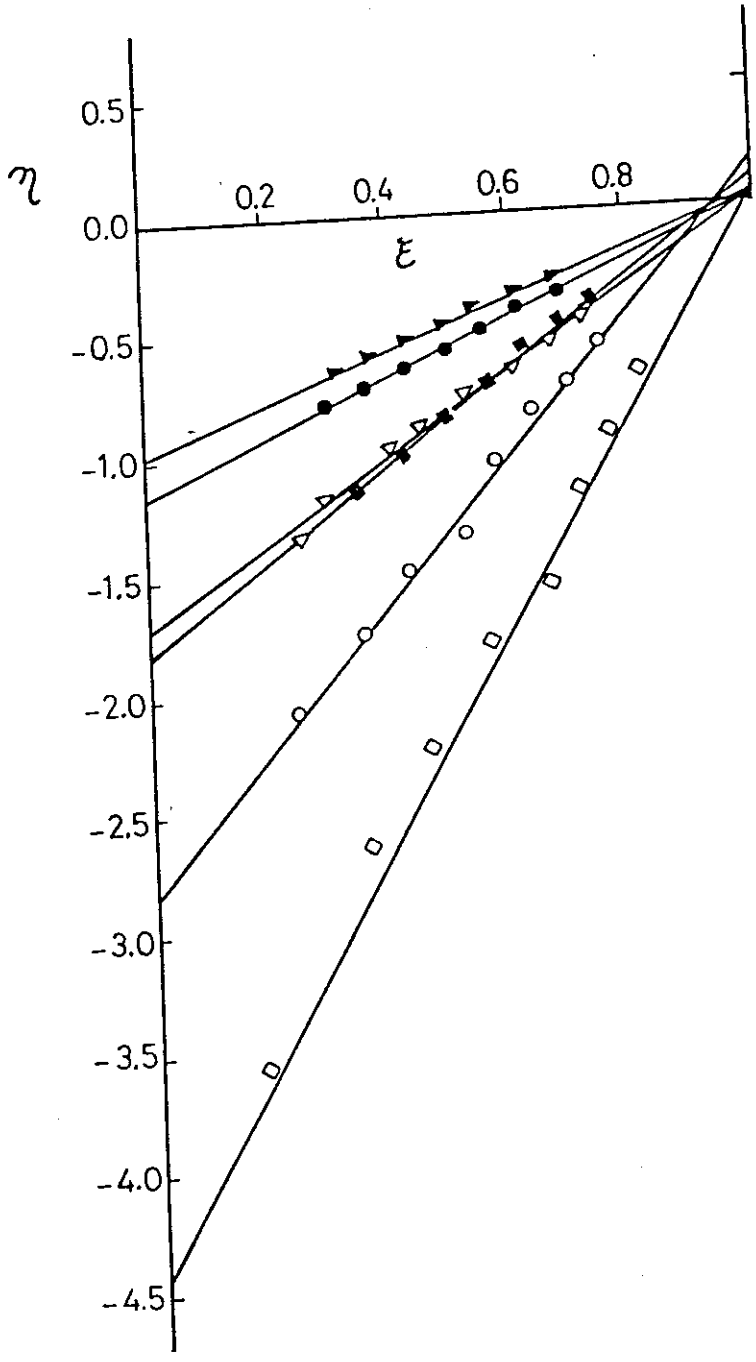

Fig(16) Kelen-Tüdős plots for copolymerizations of ABTB with (□) MA, (△) EA, (●) BA, (○) MMA, (■) ST and (▲) AN.

$$\xi = \frac{a^2}{\alpha b + a^2} \quad \text{and} \quad \eta = \frac{a(b-1)}{\alpha b + a^2}$$

where a and b are the molar ratios (M_1/M_2) of the comonomer in the feed and copolymer, respectively, and

$$\alpha = \frac{a_{min} \cdot a_{max}}{(b_{min} \cdot b_{max})^{\frac{1}{2}}}$$

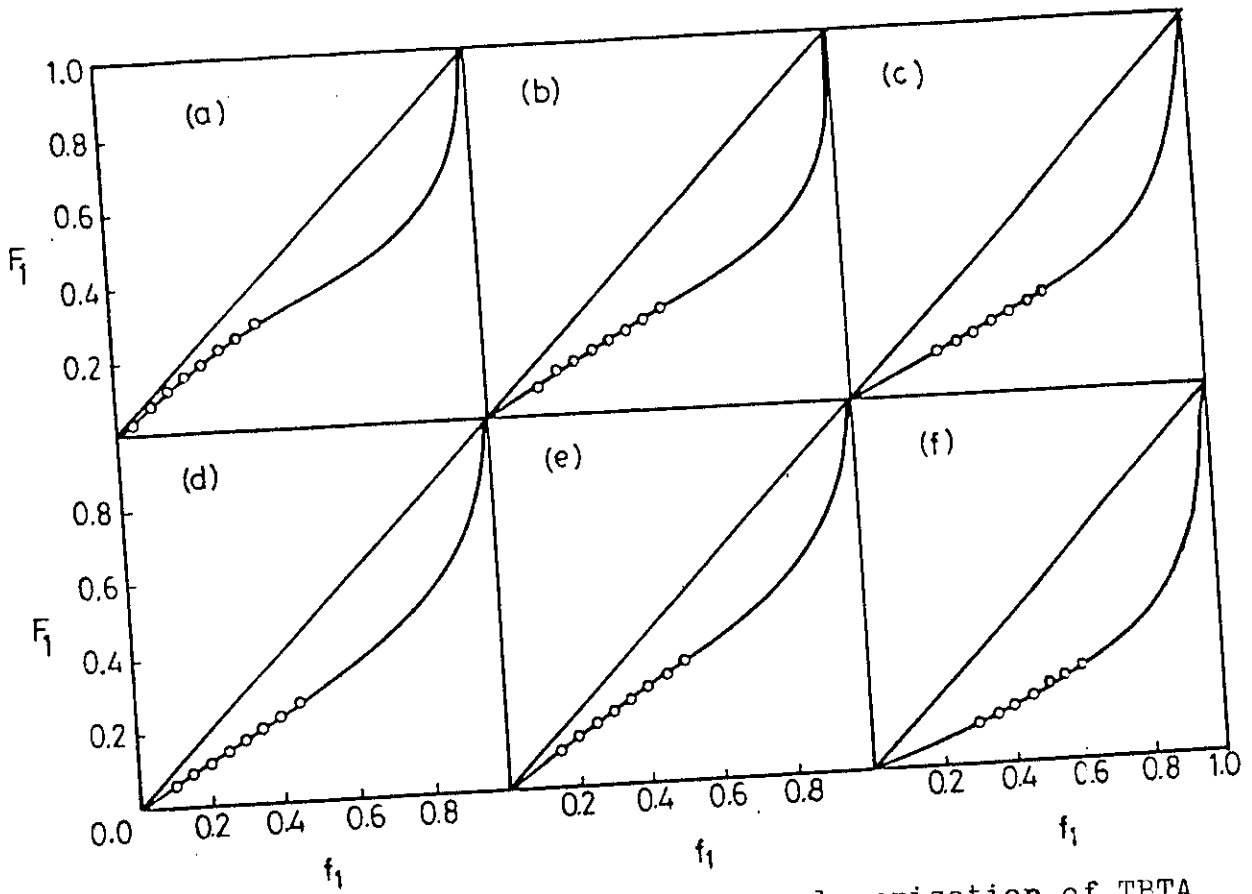

Fig(17) Composition curves for copolymerization of TBTA with (a) MA, (b) EA, (c) BA, (d) MMA, (e) ST and (f) AN. Line represents calculated values and (○) represent experimental values.

f_1 = molar fraction of M_1 in feed and

F_1 = molar fraction of M_1 in copolymer.

2--Copolymerization Reactions of tri-n-Butyltin Acrylate (TBTA) with Itaconic Acid (IA), Dimethyl Itaconate (DMI), p-Acryloyloxybenzoic Acid (ABA) and N-methacryloyloxytetrabromophthalimide (NMTP).

The copolymerization reactions of ABTB with each of IA, DMI and ABA were carried out by the solution copolymerization technique in toluene (3 mole/L) at 70 °C in the presence of 1 mole % AIBN according to the method described in page (46). In case of the copolymer system TBTA-NMTP the copolymerization reaction was carried out in dioxane as a solvent. The reactions can be illustrated as follows :

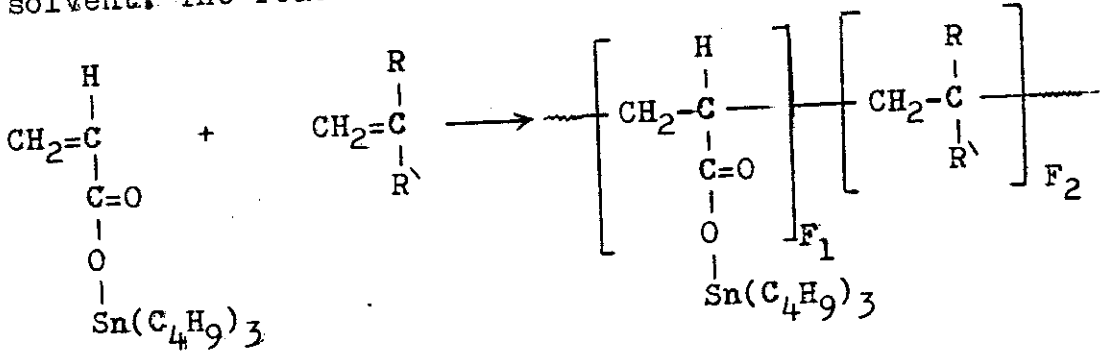

where :

M_1-M_2	R	R'
TBTA-IA	-COOH	$-CH_2-COOH$
TBTA-DMI	$-COOCH_3$	$-CH_2-COOCH_3$
TBTA-ABA	-H	$-p-COO-C_6H_4-COOH$
TBTA-NMTP	$-CH_3$	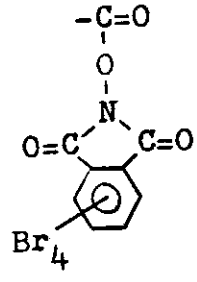

The experimental conditions and results of the copolymerization reactions of the four systems studied are illustrated in Tables (8-11). The copolymer composition of each sample was determined from tin analysis : From the experimental data the monomer reactivity ratios (r_1 and r_2) for each system were calculated by both Fineman-Ross and Kelen-Tüdös methods described in pages (19 & 20) and the standard deviations of the results were calculated by regression analysis. Fig. (18) illustrates the Kelen-Tüdös plots for the four systems studied, which give r_1 and $-r_2/\alpha$ both as intercepts. The results are summarized in Table (12) . The data illustrated in Table (12) show that there is a good agreement between the monomer reactivity ratios calculated by the two methods. Also, the range of the standard deviations calculated for r_1 and r_2 is quite small and can be considered as within the experimental error . From Table (12), it is clear that the monomer reactivity ratio values of TBTA (r_1) are greater than r_2 values for IA, DMI, and ABA, while in case of TBTA-NMTP-system the r_1 value is lower than the r_2 value . This is clear from Fig. (19) which illustrate the composition curves of the four systems studied and show that the copolymers produced have a high content of F_1 than the comonomer mixture for the system TBTA-IA, TBTA-DMI, and TBTA-ABA, while in case of TBTA-NMTP- system show a lower content of F_1 than the comonomer mixture . From Table (12) and Fig. (19) it is clear that the r_1 and r_2 value of the copolymer systems TBTA-DMI and TBTA-NMTP- are less than unity and should have azeotropic compositions at $F_1 = f_1$ at the mole

fractions of 0.77 and 0.25 respectively . However the copolmer systems TBTA-IA and TBTA-ABA gave no azeotropic copolymers .

The prepared copolymers are colourless solids soluble in most organic solvents and suitable for film formation . The structure of the prepared copolymers was investigated by IR spectroscopy . Thus, the IR spectra of the copolymer systems were similar and show a strong bands at 3000-2800 cm^{-1} characteristic for C-H vibrations of $-CH_3$ groups, a strong band at 1720 cm^{-1} due to the carboxylic carbonyl groups and a strong band at 1640 cm^{-1} due to the C=O of the tributyltin carboxyl group . Figures (20 & 21) show the IR spectra of the azeotropic copolymers of TBTA-DMI and TBTA-NMTP .

The sequence distribution of the monomer units along the copolymer chains were calculated from the monomer reactivity ratios on the basis of terminal copolymerization model[13] . The variation in the sequence distribution of the triad fractions (f_{111}, f_{112}, f_{212}) with feed composition are represented in Fig. (22) . It is clear that the triad fractions f_{111} increase with increasing of f_1 while triad fractions f_{212} decrease with increasing of f_1 . Triad fractions f_{122} have maximum values at f_1 equal to 0.50, 0.50, 0.50 and 0.55 for TBTA-IA, TBTA-DMI, TBTA-ABA and TBTA-NMTP systems respectively .

The Q and e values were calculated from the monomer reactivity ratios by Alfrey-Price equations[72] . The Q and e values which represent the extent of resonance stabilization and the polarity of the double bond, respectively in

the monomer and its extensively tabulated by Young[71] from earlier copolymerization data. Thus, the Q and e values for TBTA is obtained by using the monomer reactivity ratios determined for the system TBTA-DMI and using Q and e values for the dimethyl itaconate[73&74]. The Q and e values for TBTA is Q=0.313 and e=0.774 which are in good agreement with values reported in the literature[71].

Table (8) : Copolymerization of TBTA (M_1) with IA (M_2) •

Initial monomer composition		Conversion%	Sn%	Copolymer composition		Fineman-Ross method		Kelen-Tüdős method	
a^*	f_1^o			b^*	F_1^o	a-a/b	a^2/b	η	ξ
1.5003	0.6000	8.9462	28.7650	2.4669	0.7116	0.8921	0.9124	0.3024	0.3093
1.8571	0.6500	6.7456	29.1895	2.7849	0.7358	1.1903	1.2384	0.3633	0.3780
2.3333	0.6999	7.3028	30.0897	3.7698	0.7903	1.7144	1.4442	0.4924	0.4148
2.9999	0.7514	5.6247	30.4576	4.3761	0.8139	2.3144	2.0565	0.5653	0.5023
3.9997	0.7999	8.4027	30.9107	5.4211	0.8443	3.2619	2.9510	0.6539	0.5916
5.6667	0.8500	5.0164	31.3637	7.0577	0.8759	4.8638	4.5498	0.7371	0.6907

* Molar ratio

o Mole fraction

Table (9) : Copolymerization of TBTA (M_1) with DMI (M_2) .

Initial monomer composition		conversion%	Sn%	Copolymer composition		Fineman-Ross method		Kelen-Tüdös method	
a^*	f_1^o			b^*	F_1^o	a-a/b	a^2/b	η	ξ
1.8572	0.6500	6.7214	27.1836	2.0583	0.6654	0.9549	1.6758	0.1810	0.3177
2.3333	0.6999	7.8920	27.5071	2.2062	0.6939	1.2757	2.4677	0.2103	0.4068
2.9999	0.7499	7.1642	28.5438	2.8263	0.7437	1.9385	3.1842	0.2858	0.4694
4.0002	0.8000	5.6274	29.8129	4.1408	0.8055	3.0341	3.8643	0.4065	0.5178
5.6670	0.8490	8.2107	30.7176	5.9848	0.8509	4.7201	5.3661	0.5265	0.5986
7.3459	0.8802	5.9998	31.0194	6.9816	0.8747	6.2937	7.7293	0.5558	0.6823

* Molar ratio

o Mole fraction

Table (10) : Copolymerization of TBTA (M_1) with ABA (M_2) .

Initial monomer composition		Conversion%	Sn%	Copolymer composition		Fineman-Ross method		Kelen-Tüdős method	
a^*	f_1^o			b^*	F_1^o	a-a/b	a^2/b	η	ξ
0.6666	0.3999	6.2714	21.9816	1.0645	0.5157	0.0404	0.4175	0.0176	0.1822
0.9999	0.4999	8.3127	24.1348	1.4538	0.5925	0.3621	0.6877	0.1218	0.2685
1.5000	0.6000	5.9871	25.7962	1.9141	0.6568	0.7164	1.1755	0.2349	0.3855
2.3335	0.7000	9.0124	27.8222	2.8779	0.7421	0.5227	1.8921	0.4043	0.5024
4.0000	0.8000	7.2102	29.6136	4.7009	0.8246	3.1481	3.4035	0.5967	0.6449
8.9994	0.8999	5.7561	31.2382	9.6272	0.9059	8.0647	8.4126	0.7839	0.8178

* Molar ratio

o Mole fraction

Table (12) :Monomer reactivity ratios for copolymerization of TBTA with IA , DMI , ABA and NMTP.

M_1—M_2	Fineman-Ross Method		Kelen-Tüdős Method		$r_1 r_2$	α
	r_1	r_2	r_1	r_2		
TBTA-IA	1.088±0.044	0.011±0.109	1.086±0.113	0.070±0.121	0.076	2.038
TBTA-DMI	0.932±0.040	0.767±0.181	0.942±0.072	0.805±0.166	0.758	0.758
TBTA-ABA	1.000±0.040	0.360±0.150	1.014±0.026	0.399±0.029	0.405	1.874
TBTA-NMTP	0.691±0.014	0.902±0.060	0.689±0.045	0.896±0.110	0.617	3.630

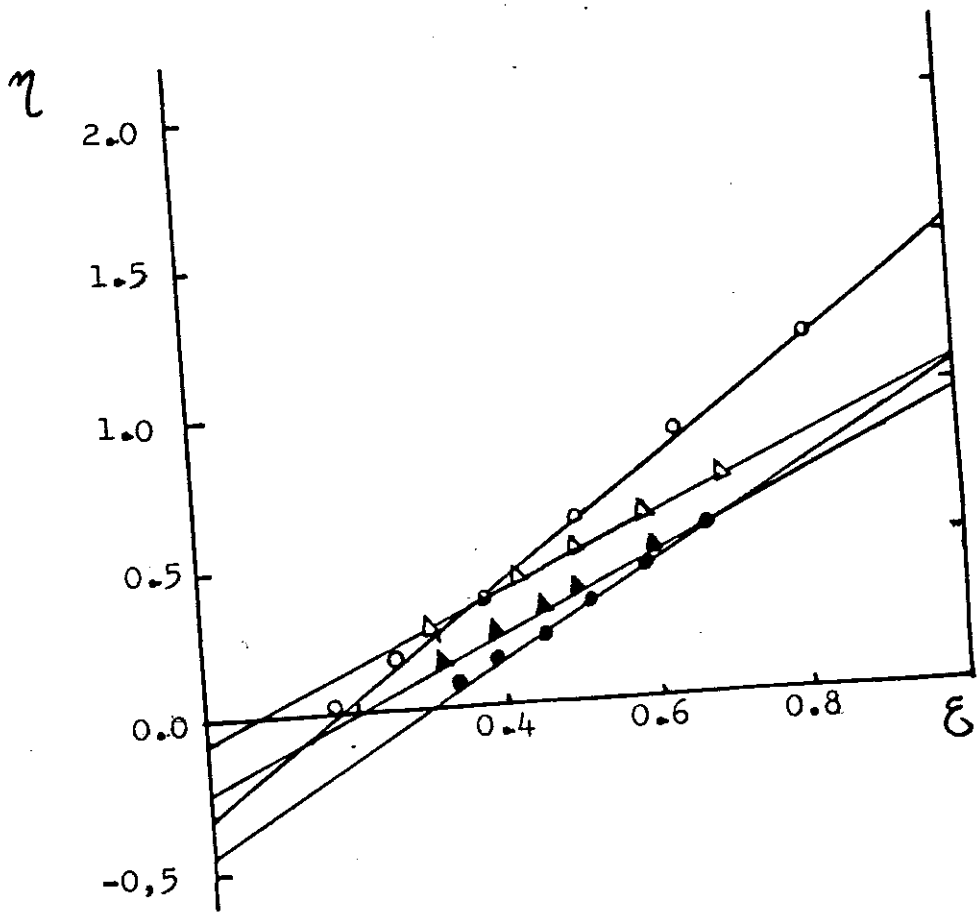

Fig.(18) : Kelen-Tüdös plot for copolymerization reaction of TBTA with (Δ) IA, (▲) DMI, (⊙) ABA and (●) NMTP .

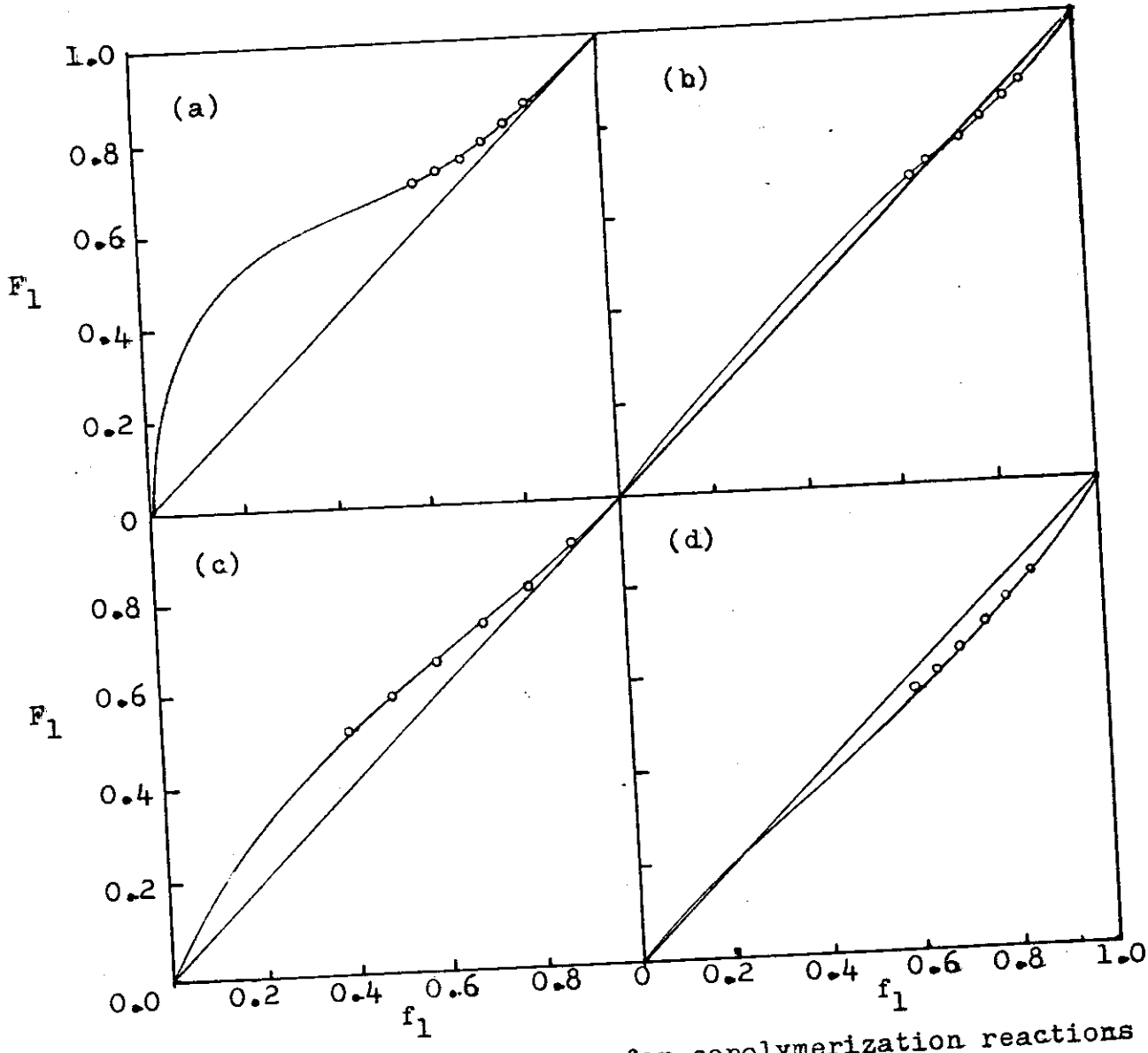

Fig.(19) : Composition curves for copolymerization reactions of TBTA with (a) IA, (b) DMI, (c) ABA and (d) NMTP .

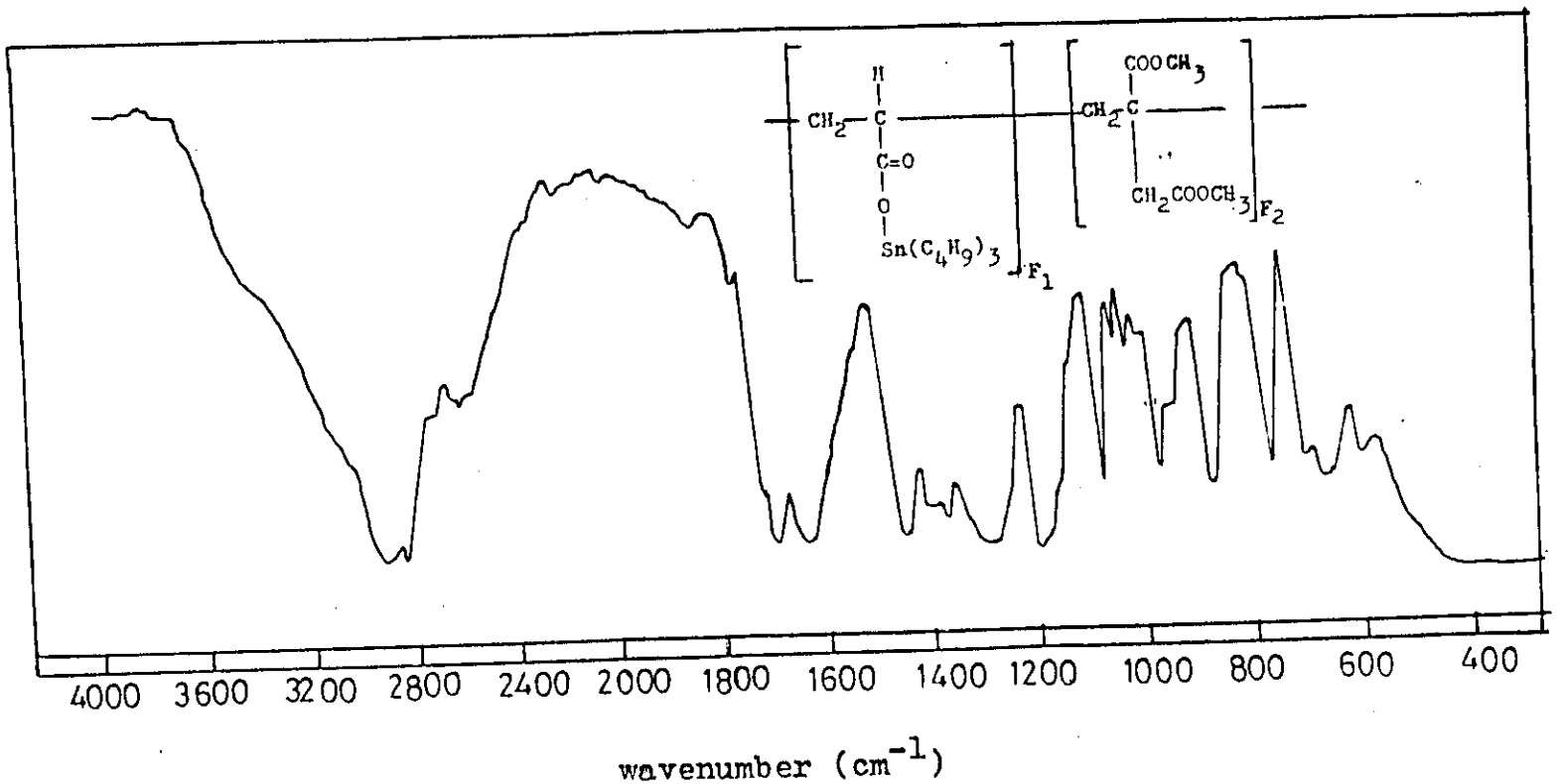

Fig. (20): IR spectrum of TBTA-DMI copolymer .

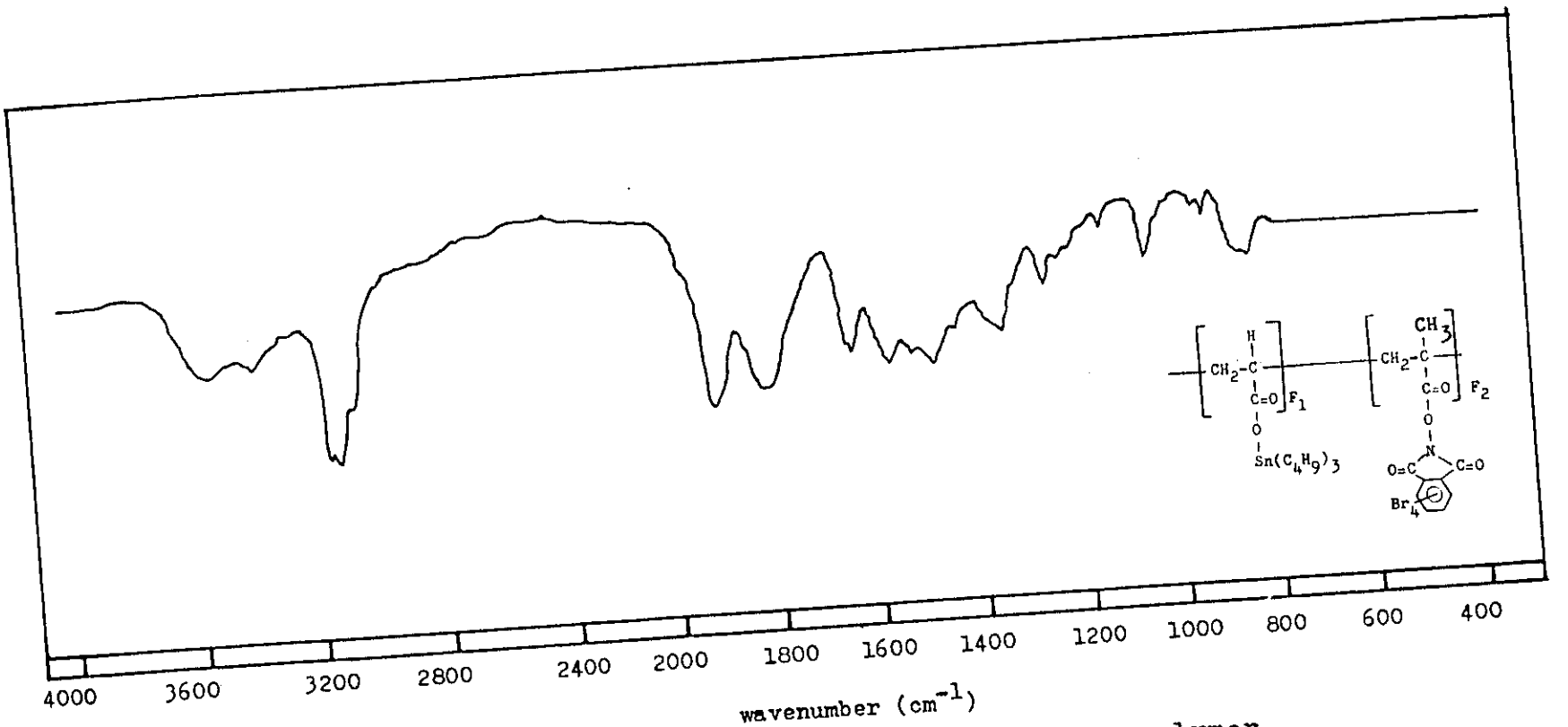

Fig. (21): IR spectrum of TBTA-NMTP copolymer .

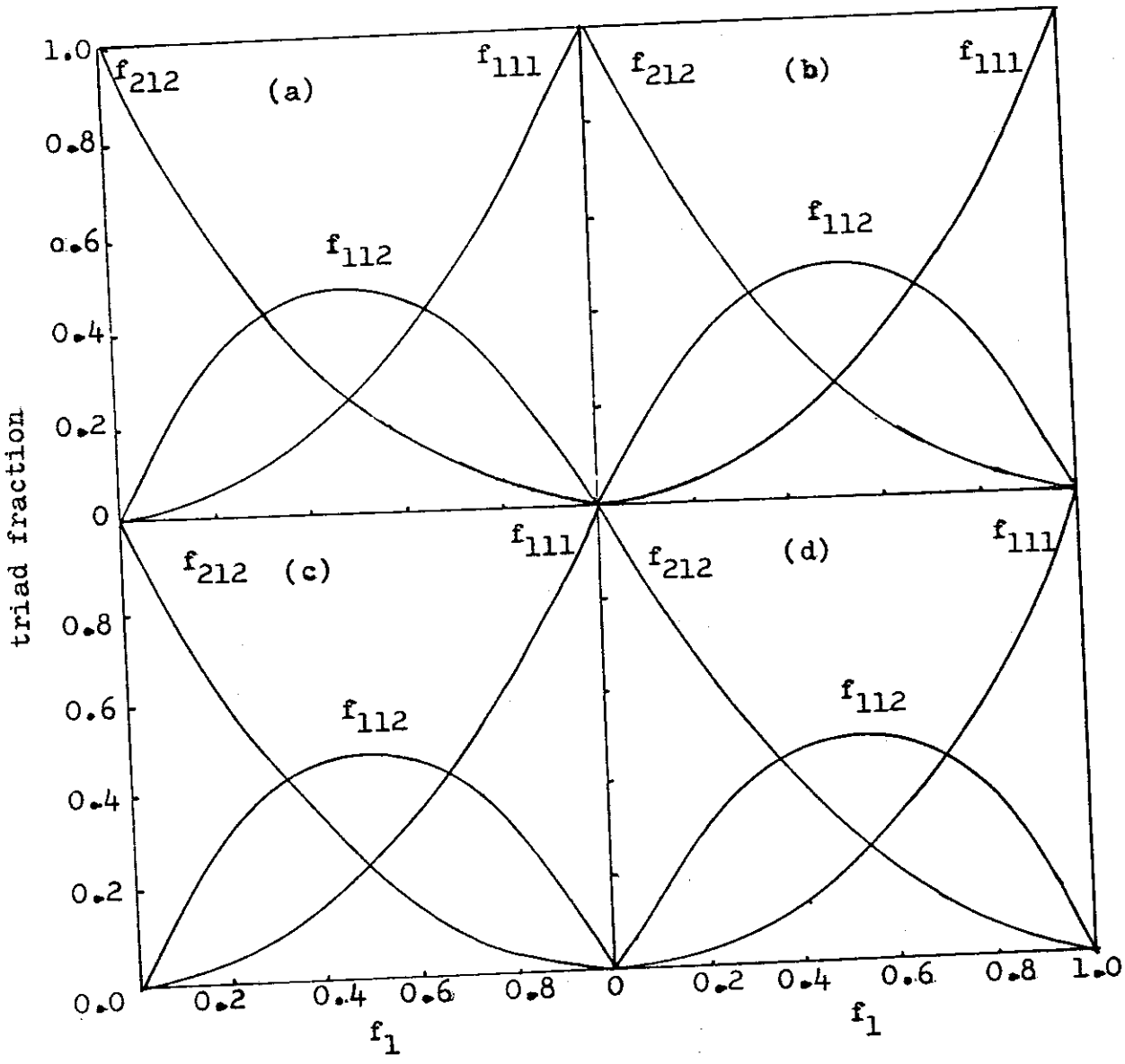

Fig.(22):Dependence of triad fractions (f_{111}, f_{112} and f_{212}) on comonomer composition f_1 for TBTA with (a) IA, (b) DMI, (c) ABA and (d) NMTP .

3-Copolymerization Reactions of tri-n-Butyltin Methacrylate (TBTMA) with Itaconic Acid (IA), Dimethyl Itaconate (DMI), p-Acryloyloxybenzoic Acid (ABA) and N-Methacryloyloxytetrabromophthalimide (NMTP).

The copolymerization of TBTMA with each of IA, DMI and ABA were carried out by the solution copolymerization technique in toluene (3 mole/L) at 70°C in the presence of 1 mol % AIBN, according to the method described in page (46). In case of copolymer system TBTMA-NMTP, the copolymerization reaction was carried out in dioxane as a solvent. The reaction can be represented as :

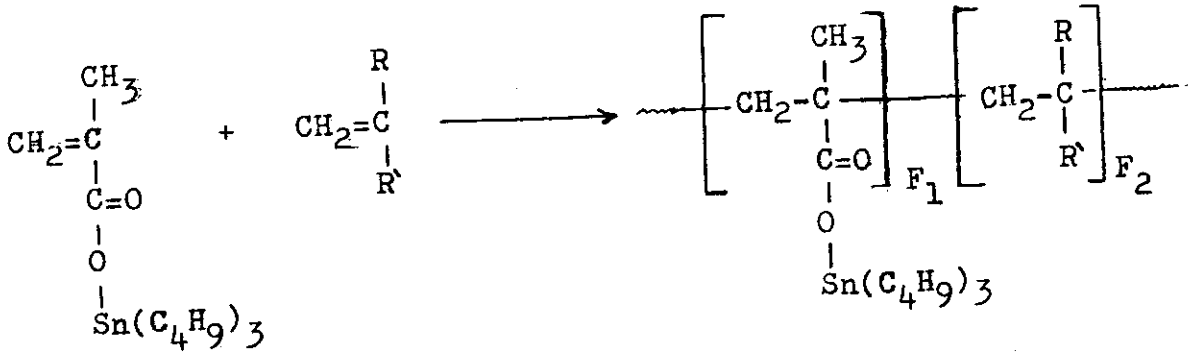

where :

M_1-M_2	R	R`
TBTMA-IA	-COOH	$-CH_2-COOH$
TBTMA-DMI	$-COOCH_3$	$-CH_2-COOCH_3$
TBTMA-ABA	-H	$-p-COO-C_6H_4-COOH$
TBTMA-NMTP	$-CH_3$	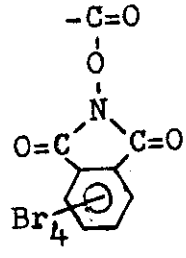

The experimental conditions and the results of the copolymerization reactions of the four systems studied are illustrated in Tables (13-16) . The copolymer composition of each sample was determined from tin analysis. From the experimental data tabulated in Tables (13-16) , the monomer reactivity ratios (r_1 and r_2) for each system were calculated by both Fineman-Ross and Kelen-Tüdös methods . The standard deviations of the results were calculated by regression analysis . Fig. (23) illustrates the kelen-Tüdös plots for the four systems studied, which give r_1 and $-r_2/\alpha$ both as intercepts . The results are summarized in Table (17). From Table (17), it clear that the monomer reactivity ratio values of TBTMA (r_1) are greater than (r_2) values for IA, DMI and ABA, while in case of TBTMA-NMTP system the (r_1) value is lower than (r_2) value . This is clear from Fig. (24) which illustrate the composition curves of the four systems studied and show that the copolymers produced have a high content of F_1 than the comonomer mixtures for the systems TBTMA-IA , TBTMA-DMI and TBTMA-ABA , while in case of TBTMA— NMTP system show a lower content of F_1 than the comonomer mixture . From Table (17) and Fig. (24) the results indicate that the copolymerization reactions of TBTMA with IA, DMI, ABA and NMTP gave no azeotropic copolymers .

The prepared copolymers are colourless solids soluble in most organic solvents and suitable for film formation . The structure of the prepared copolymers was investigated by IR spectroscopy . Thus, the IR spectra of the copolymer

systems were similar and show bands at 3000-2800 cm^{-1} characteristic for C-H vibrations of $-CH_3$ groups, a strong band at 1730 cm^{-1} due to the carboxylate carbonyl groups and a strong band at 1640 cm^{-1} due to the C=O tributyltin carboxyl group . Fig. (25) show the IR spectra of TBTMA--ABA copolymer as example .

The sequence distribution of the monomer units along the copolymer chains were calculated from the monomer reactivity ratios according to IZU and O'Driscoll[75]. The variation in the sequence distribution of the triad fraction (f_{111}, f_{112}, f_{212}) with the feed composition are represented in Fig. (26) . It is clear that the triad fraction f_{111} increases with increasing of f_1, while triad fraction f_{212} decreases with increasing of f_1 . Triad fraction f_{112} have maximum values at f_1 equal to 0.30, 0.45, 0.30 and 0.60 of TBTMA-IA , TBTMA-DMI , TBTMA-ABA and TBTMA-NMTP systems respectively .

The Q and e values were calculated from the monomer reactivity ratios by using the Alfrey-Price equation[72] . The Q and e values which represent the extent of resonance stabilization and the polarity of the double bond respectively, in a monomer and its radical are extensively tabulated by Young[71] from earlier copolymerization data . Thus, the Q and e values for TBTMA is obtained by using monomer reactivity ratios determined for the system TBTMA-DMI . The Q and e values for TBTMA were Q = 0.575 and e = 1.300 which are in good agreement with the values reported in the literature[71].

Table (13) : Copolymerization of TBTMA (M_1) with IA (M_2) .

Initial monomer composition		Conversion%	Sn%	Copolymer composition		Fineman-Ross method		Kelen-Tüdős method	
a^*	f_1^o			b^*	F_1^o	a-a/b	a^2/b	η	ξ
0.5385	0.3500	9.0124	27.4834	2.2418	0.6915	0.2983	0.1293	0.4564	0.1979
0.8182	0.4500	7.8462	28.2808	2.8397	0.7395	0.5301	0.2357	0.6975	0.3102
1.2222	0.5500	5.9981	29.0215	3.7099	0.7877	0.8928	0.4027	0.9632	0.4344
1.8571	0.6499	7.1029	29.5623	4.7205	0.8252	1.4637	0.7306	1.1665	0.5823
3.0001	0.7500	6.4147	30.2674	7.1578	0.8774	2.5810	1.2575	1.4486	0.7058
5.6672	0.8500	6.2892	30.9674	14.0161	0.9340	5.2629	2.2914	1.8692	0.8138

* Molar ratio

o Mole fraction

Table (14) : Copolymerization of TBTMA (M_1) with DMI (M_2) .

Initial monomer composition		Conversion%	Sn%	Copolymer composition		Fineman-Ross method		Kelen-Tüdős method	
a^*	f_1^o			b^*	F_1^o	a-a/b	a^2/b	η	ξ
1.4999	0.5999	7.1126	25.6596	1.7800	0.6403	0.6573	1.2639	0.1778	0.3419
1.8571	0.6499	6.9553	26.7999	2.2888	0.6959	1.0457	1.5069	0.2655	0.3826
2.3333	0.6999	7.3488	27.5201	2.7521	0.7335	1.4855	1.9782	0.3368	0.4486
2.9992	0.7499	8.0421	28.5654	3.7992	0.7916	2.2098	2.3688	0.4603	0.4934
4.0000	0.8000	6.7899	29.2467	4.9556	0.8321	3.1928	3.2287	0.5640	0.5704
5.6669	0.8500	5.9714	29.8979	6.8634	0.8619	4.8412	4.6786	0.6809	0.6579

* Molar ratio

o Mole fraction

Table (15) : Copolymerization of TBTMA (M_1) with ABA (M_2) .

Initial monomer composition		Conversion%	Sn%	Copolymer composition		Fineman-Ross method		Kelen-Tüdős method	
a*	f_1^o			b*	F_1^o	a-a/b	a^2/b	η	ξ
0.6667	0.3999	7.2173	21.4539	1.0686	0.5166	0.04279	0.4157	0.0271	0.2639
1.0000	0.4999	8.4182	24.6665	1.7871	0.6412	0.4404	0.5596	0.2333	0.2964
1.5000	0.6000	6.8935	26.9064	2.8540	0.7405	0.9744	0.7884	0.4603	0.3724
2.3334	0.7000	8.3982	28.5843	4.6475	0.8229	1.8313	1.1716	0.7325	0.4686
4.0000	0.8000	5.5605	29.7919	7.8165	0.8866	3.4883	2.0469	1.0334	0.6064
9.0000	0.9000	7.0140	30.9044	19.0889	0.9502	8.5285	4.2433	1.5307	0.7616

* Molar ratio

o Mole fraction

Table (16) : Copolymerization of TBTMA (M_1) with NMTP (M_2) •

Initial monomer composition		Conversion%	Sn%	Copolymer composition		Fineman-Ross method		Kelen-Tüdös method	
a^*	f_1^o			b^*	F_1^o	a-a/b	a^2/b	η	ξ
5.6667	0.9000	8.4216	23.9599	4.4960	0.8181	4.4063	7.1421	0.4180	0.6776
4.0000	0.8499	7.0125	21.6624	3.1376	0.7583	2.7251	5.0994	0.3207	0.6001
3.0000	0.8000	5.4389	19.5331	2.3354	0.7002	1.7154	3.8537	0.2365	0.5314
2.3333	0.7499	5.9247	17.8085	1.8655	0.6510	1.0825	2.9185	0.1714	0.4620
1.8571	0.6999	6.2548	15.9075	1.4662	0.5945	0.5905	2.3523	0.1027	0.4090
1.5000	0.6499	7.9896	14.0571	1.1600	0.5370	0.2069	1.9396	0.0388	0.3634
1.2222	0.5999	5.4216	12.3042	0.9238	0.4802	-0.1008	1.6170	-0.0201	0.3224

* Molar ratio

o Mole fraction

Table (17) : Monomer reactivity ratios for copolymerization of TBTMA with IA , DMI , ABA and NMTP.

M_1—M_2	Fineman-Ross Method		Kelen-Tüdös Method		$r_1 r_2$	α
	r_1	r_2	r_1	r_2		
TBTMA-IA	2.272±0.080	0.073±0.090	2.157±0.161	0.006±0.046	0.013	0.524
TBTMA-DMI	1.223±0.036	0.829±0.101	1.242±0.064	0.869±0.099	1.079	2.432
TBTMA-ABA	2.190±0.030	0.820±0.070	2.207±0.110	0.861±0.090	1.900	1.329
TBTMA-NMTP	0.804±0.011	1.343±0.044	0.851±0.062	1.355±0.148	1.153	3.398

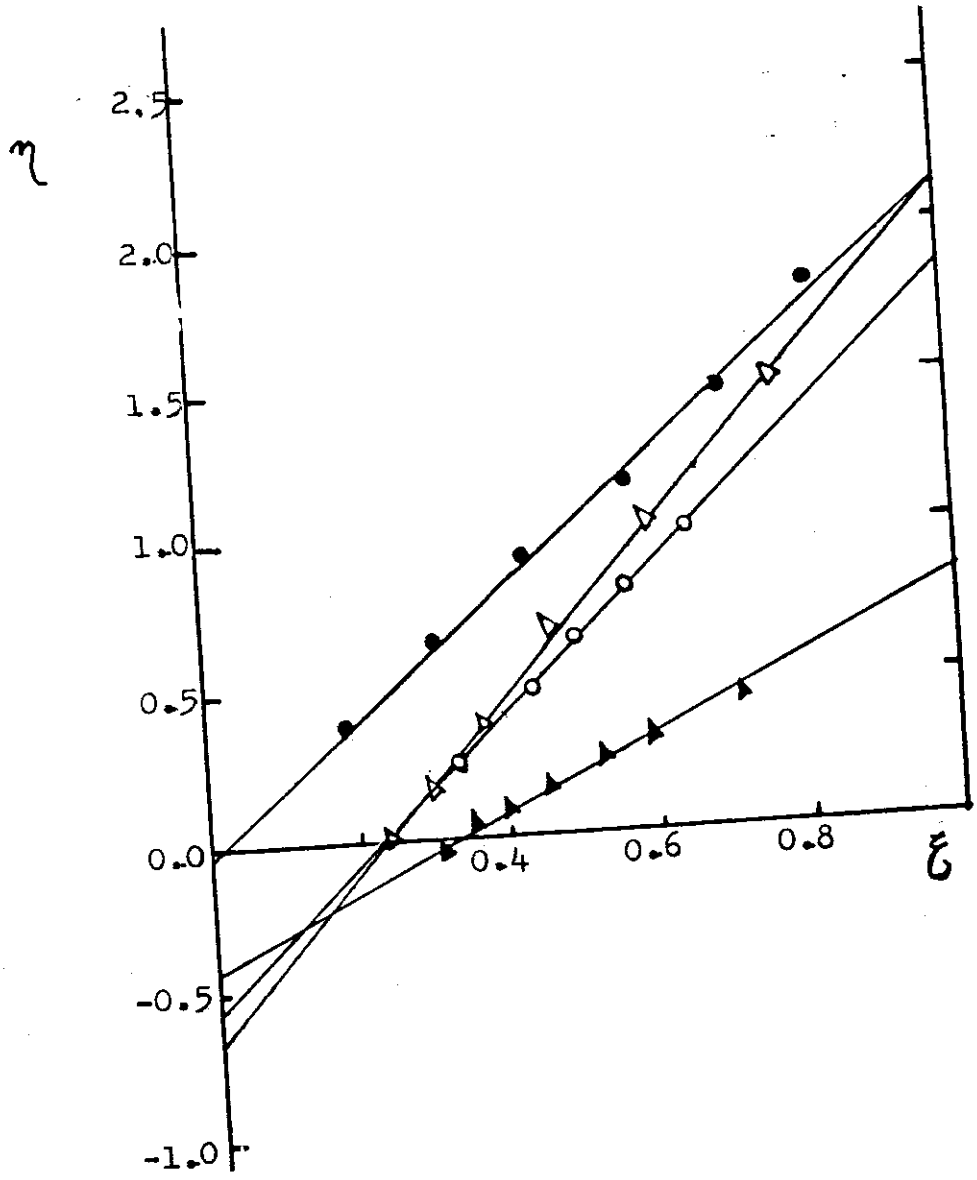

Fig. (23) Kelen-Tüdős plot for copolymerization of TBTMA with (●) IA, (○) DMI, (▲) ABA, and (Δ) NMTP .

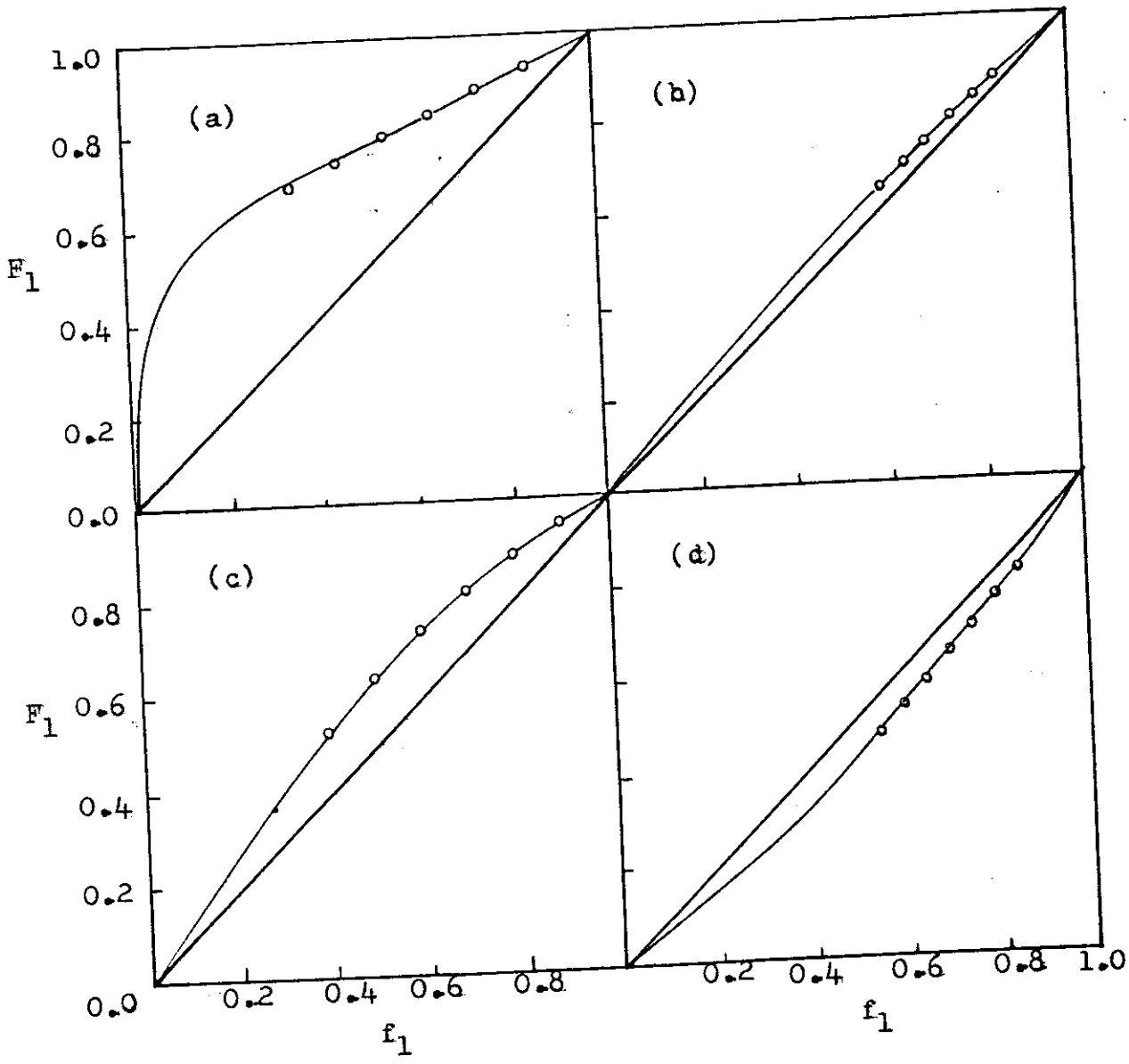

Fig. (24) : Composition curves for copolymerization of TBTMA with (a) IA, (b) DMI, (c) ABA and (d) NMTP.

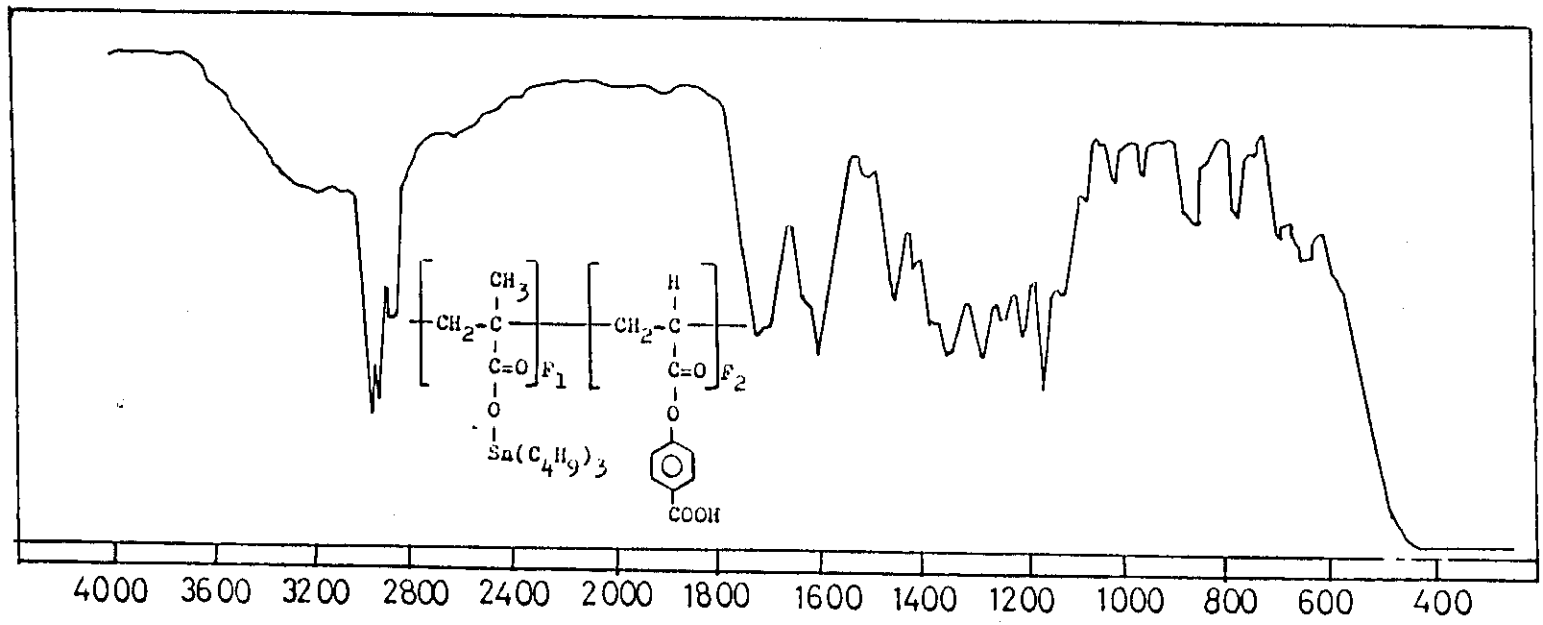

Fig. (25): IR spectrum of TBTMA-ABA copolymer .

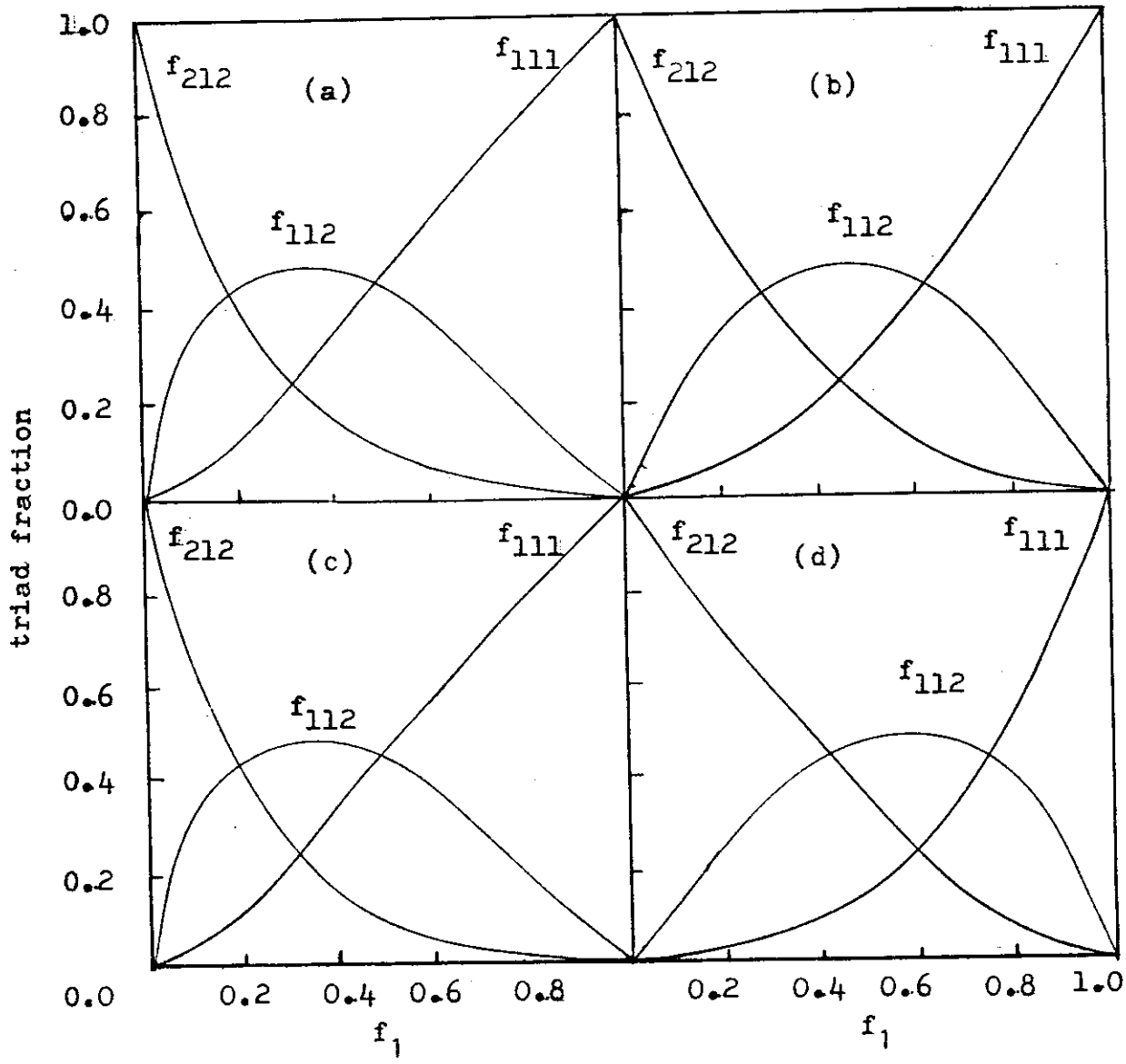

Fig. (26): Dependence of triad fractions (f_{111}, f_{112}, f_{212}) on comonomer composition f_1 for TBTMA with (a) IA, (b) DMI, (c) ABA and (d) NMTP .

C-TERNARY COPOLYMERIZATION REACTIONS

1- Azeotropy in Binary and Ternary Copolymerization Reactions of tri-n-Butyltin Acrylate or Methacrylate with Itaconic Acid or Dimethyl Itaconate and Acrylonitrile .

The monomer reactivity ratio values determined for binary system TBTA-DMI in the present work Table (12) were found to be r_1=0.942 and r_2=0.805 . These results indicate that the TBTA-DMI system should have a binary azeotropic composition at F_1=77 mole % .Thus, the comonomer composition corresponding to the binary azeotropy was polymerized to several degrees covering a wide range of conversions. Table (18) show that the azeotropic feed composition as a function of conversion remains constant up to high degrees of conversion . Fig. (27) show F_1(mole fraction of TBTA) against % conversion for TBTA-DMI system indicates that the experimental points,calculated from tin content of eash sample, are in good agreement with the lines representing the azeotropic composition of the copolymer . These results indicate the correctness of the reactivity ratio values determined for the studied binary copolymerization reaction of TBTA with DMI .

Four terpolymer systems involving tri-n-butyltin acrylate or methacrylate with itaconic acid, dimethyl itaconate and acrylonitrile were prepared by solution polymerization in DMF (1.5 mole/L) in presence of 1 mole % AIBN as initiater at 70°C .

The structure of the prepared terpolymers can be represented by the following general formula as:

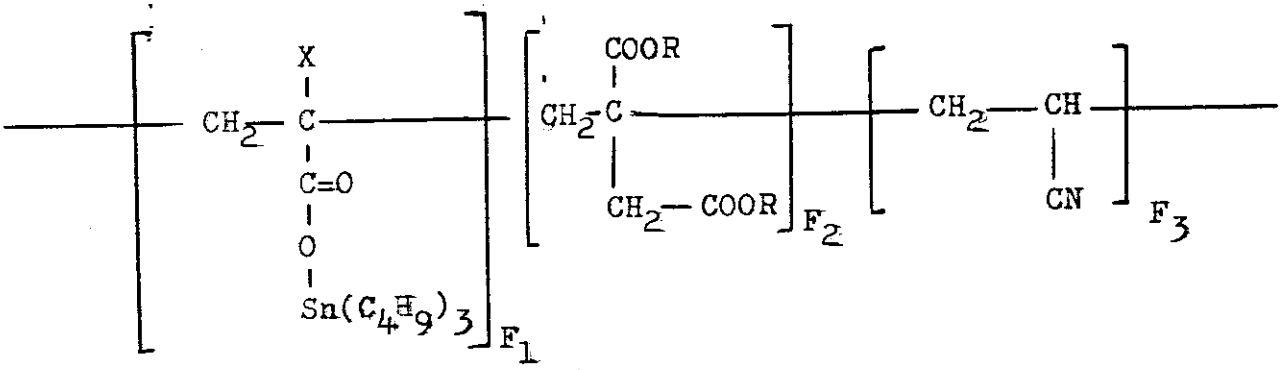

where x and R = H or $-CH_3$

The terpolymer samples were polymerized to low conversion (less tham 10 %) to allow us to use the terpolymer composition equation . The terpolymer composition of each sample was calculated from tin and nitrogen analysis . The theoritical terpolymer composition were obtained by the use of Alfrey-Goldfinger terpolymerization equation [20] page (26) in the form proposed by Khan and Horowitz [26] page (26) . The monomer reactivity ratios determined for TBTA-IA , TBTA-DMI , TBTMA-IA and TBTMA-DMI systems determined in the present studies Table (12&17) as well as the literature values [71] for the systems IA-AN and DMI-AN Table (19) were used for calculating the terpolymer composition. A computer program written in basic based on the equation proposed by Kham and Horowitz [26] was used to

facilitate the calculations of the ternary monomer-polymer composition relationship and to study the behaviour of each monomer during polymerization. All possible compositions were screened and the different azeotropic curves of binary and ternary azeotropies can be graphically plotted. The relation between monomer composition in the feed and the composition of the monomers in the resulting terpolymer is represented in the form of triangular plots Figs. (28-30). Slocombe[19] proposed the representation of experimental points by means of arrows, the head of arrows indicate the instantaneous terpolymer composition and the tails the composition of the monomer feed. Terpolymerization of both TBTA-IA-AN and TBTMA-IA-AN systems Figs. (28 & 29), produced compositions represented by arrows pointing towards a well defined point corresponding to the ternary azeotropic compositions at 39.00:26.10:10.90 and 51.70:10.50:37.80 mole % respectively. In both cases the arrows were shorter near the ternary azeotropic point. Also, compositions obtained for TBTMA-DMI-AN system produced arrows pointing toward a point representing the ternary azeotropic composition at 00.30:66.30:33.40 mole % as shown in Fig. (30). However, compositions obtained for TBTA-DMI-AN system did not show any ternary azeotropy.

The true or ternary composition is defined as the net of monomer feed fractions $M_i = m_i$ (i= 1,2,3) where M_i and m_i are the mole fractions of monomer (i) in the feed and

terpolymer, respectively. In unitary azeotropy the amount of one of the three monomers was the same in the feed and terpolmer($M_i=m_i$), whereas in the binary azeotropy the ratio of the two monomers was the same in the monomer feed and terpolymer ($M_i/M_j=m_i/m_j$). The intersection of the unitary azeotropic lines, if any, corresponding to the true or ternary azeotropy and indicate the region of lower compositional drift . It is also interesting to determine not only the azeotropic points, but also domains in which the compositional drift is very low . These areas might be termed "pesudo azeotropic domains"(76) and are hatched on the digrams. The unitary azeotropic curves and the difference between the instantaneous terpolymer composition (dotted lines) and the monomer feed composition (full lines) for the four systems studied are illustrated in Figs. (31-34). Thus in case of TBTA-IA-AN, TBTMA-IA-AN and TBTMA-DMI-AN Figs. (31-33) The three unitary azeotropic lines intersect at one point .These points of intersection correspond to the ternary azeotropic composition yielding homogeneous terpolymer regardless of conversion. In case of TBTA-DMI-AN system Fig.(34), the three unitary azeotropic lines do not intersect indicating that there is no ternary azeotropic composition for such system. The behaviour of TBTMA-DMI-AN system Fig. (33) is even more complex, since the lines corresponding to the unitary azeotropy for TBTMA is actually constituted of two curves . Similar behaviour was reported for the unitary azeotropic curves of AN in the acrylonitrile-styrene-4-vinyl pyrrolidone system studied by Rios and

Guillot[76] . Also, Wittmer et al[77] calculated the different unitary azeotropic curves for styrene-methyl methacrylate-methacrylonitrile system and concluded that the unitary azeotropic curve of methyl methacrylate constituted of two arcs . Our calculations shows that "pseudo azeotropic domains" may be situated along unitry azeotropic lines or between arcs of these lines close enough to one another Figs (31-33) . However, it is not all always valid, that the compositional drift remains small along the unitry azeotropic lines as in case of TBTA-DMI-AN system illustrated in Fig. (34) which represent very different shape .

The lines of binary azeotropy, which then corresponding to copolymers for which the ratios of two monomers is the same in the terpolymer mixture and in the monomer mixture and carry the same information relative to true azeotrope and "pseudo azeotropic domains". When a ternary azeotropy exist the curves intersect at the same point as expected . The binary azeotropic curves and the difference between the instantaneous terpolymer composition (dotted line) and the monomer feed composition (full line) for the four systems studied are illustrated in Figs. (35-38) . Thus in case of TBTA-IA-AN, TBTMA-IA-AN and TBTMA-DMI-AN systems Figs. (35-37) the three binary lines intersect at one point which correspond to the true terpolymer azeotropic composition . In case of TBTA-DMI-AN only two binary azeotropic curves appear for M_1/M_2 and M_2/M_3 .

The points of intersection of both unitary and binary curves for the terpolymer systems TBTA-IA-AN and TBTMA-IA-AN which correspond to the true ternary azeotropic compositions of 39.00:26.10:34.90 and 51.70:10.50:37.80 mole% respectively were polymerized to several degrees of conversions covering a wide range. The avarage compositions as a function of conversion for the two terpolymer systems are illustrated in Fig.(39). The results indicate that the azeotropic terpolymer composition of both systems is constant over a wide range of conversion which prove that the monomer reactivity ratio values illustrated in Table(19) are reliable. Also, selective feed compositions corresponding to unitary azeotropy for each system were polymerized to low conversions. The results of the terpolymer composition determined from tin and nitrogen analysis for each case are illustrated in Table(20). From Table(20) it is clear that the experimental terpolymer composition are in good agreement with those obtained from theoritical calculations. These results indicate the correctness of the six monomer reactivity ratios illustrated in Table (19) for each system.

Also, selective comonomer compositions for each binary azeotropy in the terpolymer systems studied were polymerized to low conversions(less than 10%). Table (21) show the relationship between the experimental and the theoritical

terpolymer composition, and indicate that for each system the experimental values are in good agreement with values obtained from theoretical calculations. from all results it could be concluded that the free radical terpolymerization reactions of the systems studied followed the classical copolymerization theory .

The structure of the prepared terpolymers was investigated by IR spectroscopy (as Nujol mull). Fig (40) show the IR spectra of TBTA-IA-AN and TBTMA-IA-AN systems . Their infrared spectra showed a strong band at 3000 cm^{-1} due to C-H stretching vibrations, a strong band at 2240 cm^{-1} due to -C≡N of acrylonitrile and a broad band between 1750-1720 cm^{-1} characteristic for the carbonyl group of alkyl ester.

Table (18) : Polymerization of the azeotropic composition of TBTA-DMI system.

M_1-M_2	azeotropic feed composition (mole%) M_1	conversions %	Sn%	copolymer composition mole% M_1
TBTA-DMI	22.92	18.921	14.016	22.65
		38.261	13.213	22.15
		47.560	12.985	22.37
		78.492	13.087	21.63

Table(19) : Monomer reactivity ratios for terpolymerization of TBTA or TBTMA with IA , DMI and AN

M_1 - M_2 - M_3	r_{12}	r_{21}	r_{23}	r_{32}	r_{13}	r_{31}
TBTA - IA - AN	1.068	0.070	1.750	0.250	0.240	0.997
TBTA -DMI - AN	0.942	0.805	0.630	0.260	0.240	0.997
TBTMA- IA - AN	2.157	0.006	1.750	0.250	0.471	0.474
TBTMA-DMI - AN	1.242	0.869	0.630	0.260	0.471	0.474

The values of r_{12}, r_{21}, r_{13}, and r_{31} are determined in the present work (Table 13 &18), while the values of r_{23} and r_{32} are from literature[71] .

Table(20): Terpolymerization of selective unitry azeotropic compositions.

M_1 -M_2 -M_3	Feed composition mole%			Conversion%			unity azeotropy	Instantaneous terpolymer composition mole %					
								Theoretical					
	M_1	M_2	M_3	Sn%	N%			M_1	M_2	M_3	M_1	M_2	M_3
TBTMA-IA -AN	60.00	18.70	21.30	5.64	37.61	1.41	TBTMA	60.00	13.65	26.32	59.25	15.02	25.72
	32.30	18.30	49.40	7.20	24.16	2.80	IA	41.48	18.30	40.21	40.20	20.19	39.61
	30.20	42.10	27.70	6.92	24.52	1.64	AN	45.66	26.64	27.70	45.76	28.22	26.09
TBTMA-DMI-AN	14.00	75.80	10.10	5.73	10.06	6.97	TBTMA	14.10	71.70	14.20	15.02	72.67	12.31
	20.00	17.20	62.80	6.95	15.98	5.16	TBTMA	20.00	25.78	54.22	19.37	27.47	53.17
	25.70	45.50	28.80	8.64	15.24	2.47	DMI	22.50	45.50	31.95	22.31	46.97	30.72
	27.30	33.20	39.50	7.33	16.75	3.19	AN	23.88	36.62	39.50	23.82	37.62	38.56
TBTA -IA -AN	35.60	17.80	46.60	4.69	23.60	3.16	TBTA	35.60	22.50	41.85	36.05	23.00	41.00
	22.80	29.50	47.70	8.49	21.65	2.80	IA	32.70	29.50	37.80	32.25	32.25	35.43
	25.90	45.50	28.60	5.74	23.02	2.00	AN	37.43	33.97	28.60	37.92	34.09	27.99
TBTA -DMI-AN	6.40	83.10	10.50	6.28	4.69	1.23	TBTA	6.40	78.91	14.69	6.15	80.10	13.75
	25.60	51.50	22.90	4.92	12.99	2.37	DMI	19.55	51.50	28.95	18.03	54.01	27.95
	44.30	43.10	12.60	7.86	19.89	1.40	DMI	35.36	43.10	21.54	34.49	44.83	20.68
	26.40	29.10	44.50	5.76	14.02	4.11	AN	17.72	37.78	44.50	17.41	38.67	43.41

Table (21) : Terpolymerization of selective binary azeotropic compositions.

M_1 -M_2 -M_3	Feed composition mole%			Conversion%	Sn%	N%	Binary azeotropy	Instantaneous terpolymer composition (mole%)					
								Theoretical			Found		
	M_1	M_2	M_3					M_1	M_2	M_3	M_1	M_2	M_3
TBTMA-IA -AN	29.90	10.60	59.70	9.42	24.46	3.45	TBTMA/IA	38.68	13.81	47.51	38.98	14.28	46.80
	42.90	40.40	16.70	5.97	26.41	1.15	TBTMA/AN	54.87	23.77	21.36	55.54	23.90	20.56
	25.90	30.10	44.00	8.46	22.91	2.43	IA /AN	40.39	24.21	35.40	37.81	28.10	34.09
TBTMA-DMI-AN	10.40	73.10	16.50	6.04	11.89	4.30	TBTMA/DMI	9.87	69.40	20.72	9.14	72.30	18.55
	15.00	34.20	50.80	5.21	16.12	2.85	TBTMA/AN	13.43	41.06	45.50	14.28	41.82	43.90
	26.20	39.40	34.40	9.22	25.59	2.20	DMI /AN	22.80	41.20	35.98	23.27	41.75	34.97
TBTA -IA -AN	52.90	27.90	19.20	6.67	25.50	1.69	TBTA /IA	47.65	25.13	27.23	46.59	27.18	26.23
	38.60	14.00	47.40	9.25	24.12	3.35	TBTA /AN	36.02	19.79	44.22	36.82	19.77	43.41
	16.50	43.60	39.90	5.99	21.64	2.49	IA /AN	32.30	35.35	32.34	32.98	34.79	32.22
TBTA -DMI-AN	16.00	73.60	10.40	8.29	10.14	1.19	TBTA /DMI	15.08	69.24	15.67	14.71	70.69	14.60
	20.40	45.80	33.80	7.62	11.67	3.29	DMI /AN	14.62	49.13	36.25	14.79	49.74	35.46
	60.40	13.30	26.30	7.10	24.82	2.60	DMI /AN	41.93	19.50	38.57	42.75	19.27	37.98

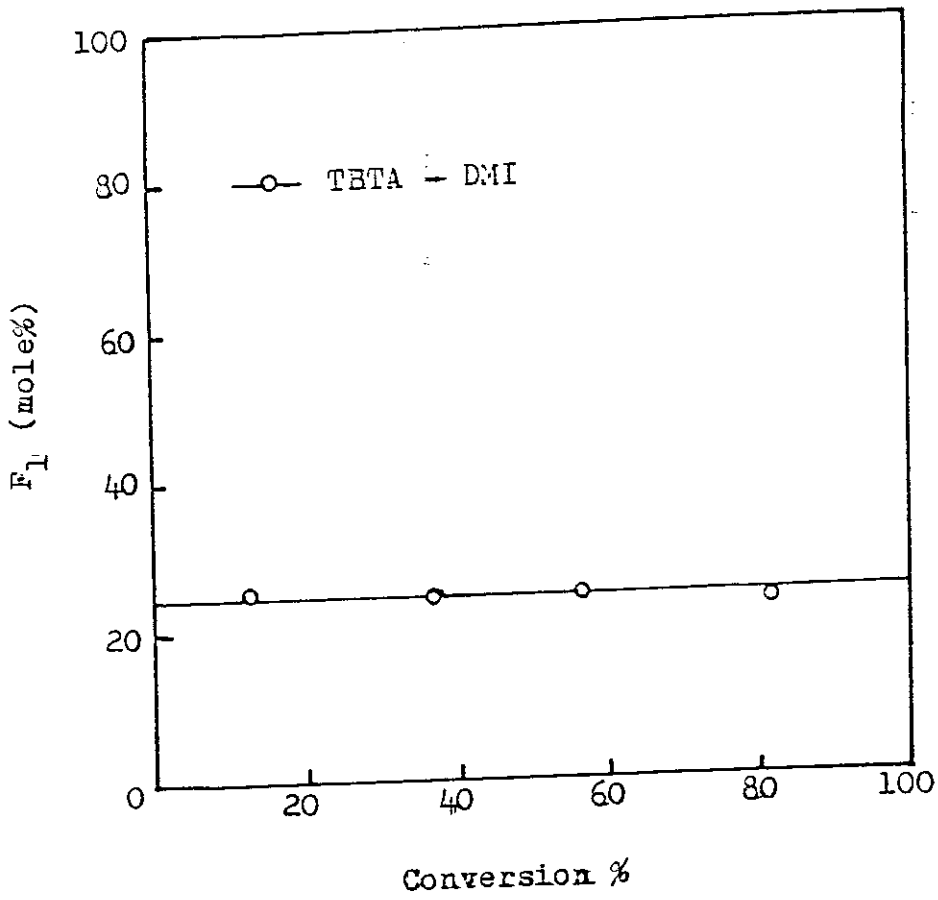

Fig. (27) : F_1 as a function of conversion for azeotrpic copolymerization of TBTA - DMI system .

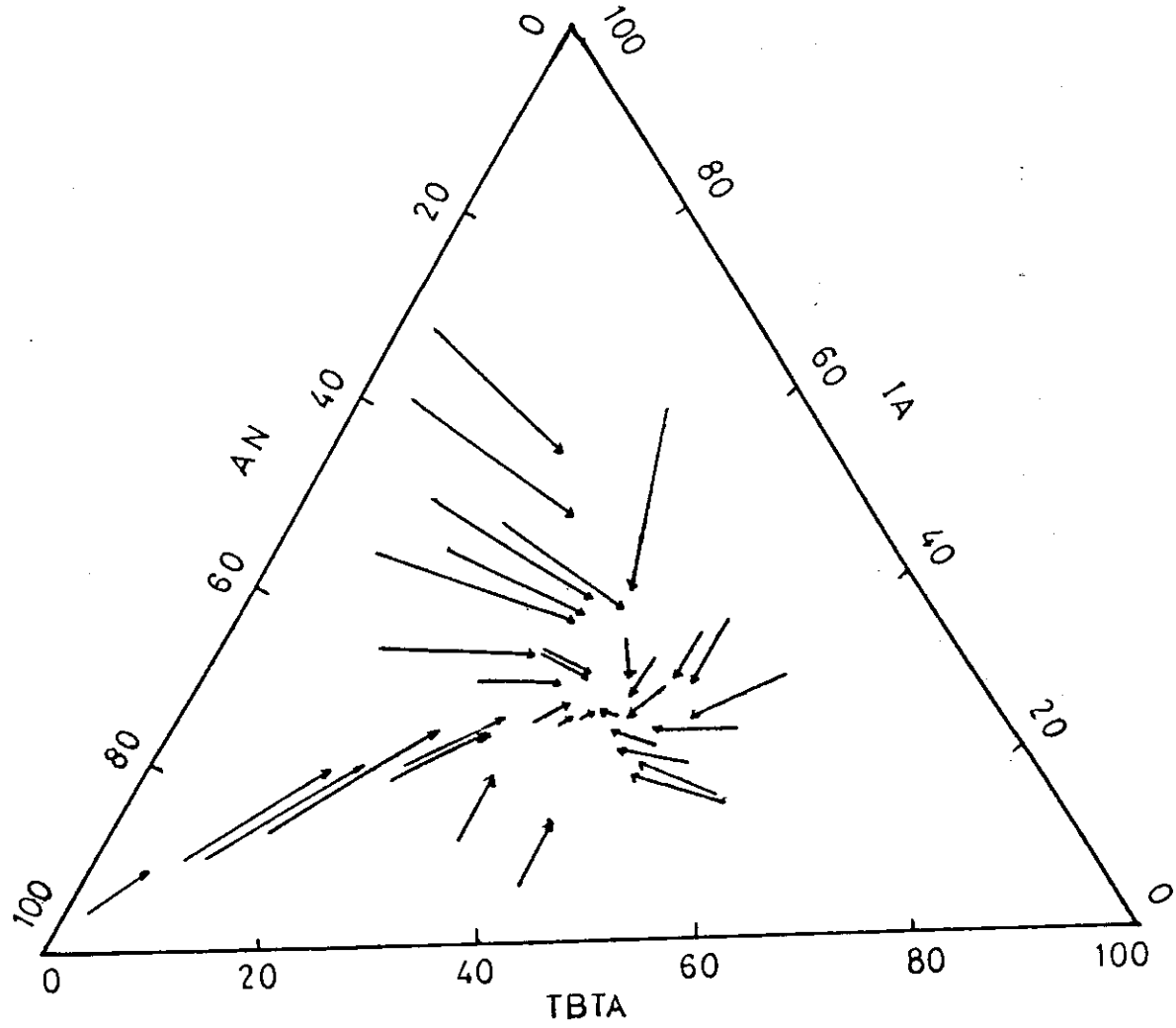

Fig. (28): Instantaneous terpolymer composition as a function of monomer composition for the system TBTA-IA-AN

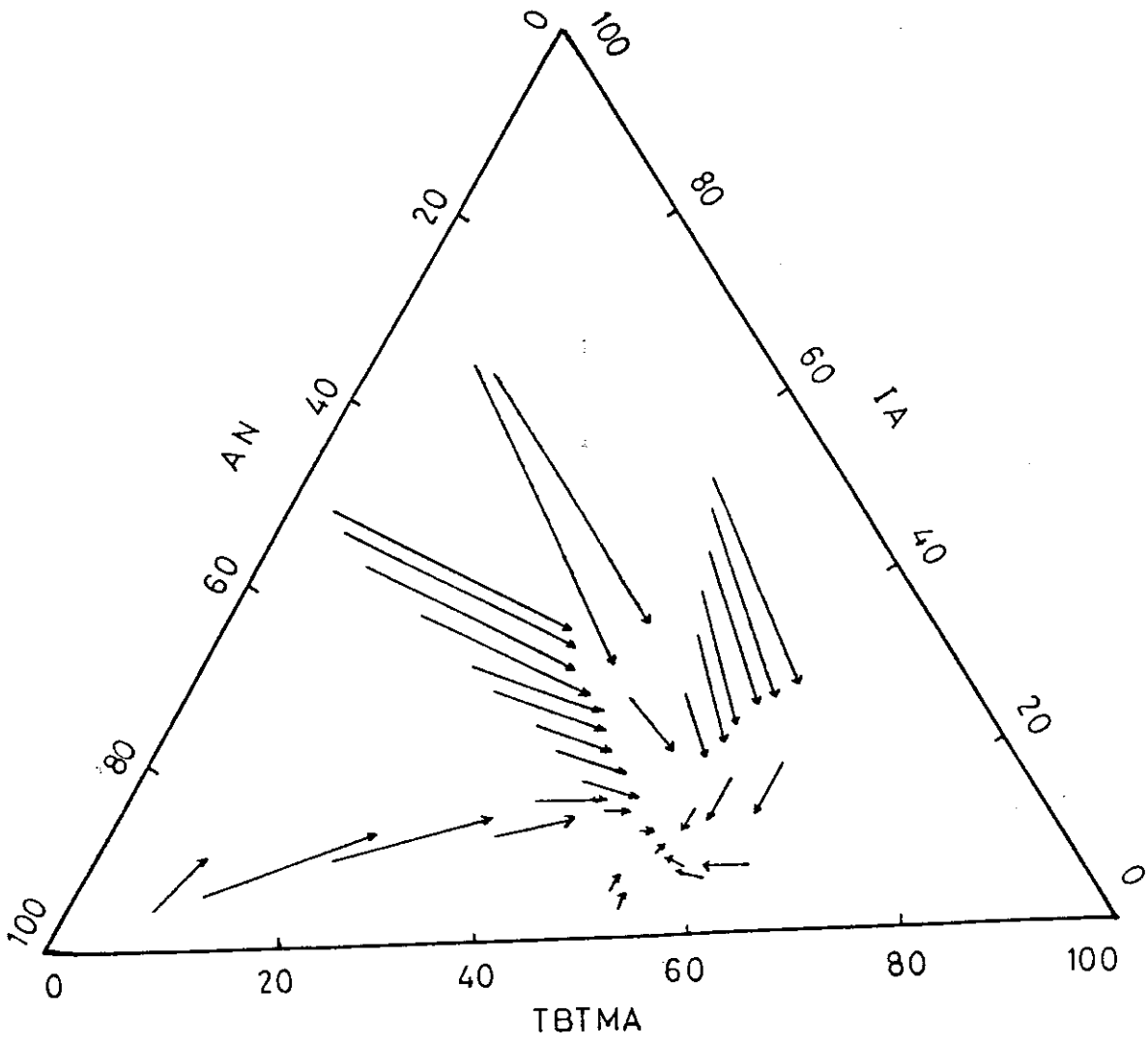

Fig. (29): Instantaneous terpolymer composition as a function of monomer composition for the system TBTMA-IA-AN

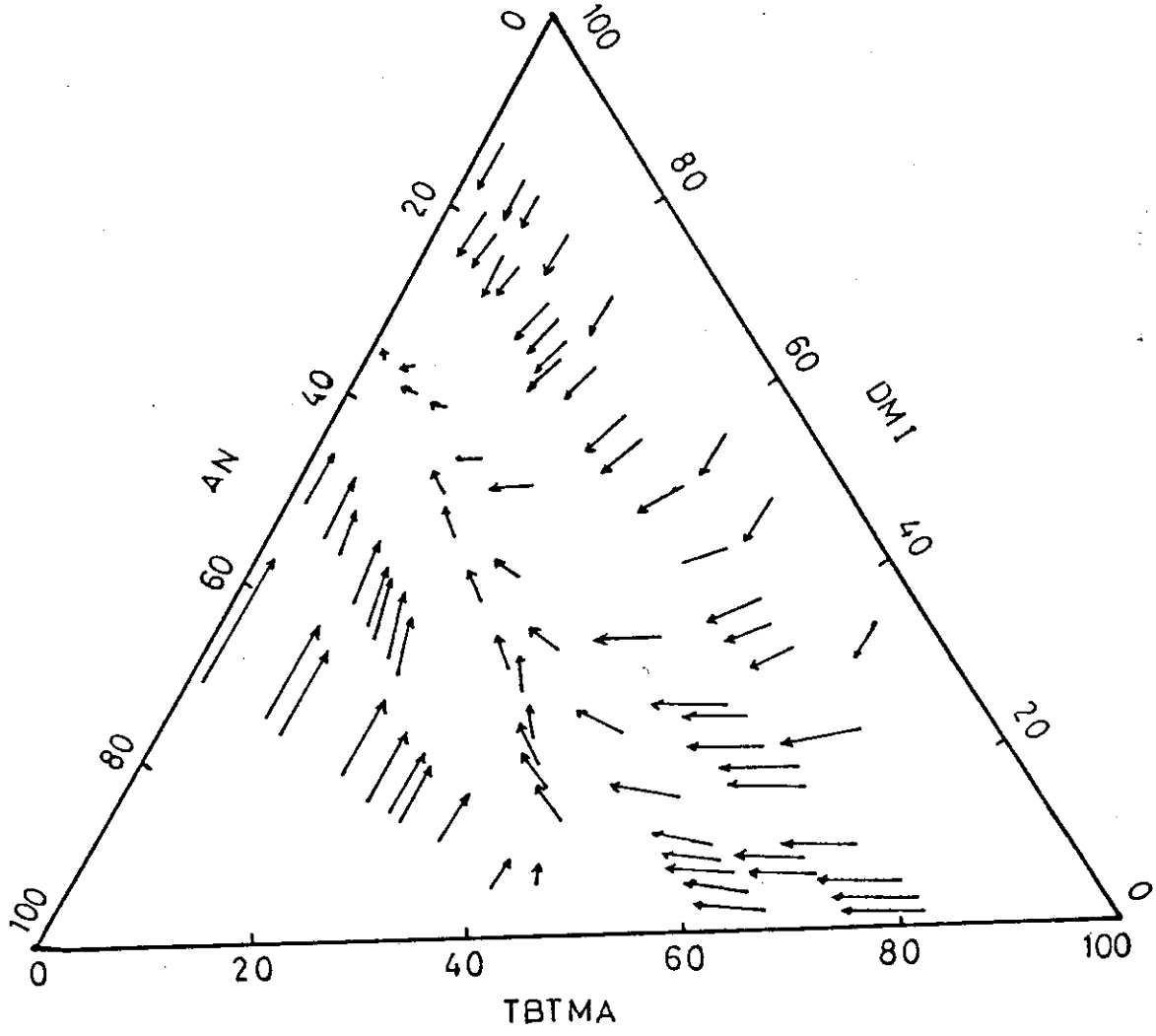

Fig. (30): Instantaneous terpolymer composition as a function of monomer composition for the system TBTMA-DMI-AN

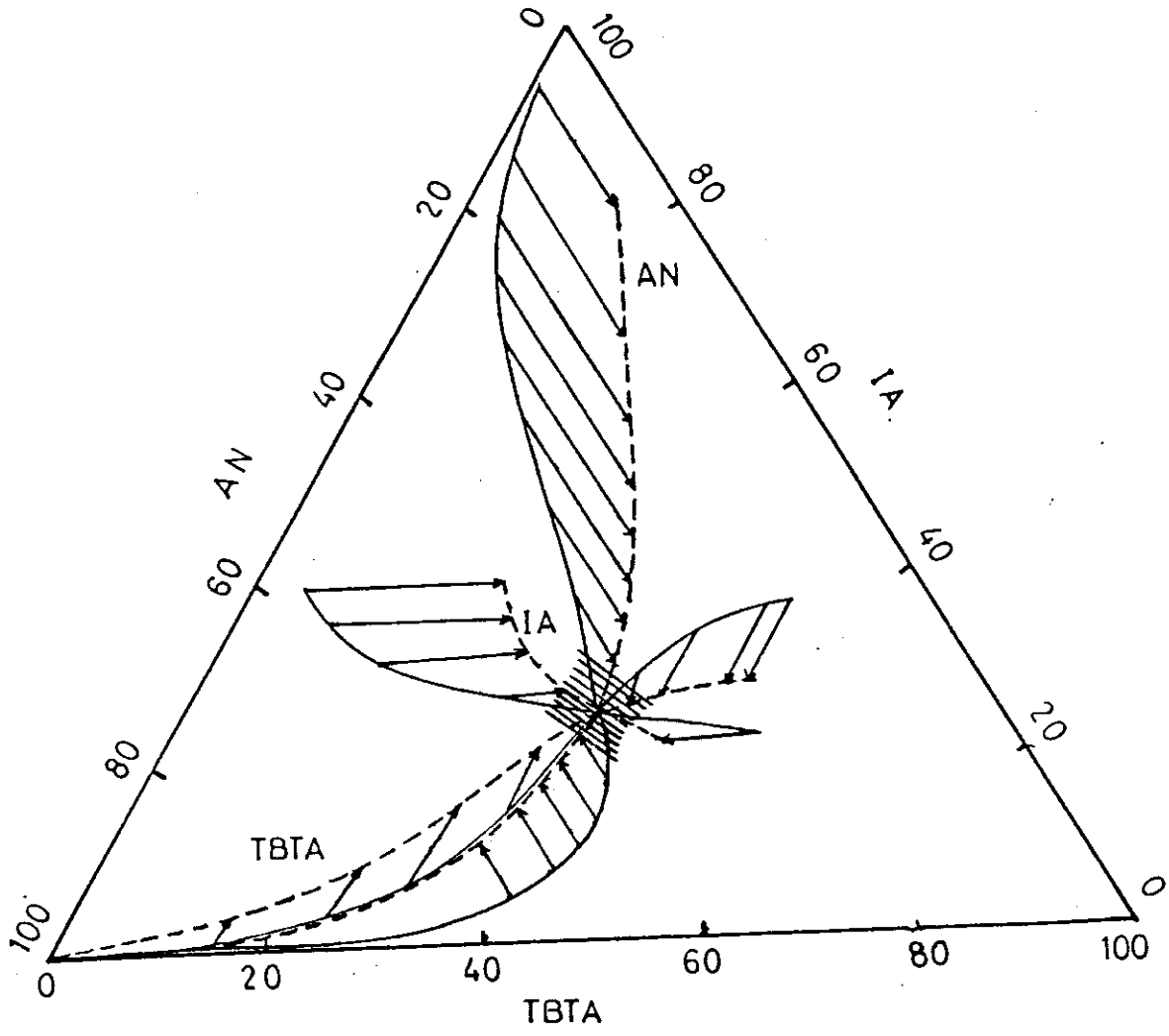

Fig. (31): The unitry azeotropic lines for the system TBTA-IA-AN: (——) monomer composition, (-----) terpolymer composition and (hatched area) "pseudo-azeotropic" domains.

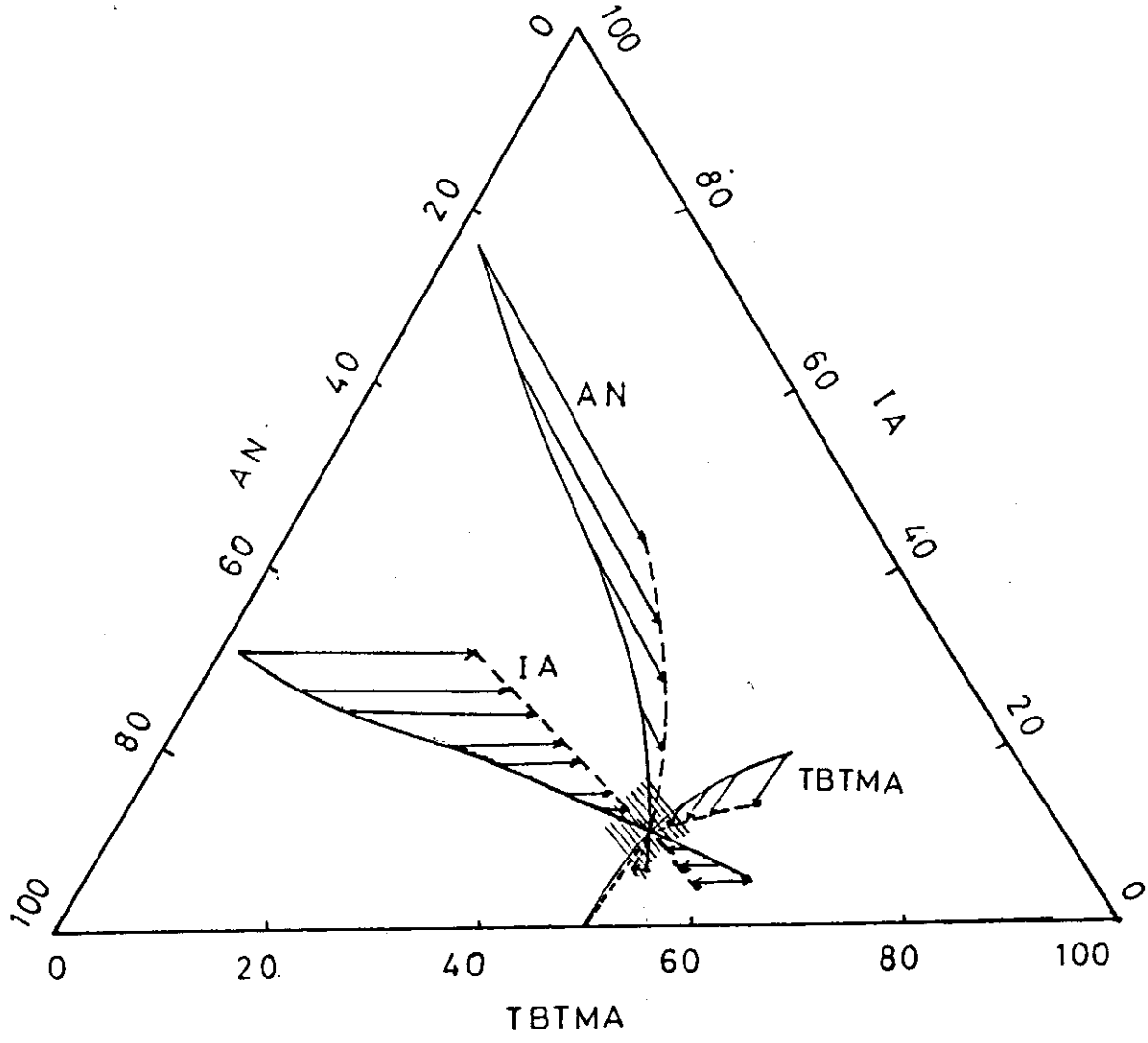

Fig. (32): The unitry azeotropic lines for the system TBTMA-IA-AN: (——) monomer composition, (----) terpolymer composition and (hatched area) "pseudo-azeotropic" domains.

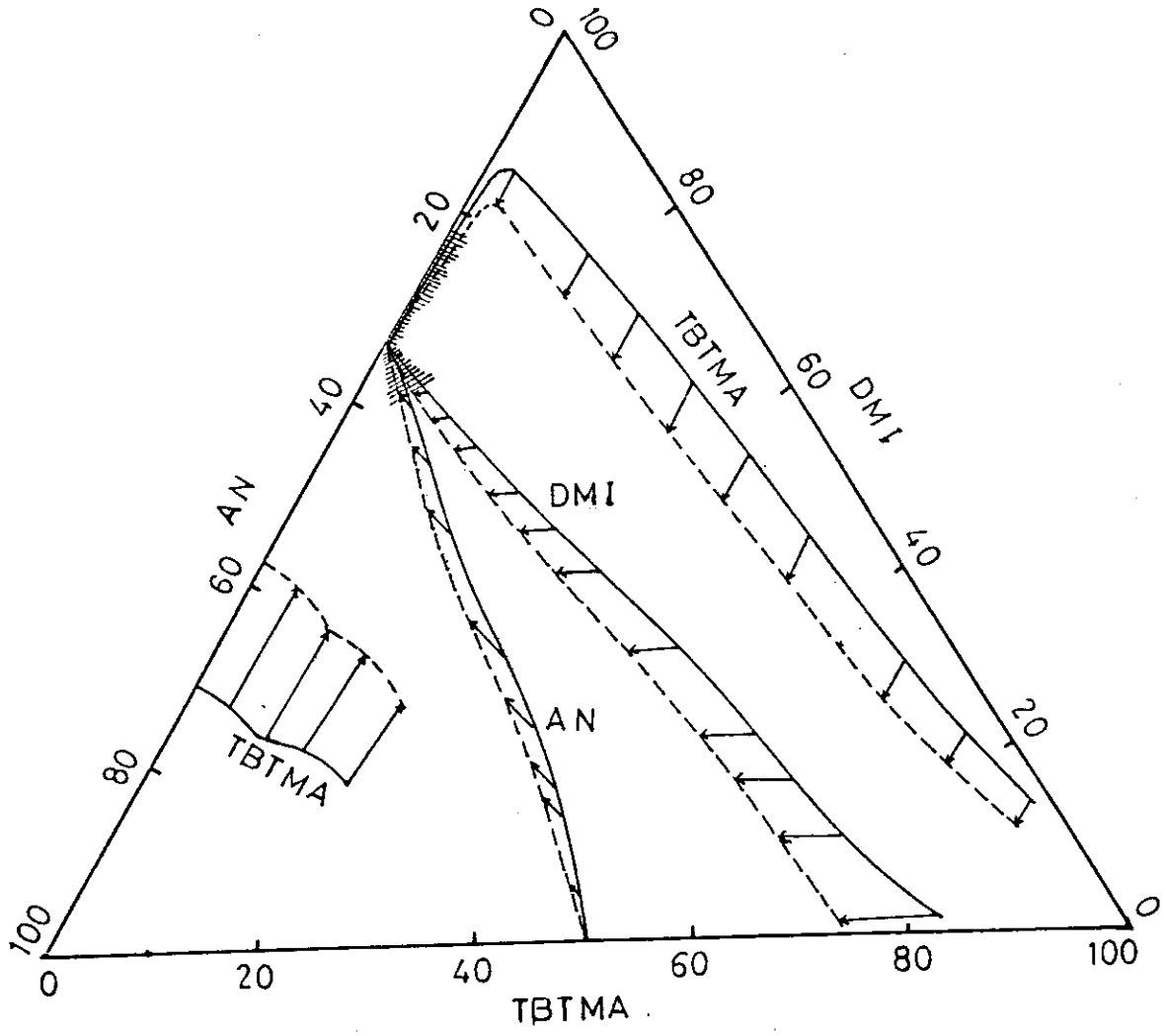

Fig. (33): The unitry azeotropic lines for the system TBTMA-DMI-AN:(——) monomer composition, (---) terpolymer composition and (hatched area) "pseudo-azeotropic" domains .

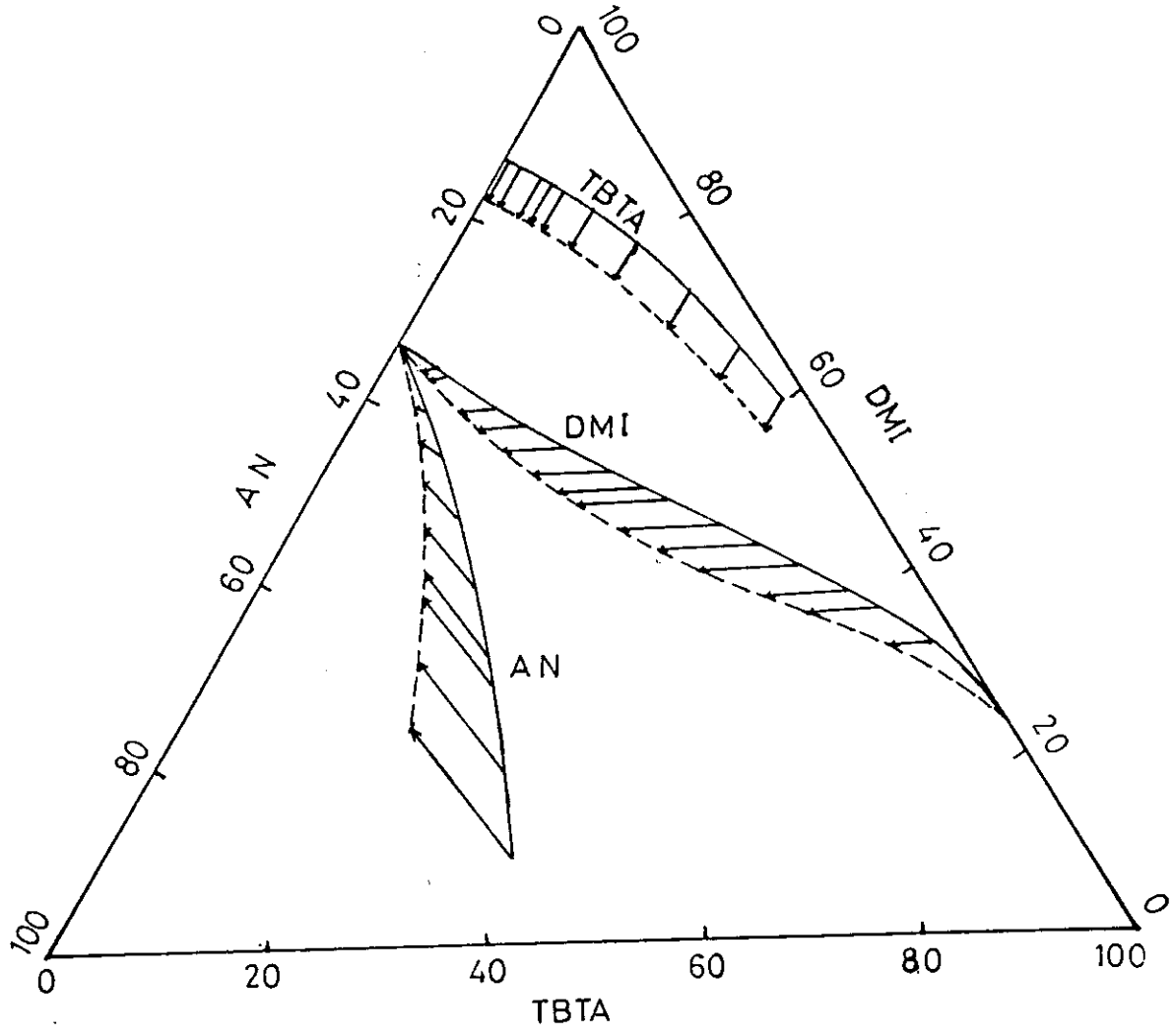

Fig. (34) : The unitry azeotropic lines for the system TBTA-DMI-AN: (——) monomer composition, (----) terpolymer composition

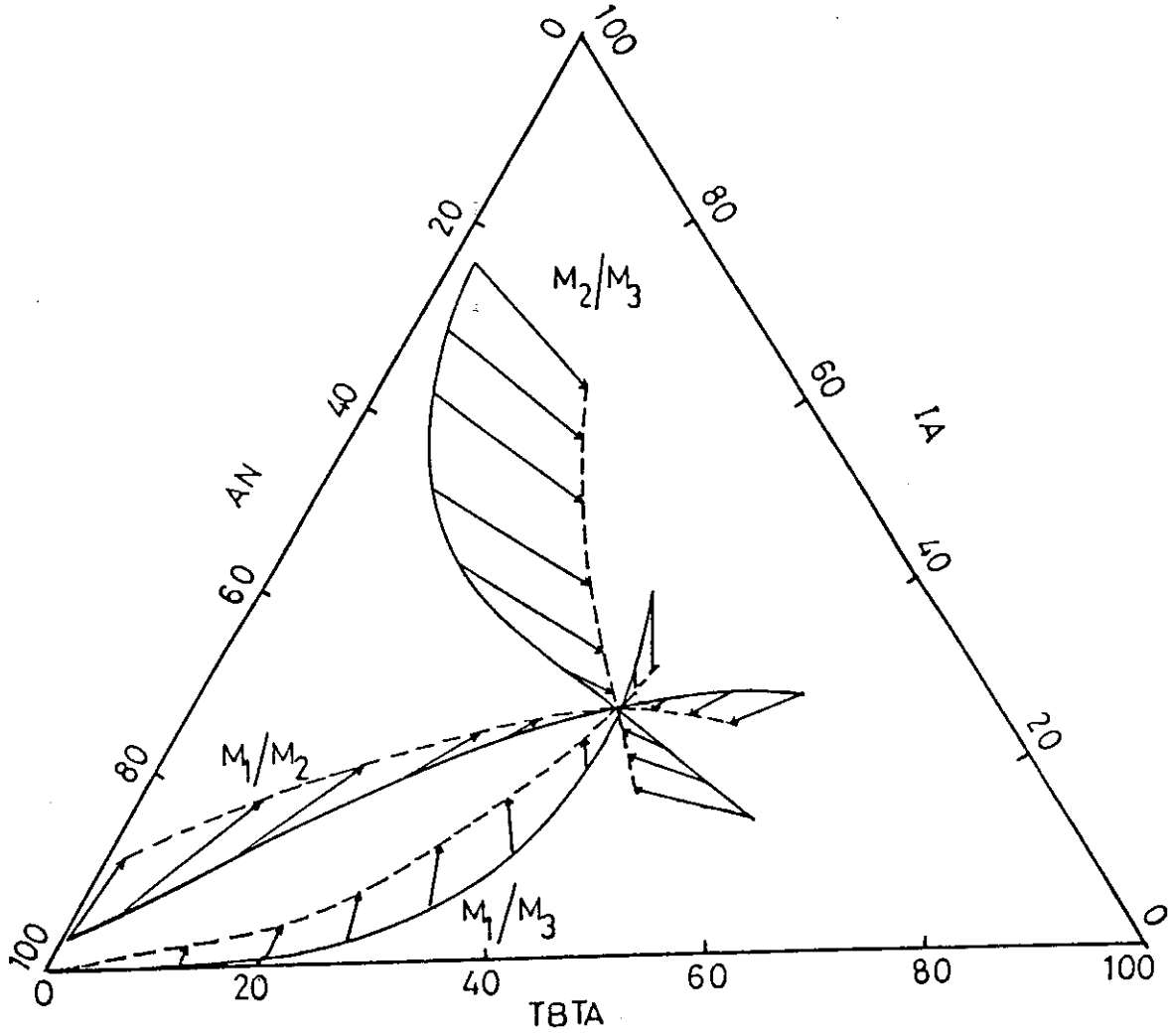

Fig. (35): The binary azeotropic lines for the system TBTA-IA-AN: (——) monomer composition and (---) terpolymer composition.

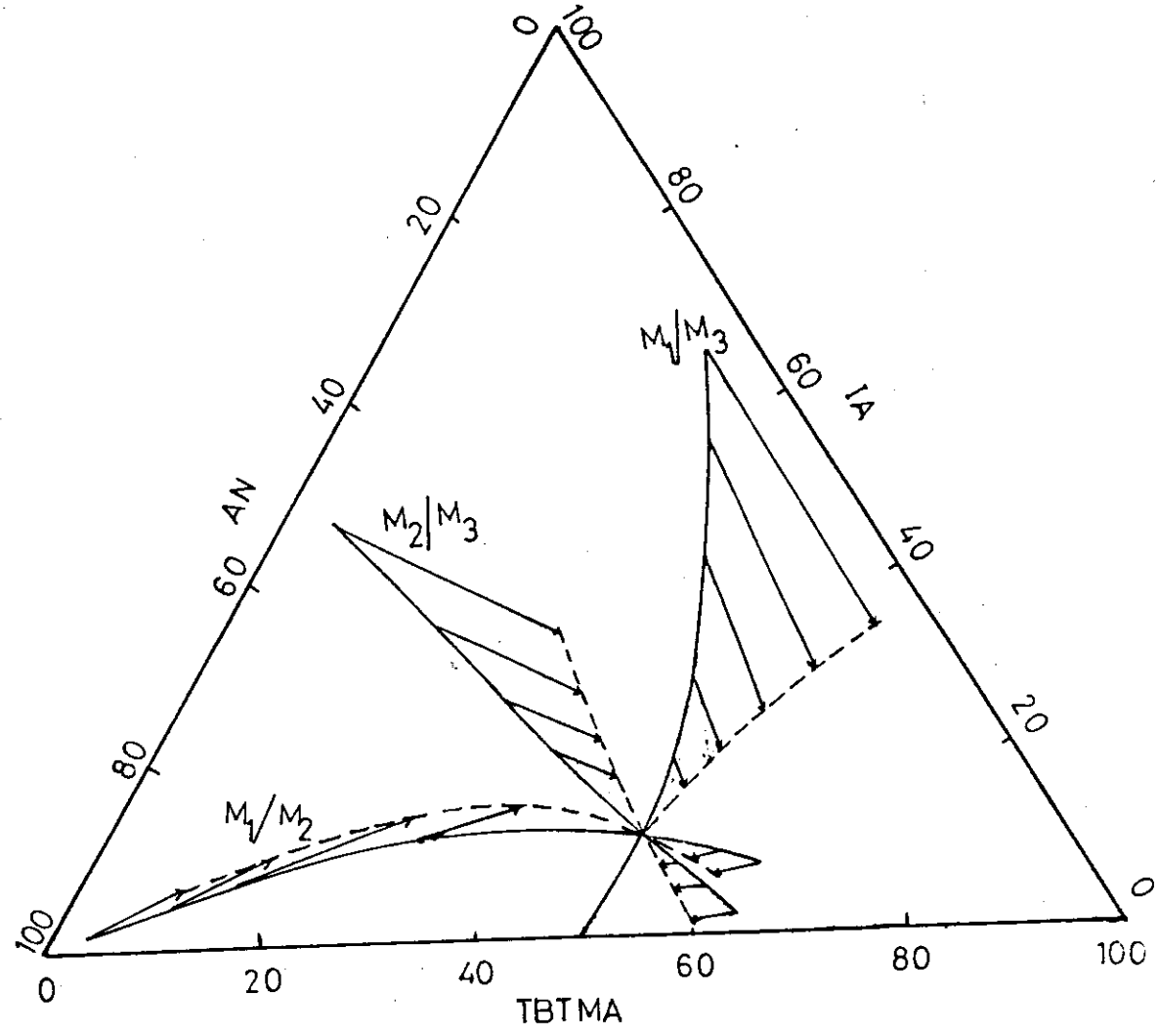

Fig. (36): The binary azeotropic lines for the system TBTMA-IA-AN: (——) monomer composition and (– – –) terpolymer composition.

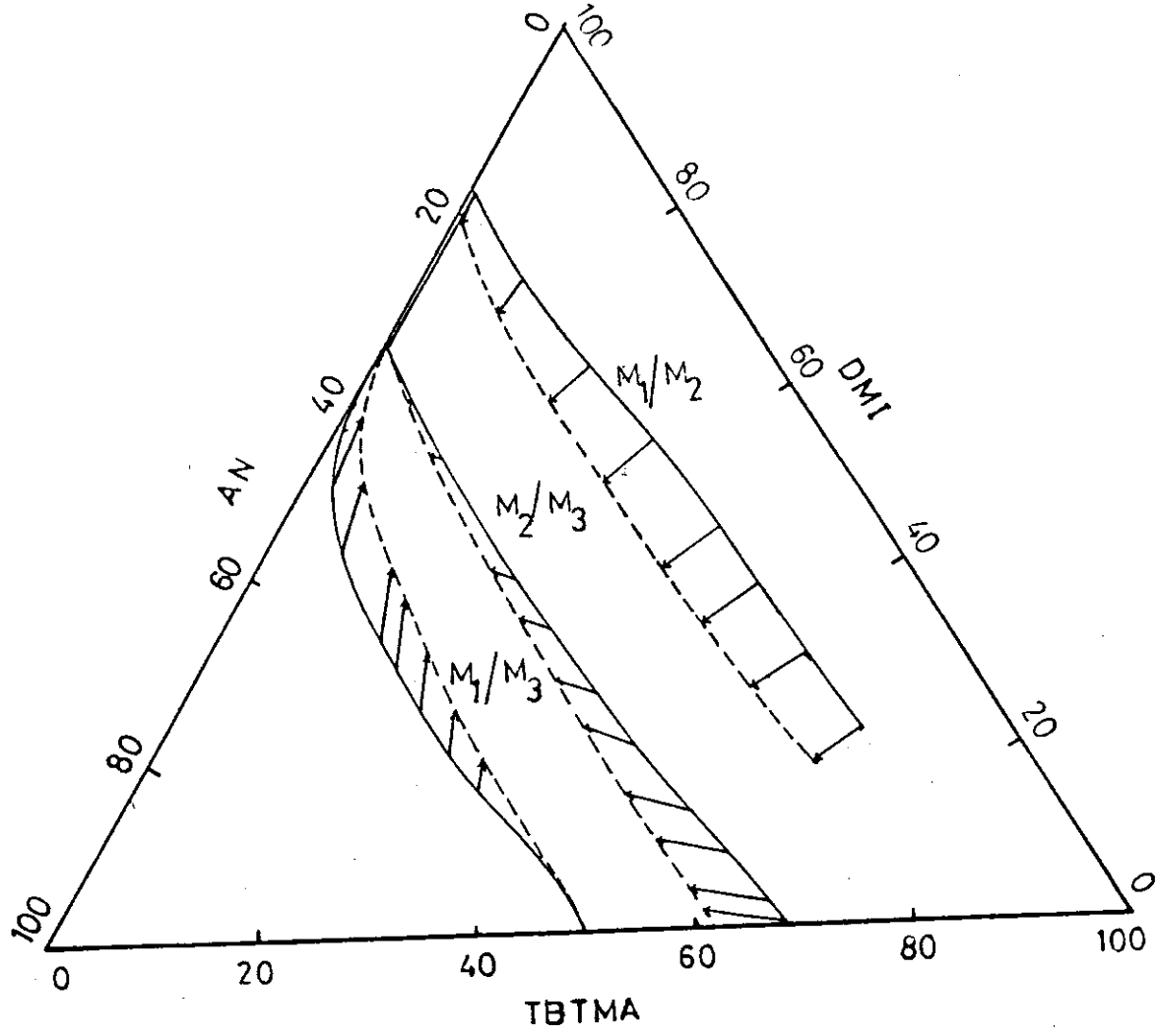

Fig. (37): The binary azeotropic lines for the system TBTMA-DMI-AN: (——) monomer composition and (----) terpolymer composition.

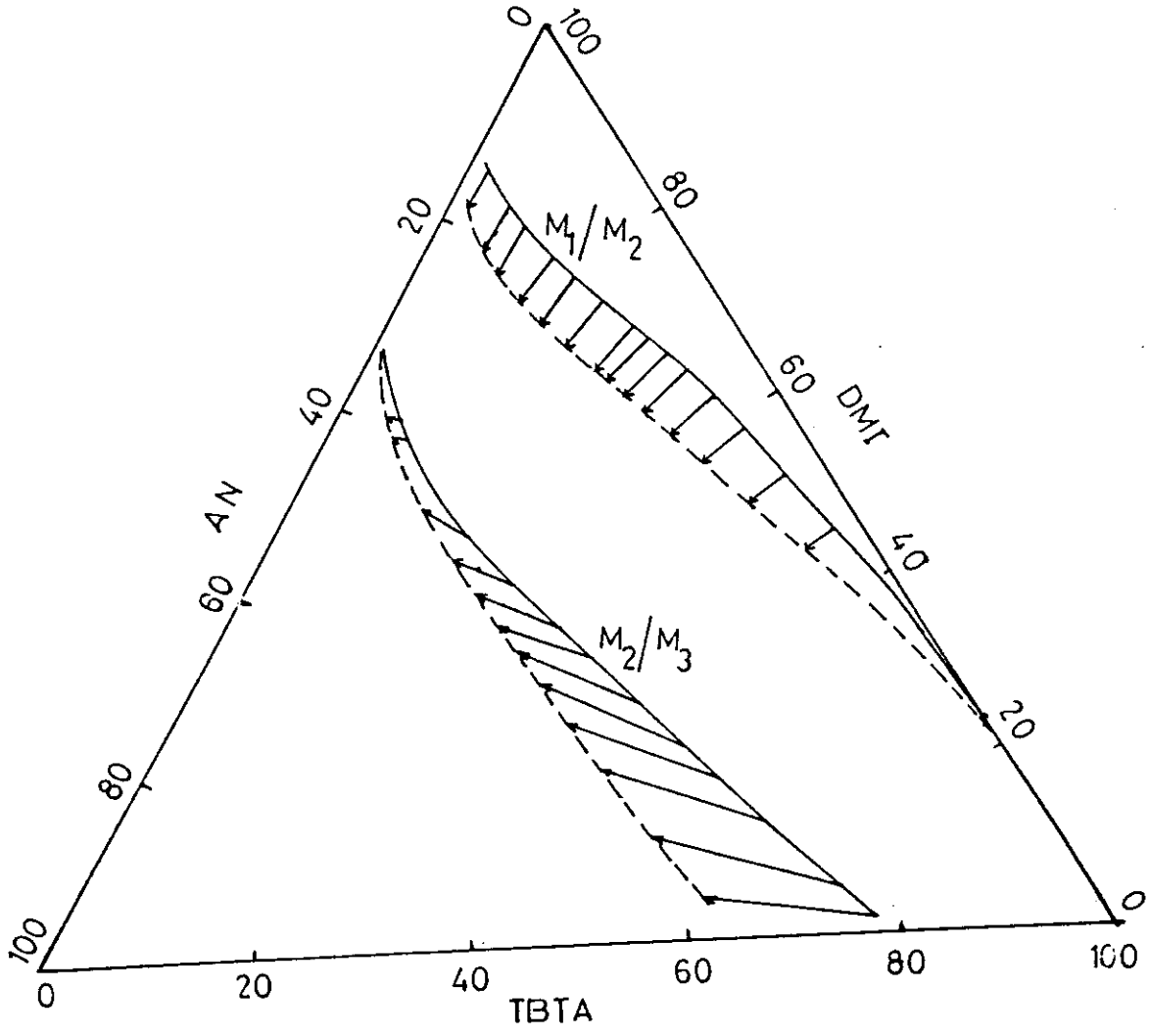

Fig. (38): The binary azeotropic lines for the system TBTA-DMI-AN: (——) monomer composition and (---) terpolymer composition.

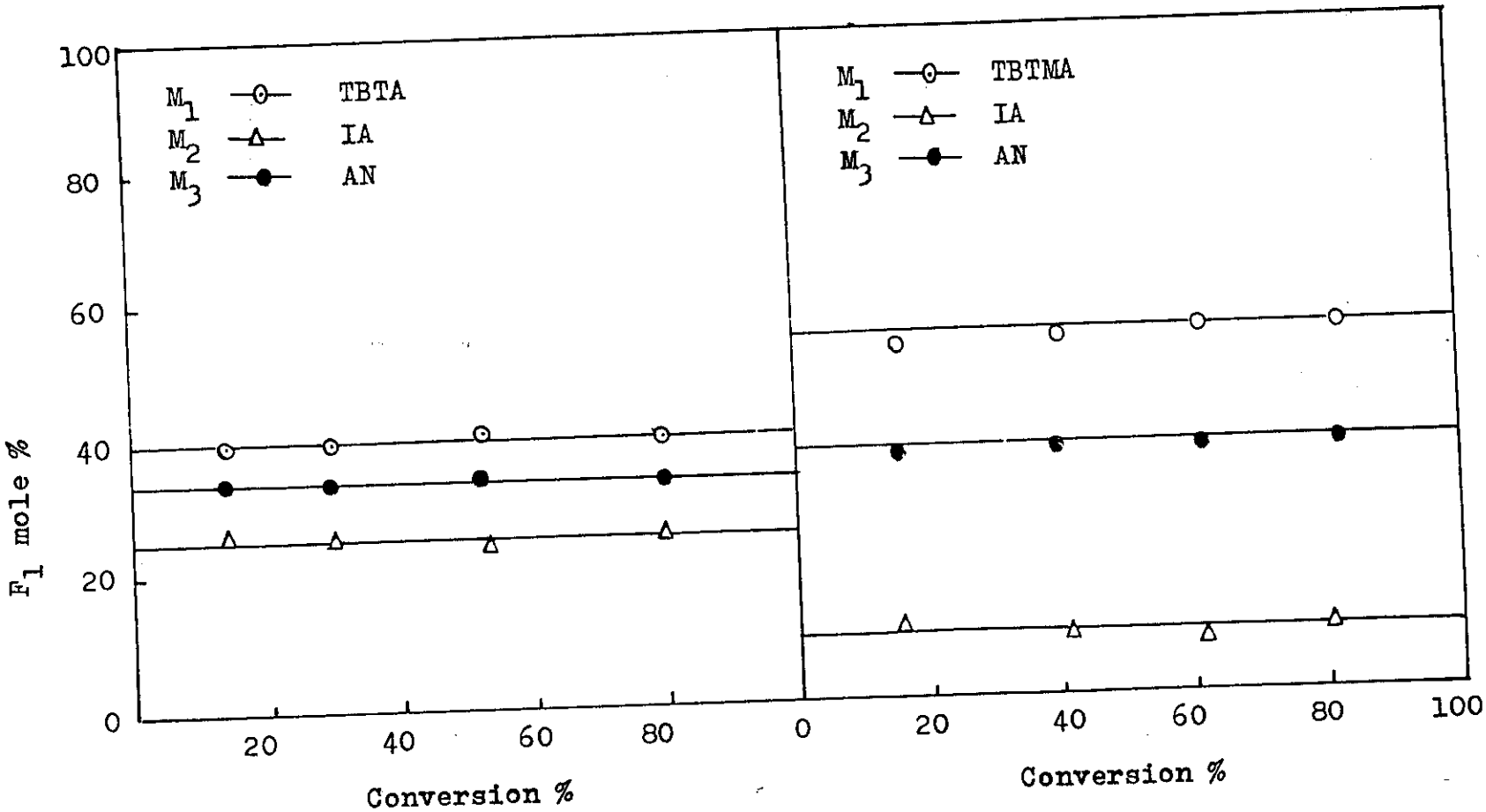

Fig. (39): Variation of average terpolymer composition with conversion for the systems TBTA-IA-AN and TBTMA-IA-AN, lines represent predicted values and (0,Δ,●) represemt values from nitrogen and tin analysis.

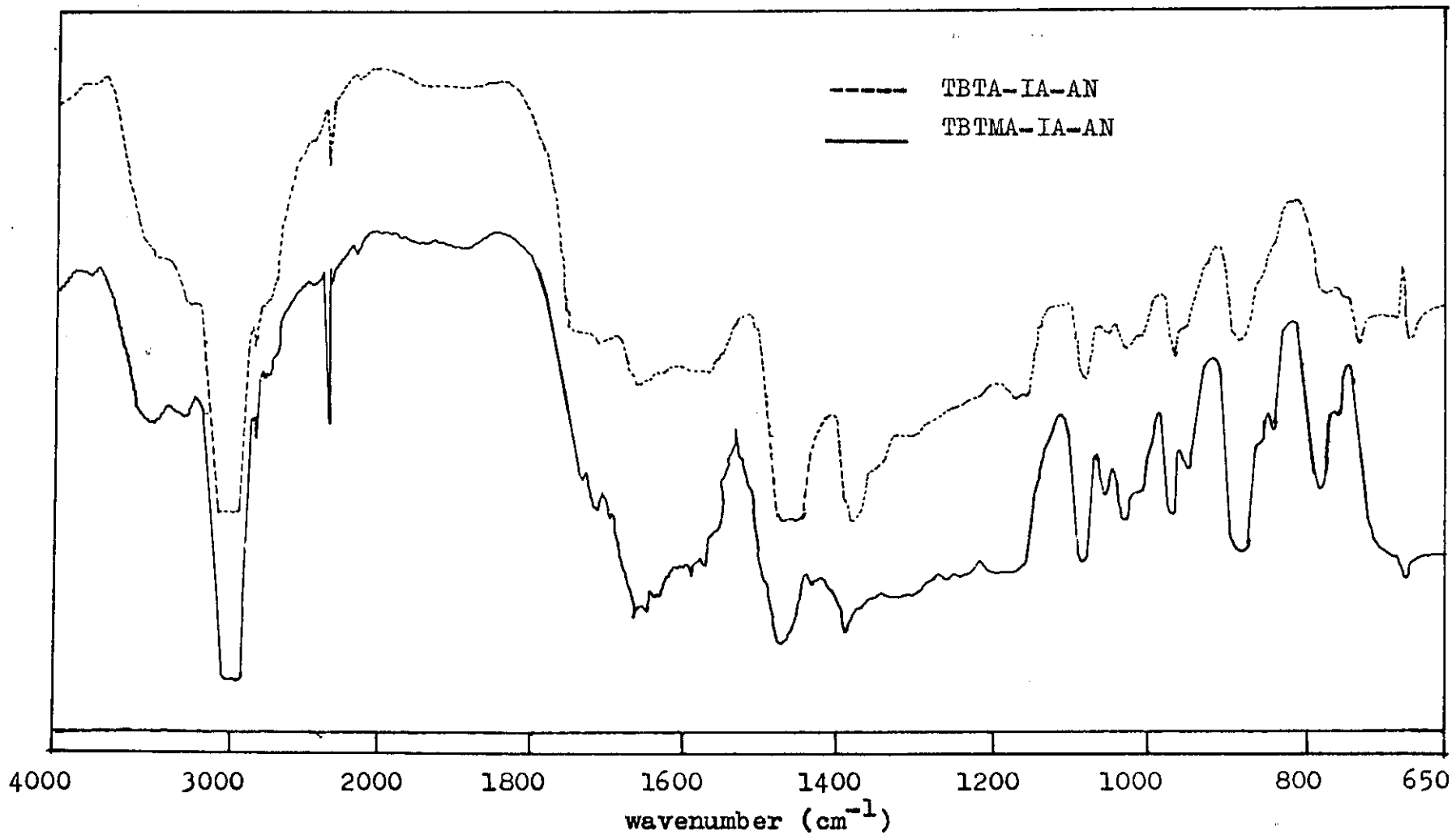

Fig. (40): The IR spectra of the azeotropic composition of terpolymers: (——) TBTMA-IA-AN and (-----) TBTA-IA-AN.

2- Ternary Copolymerization Reactions of p-Acryloyloxy-tri-n-butyltin Benzoate with Acrylonitrile and Alkyl acrylates, Methyl Methacrylate or Styrene.

Five ternary copolymerization systems involving p-acryloyloxy-tri-n-butyltin benzoate with acrylonitrile and alkyl acrylates, methyl methacrylate or styrene were prepared by solution polymerization in DMF(1.5 mole/L) in presence of 1 mole % AIBN initiator at 70 °C.

The terpolymers prepared in the present study can be represented by the following general formula:

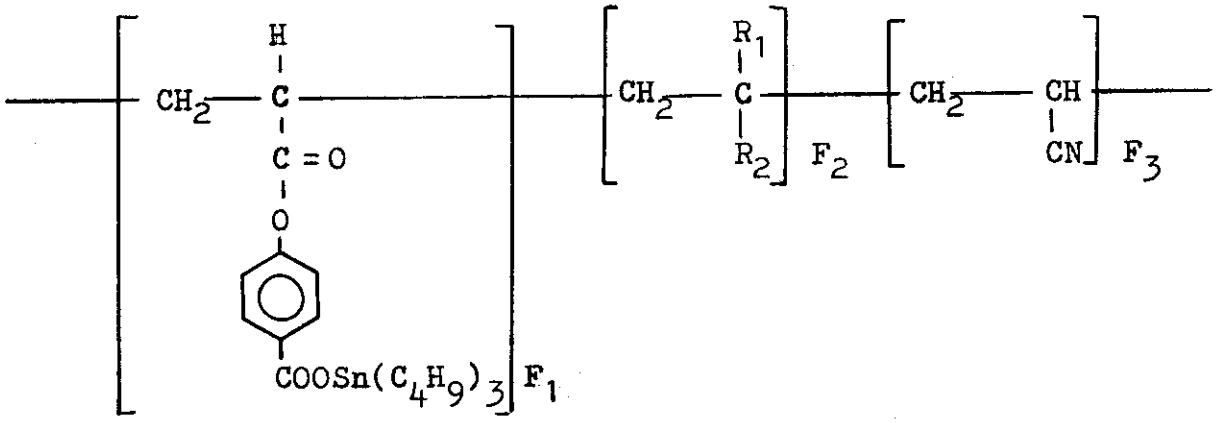

where :

M_2	R_1	R_2
MA	-H	$-COOCH_3$
EA	-H	$-COOC_2H_5$
BA	-H	$-COOC_4H_9$
MMA	$-CH_3$	$-COOCH_3$
ST	-H	$-C_6H_5$

The five terpolymers studied were polymerized to low conversions (less than 10%) and the terpolymers produced were analyzed for tin and nitrogen. From the tin content and nitrogen content of each sample, the terpolymer composition of each system could be calculated. The initially formed terpolymer composition of each system could be calculated by using the terpolymer composition equation in the form proposed by Khan and Horowitz[26] page (28). The prediction of the terpolymer composition requires the monomer reactivity ratios of the individual two-component systems. Thus, the reactivity ratios used for calculating the terpolymer composition of each system, determined in the present study from the binary copolymerization reaction of ABTB-MA, ABTB-EA, ABTB-BA, ABTB-MMA, ABTB-ST and ABTB-AN systems Table (7) as well as the literature values[71] for the binary systems MA-AN, EA-AN, BA-AN, MMA-AN and ST-AN systems are illustrated in Table (22). The relation between monomer composition in the feed and instantaneous terpolymer composition is determined for each case and compositions obtained for all systems studied did not show any azeotropic composition. Fig. (41) shows the relation between monomer composition in the feed and instantaneous terpolymer composition for ABTB-ST-AN system as an example.

All posible compositions calculated by a computer program as previously described screened and different azeotropic curves of unitary, binary and ternary azeotropies can be graphically plotted. The unitary azeotropic curves

and the difference between the instantaneous terpolymer composition for the five systems studied are illustrated in Figs (42-46). The behaviour of ABTB-MA-AN, ABTB-EA-AN, ABTB-BA-AN and ABTB-MMA-AN terpolymer systems, Figs (42-45), show only one unitry azeotropic lines corresponding to each of MA, EA, BA and AN respectively. However, the behaviour of ABTB-ST-AN system Fig. (46) show two unitary azeotropic curves corresponding to ST and AN monomers.

The binary azeotropic curves for the five terpolymer systems were also investigated. Figs (47-49) show the curves of binary azeotropic lines for ABTB-BA-AN, ABTB-MMA-AN and ABTB-ST-AN systems and indicate that only one binary azeotropic curves for BA/AN, MMA/AN and ST/AN respectively, for each case. On the other hand, no binary azeotropic lines appeared in case of ABTB-MA-AN and ABTB-EA-AN systems.

Selective feed compositions corresponding to unitary azeotropy for each system were polymerized to low conversion and the terpolymer composition of each sample was determined from tin and nitrogen analysis and the results are illustrated in Table (23). The results illustrated in Table (23) show good agreement between the theoretical values and experimental ones.

Also, selective comonomer compositions for each binary azeotropy for ABTB-BA-AN, ABTB-MMA-AN and ABTB-ST-AN terpolymer systems were polymerized to low conversions (less than 10 %). Table (24) show the relationship between

the experimental and the theoretical terpolymer compositions, and indicate that for each system the experimental values are in good agreement with values obtained from theoretical calculations. These results indicate the relibility of the monomer reactivity ratio values used for each binary system.

The structure of the prepared terpolymers was also investigated by IR spectroscopy (as Nujol mull). Fig. (50) shows the IR spectrum of ABTB-ST-AN terpolymer system (as an example). Its IR spectrum shows a strong band at 3000 cm^{-1} due to C-H stretching vibrations and a strong band at 2240 cm^{-1} due to the nitrile group. Also, the IR spectrum shows a broad band between 1760-1710 cm^{-1} due to the carbonyl group of alkyl ester and a strong band at 715 cm^{-1} characteristic for the four adjacent hydrogen atoms of benzene ring.

Table(22): Monomer reactivity ratios for terpolymerization of ABTB with MA , EA , BA , MMA , ST and AN

M_1 -M_2 -M_3	r_{12}	r_{21}	r_{23}	r_{32}	r_{13}	r_{31}
ABTB-MA -AN	0.080	1.046	0.670	1.260	0.007	2.853
ABTB-EA -AN	0.039	1.585	0.930	1.120	0.007	2.853
ABTB-BA -AN	0.019	2.076	0.890	1.200	0.007	2.853
ABTB-MMA-AN	0.150	1.710	1.090	0.150	0.007	2.853
ABTB-ST -AN	0.113	1.339	0.410	0.030	0.007	2.853

The values of r_{12}, r_{21}, r_{13}, and r_{31} are determined in the present work Table (7),while the values of r_{23} and r_{32} are from literature[71] .

Table (23): Terpolymerization of selective unitry azeotropic compositions.

M_1 - M_2-M_3	Feed composition mole%			Conversion%	Sn%	N%	unity azeotropy	Instantaneous terpolymer composition (mole%)					
								Theoretical			Found		
	M_1	M_2	M_3					M_1	M_2	M_3	M_1	M_2	M_3
ABTB-ST -AN	13.90	62.70	23.40	5.22	5.45	4.18	ST	5.09	62.70	32.70	4.87	63.39	31.74
	23.60	65.70	10.70	4.82	9.46	2.39	ST	10.79	65.70	23.51	10.52	66.93	22.55
	20.90	37.80	41.30	8.25	6.50	5.44	AN	5.62	53.08	41.30	5.73	53.52	40.75
	37.90	17.50	44.60	7.66	9.40	5.21	AN	9.40	46.00	44.60	9.21	47.34	43.45
ABTB-BA -AN	16.40	43.90	39.70	7.25	6.98	5.62	BA	7.05	43.90	49.05	6.87	46.13	47.00
	28.70	12.40	58.90	5.84	12.41	9.43	BA	11.54	12.40	76.05	11.74	12.41	75.85
ABTB-MMA-AN	17.90	55.30	26.80	5.27	8.13	8.13	AN	8.01	65.19	26.80	8.12	66.17	25.71
	32.40	27.80	39.90	8.15	11.73	4.17	AN	12.77	47.43	39.80	12.91	48.14	38.95
ABTB-EA -AN	15.00	57.00	28.00	3.32	7.90	4.18	EA	7.81	57.01	35.18	7.49	58.85	35.65
	25.00	21.00	54.00	6.84	10.92	8.52	EA	10.85	21.03	68.12	11.00	26.61	68.39
ABTB-MA -AN	55.10	32.50	12.40	8.33	18.16	2.62	MA	29.88	32.50	37.62	28.61	36.34	35.05
	60.00	10.00	30.00	6.74	18.75	4.79	MA	27.71	10.00	62.24	27.64	12.41	59.95

Table (24) : Terpolymerization of selective Binary azeotropic compositions.

M_1- M_2-M_3	Feed composition mole%			Conversion%			Binary azeotropy	Instantineous terpolymer composition(mole%)					
					Sn%	N%		Theoretical			Found		
	M_1	M_2	M_3					M_1	M_2	M_3	M_1	M_2	M_3
ABTB-ST -AN	20.90	47.90	31.70	6.22	6.89	4.68	ST /AN	6.43	56.07	37.49	6.33	57.12	36.55
	61.30	21.30	17.40	5.73	14.53	3.06	ST /AN	19.91	44.05	36.01	19.54	45.48	34.98
ABTB-BA -AN	39.50	35.00	25.50	6.22	10.06	3.40	BA /AN	12.39	50.70	36.94	12.43	52.26	35.31
	61.30	21.30	17.40	4.98	13.65	2.84	BA /AN	19.91	44.08	36.01	19.66	45.53	34.81
ABTB-MMA-AN	20.10	59.30	20.60	6.65	8.35	2.49	MMA/AN	9.25	67.36	23.39	8.61	69.56	21.83
	59.20	22.00	18.80	7.46	15.84	2.30	MMA/AN	23.69	41.15	35.16	22.71	42.23	34.06

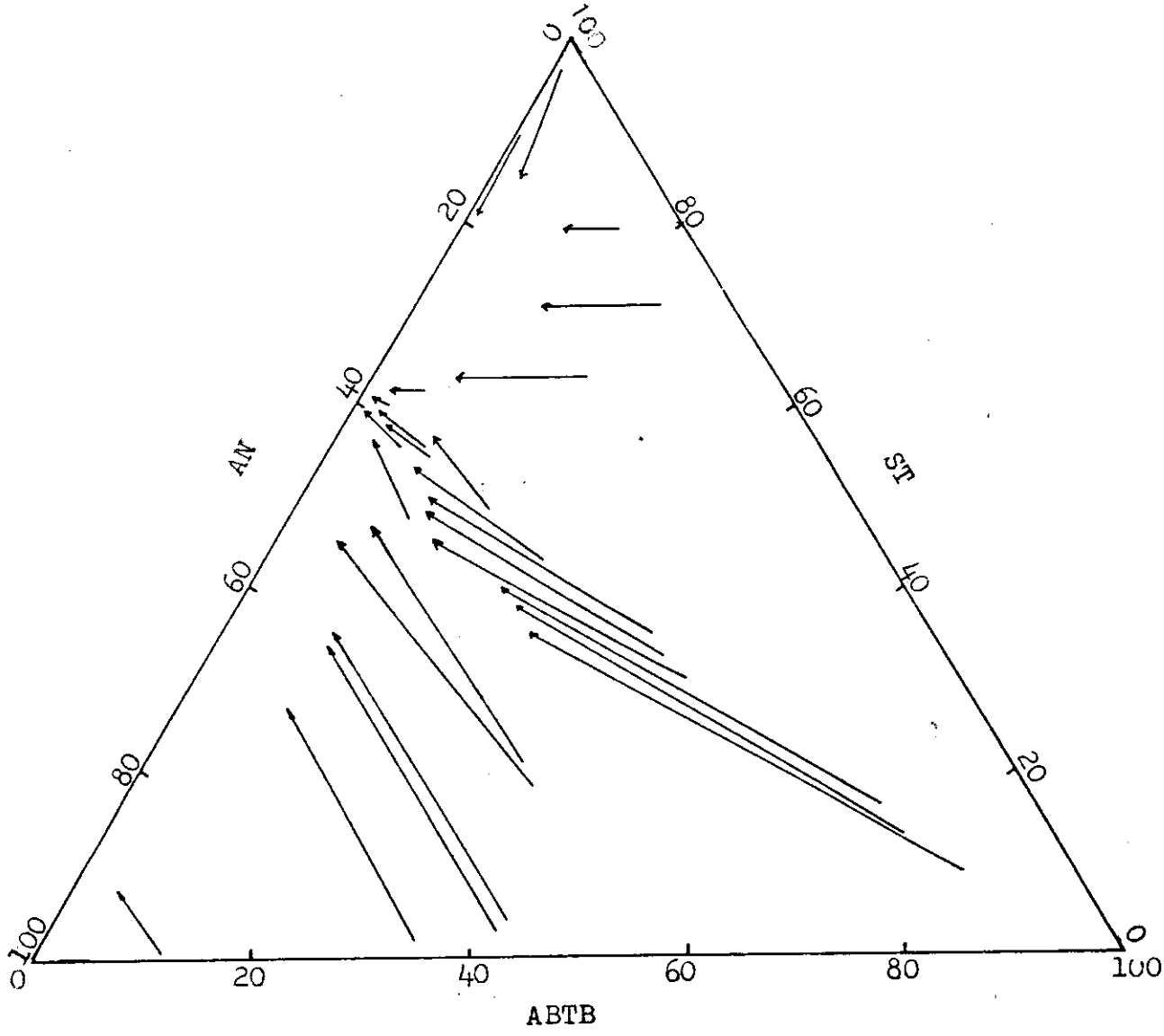

Fig. (41): Instamtaneous terpolymer composition as a function of monomer composition for the system ABTB-ST-AN .

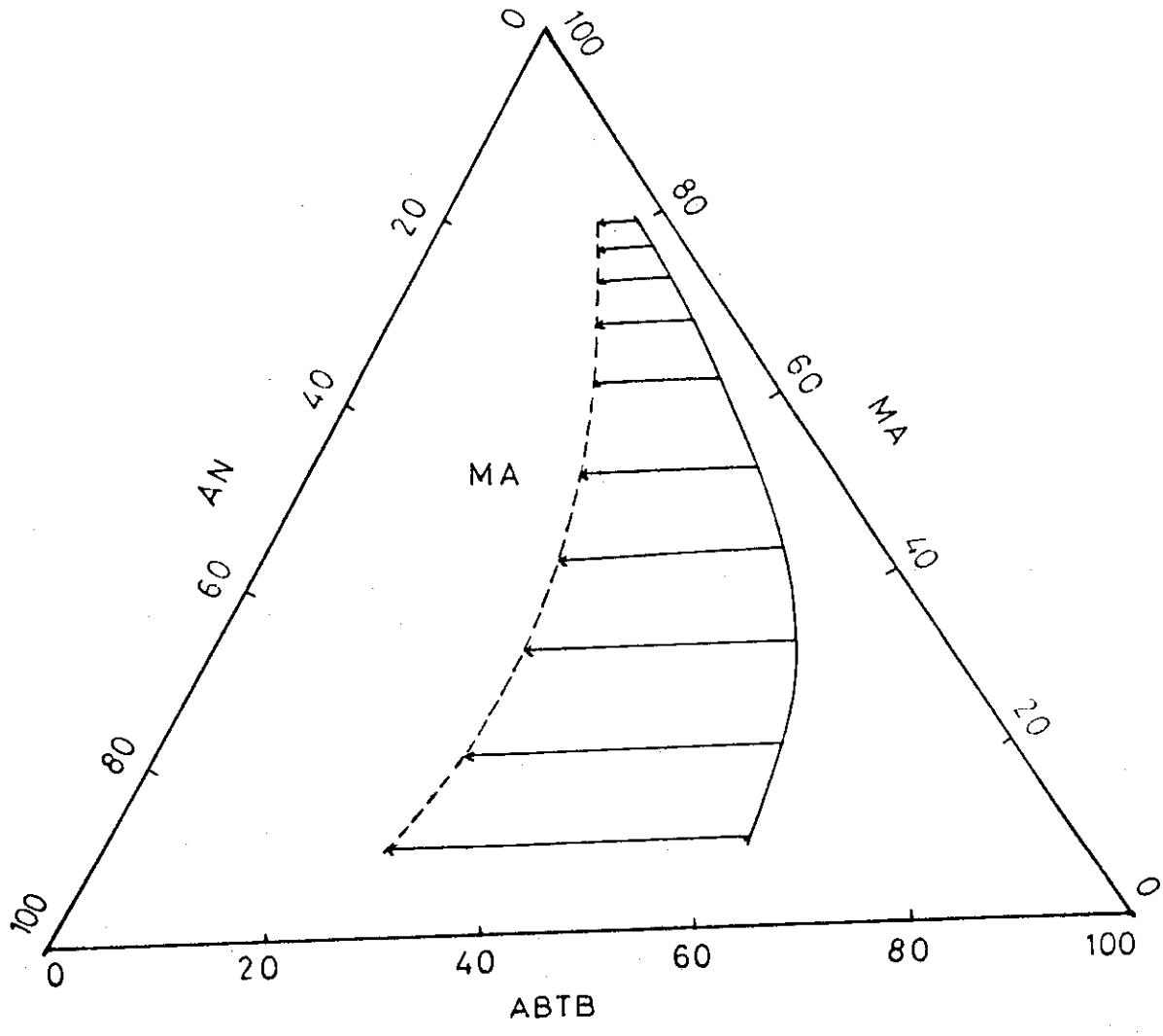

Fig. (42): The unitary azeotropic lines for the system ABTB-MA-AN: (——) monomer composition, (---) terpolymer composition .

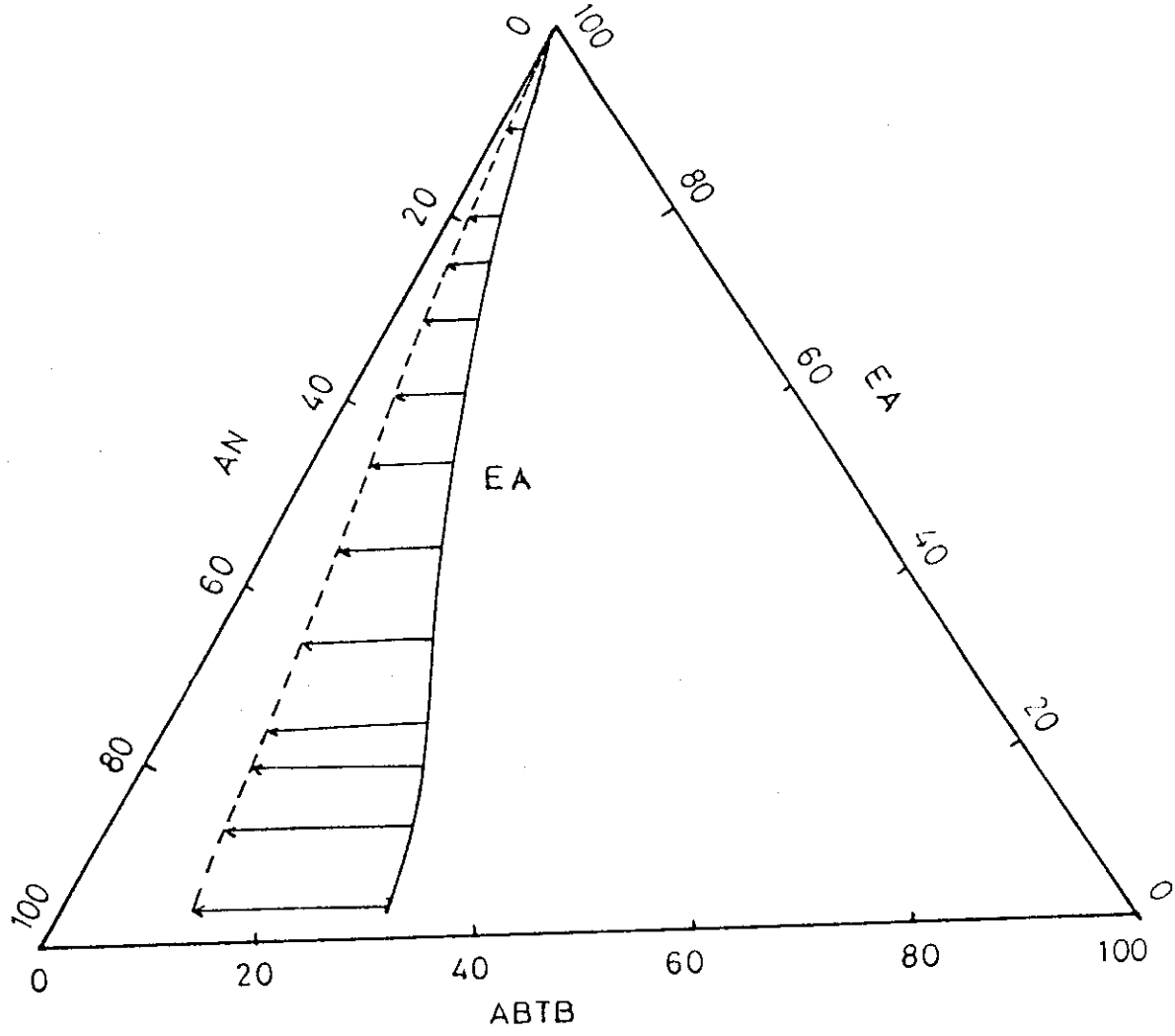

Fig. (43): The unitary azeotropic lines for the system ABTB-EA-AN: (——) monomer composition, (---) terpolymer composition

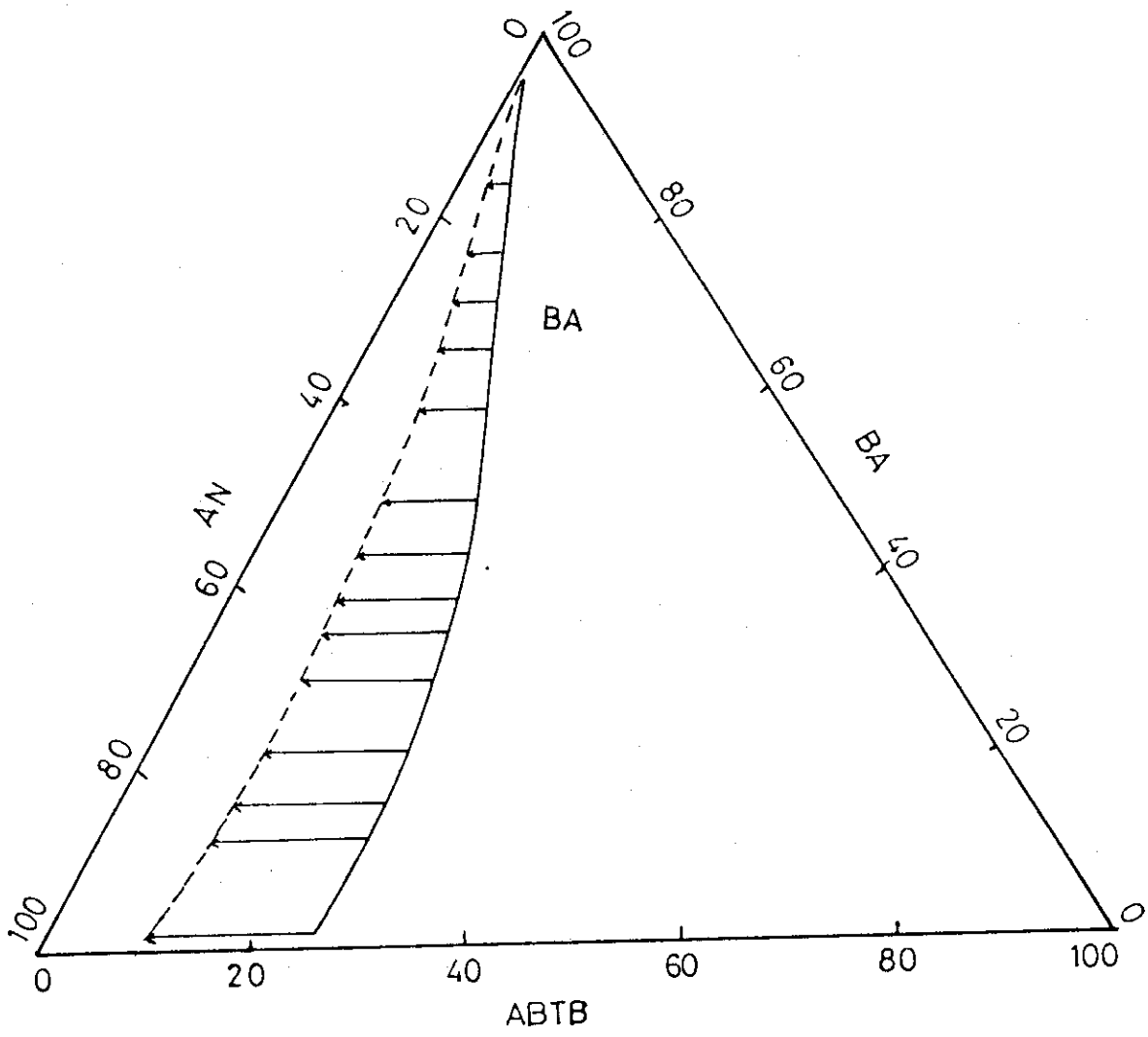

Fig. (44): The unitary azeotropic lines for the system ABTB-BA-AN: (——) monomer composition, (---) terpolymer composition

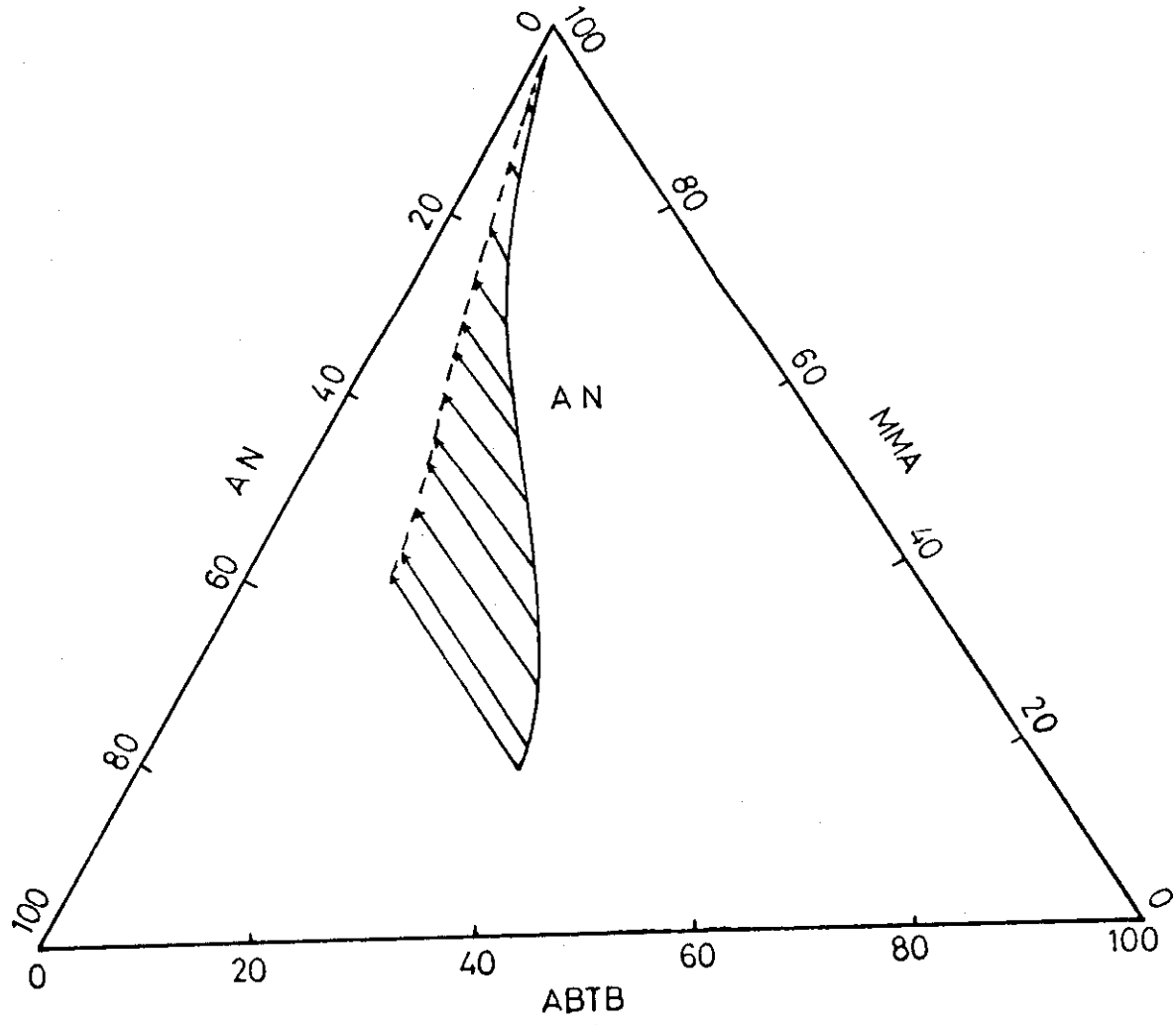

Fig. (45): The unitary azeotropic lines for the system ABTB-MMA-AN: (——) monomer composition, (---) terpolymer composition

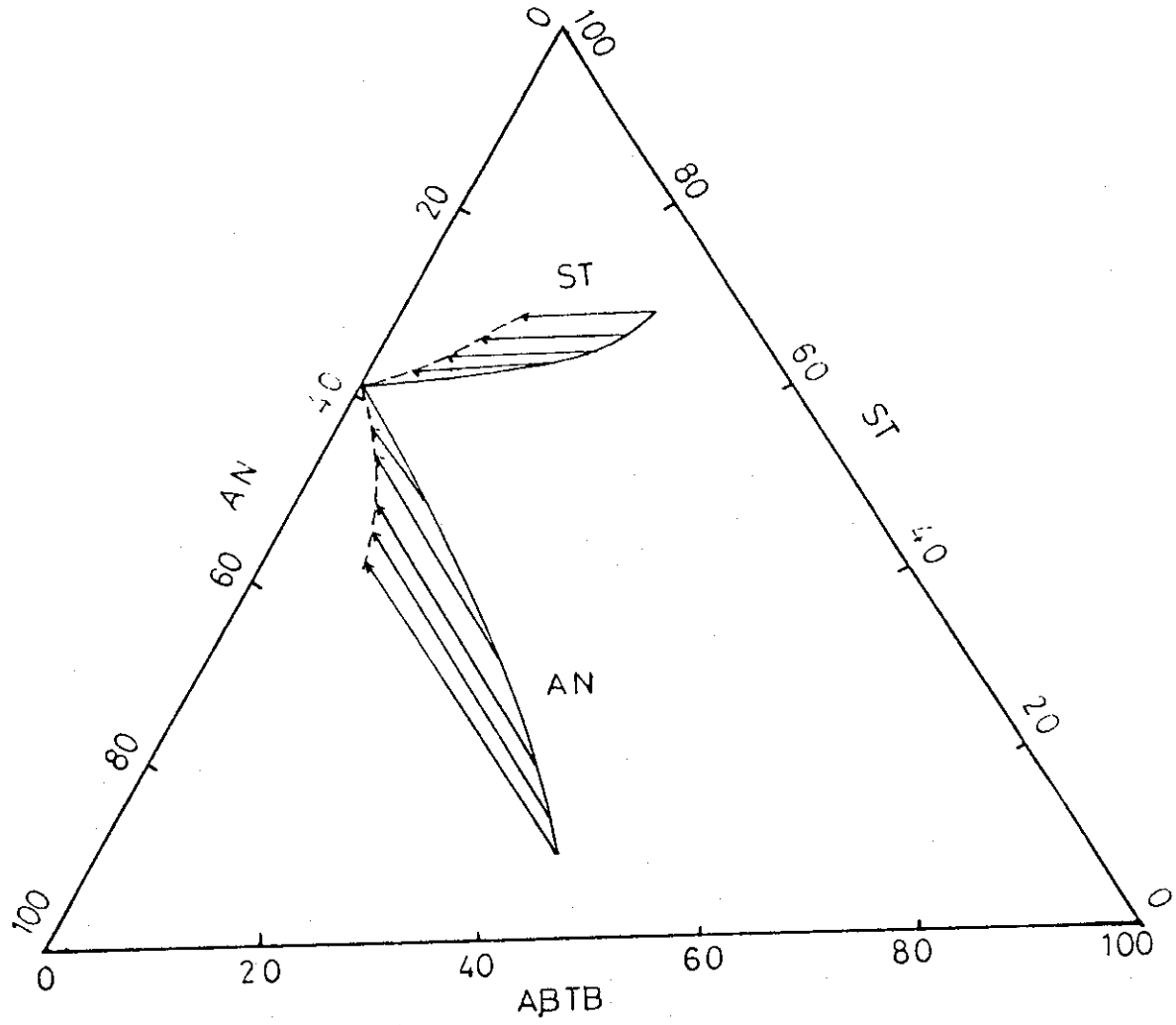

Fig. (46): The unitary azeotropic lines for the system ABTB-ST-AN: (——) monomer composition, (– – –) terpolymer composition

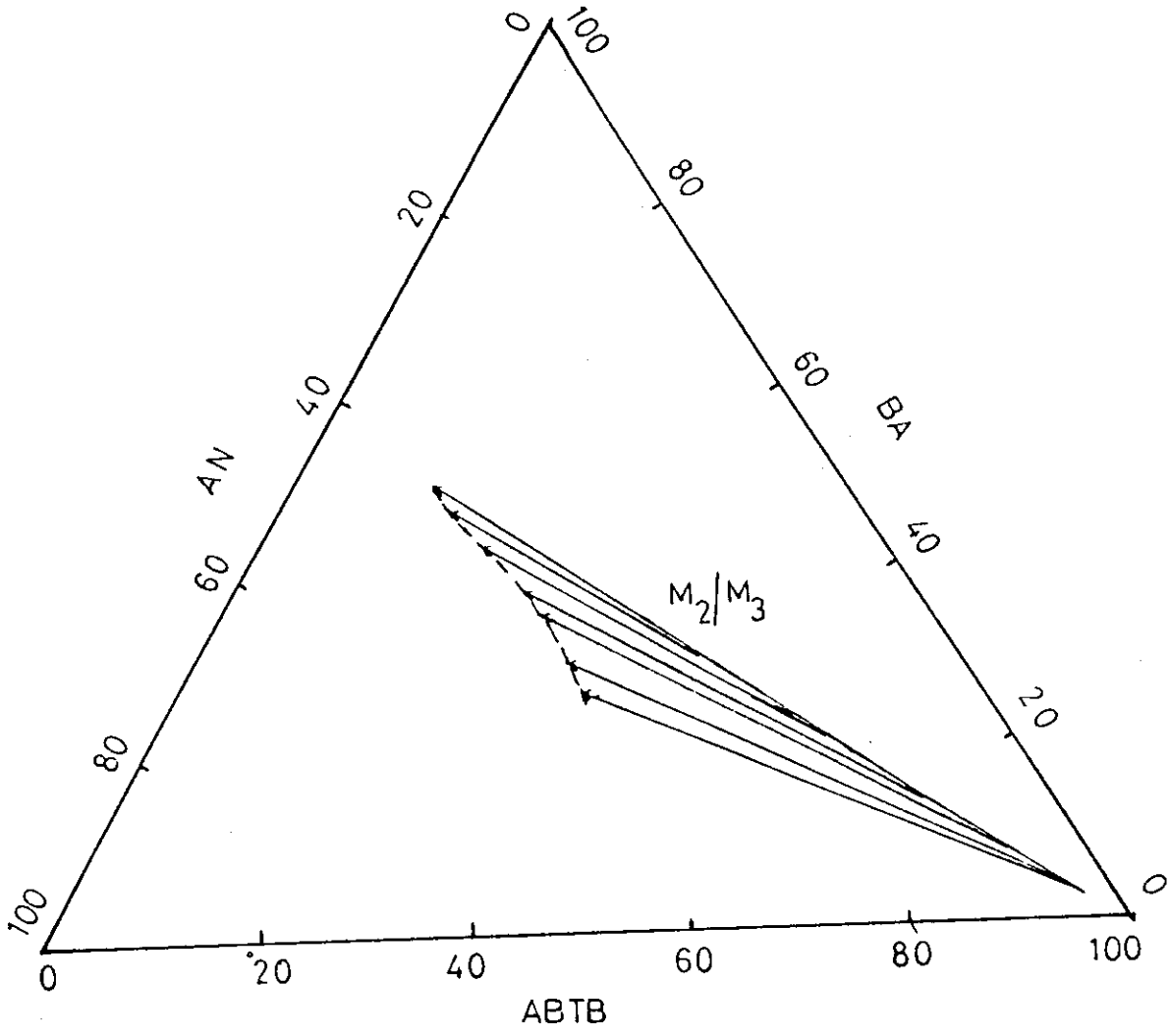

Fig. (47): The binary azeotropic lines for the system ABTB-BA-AN: (——) monomer composition, and (---) terpolymer composition .

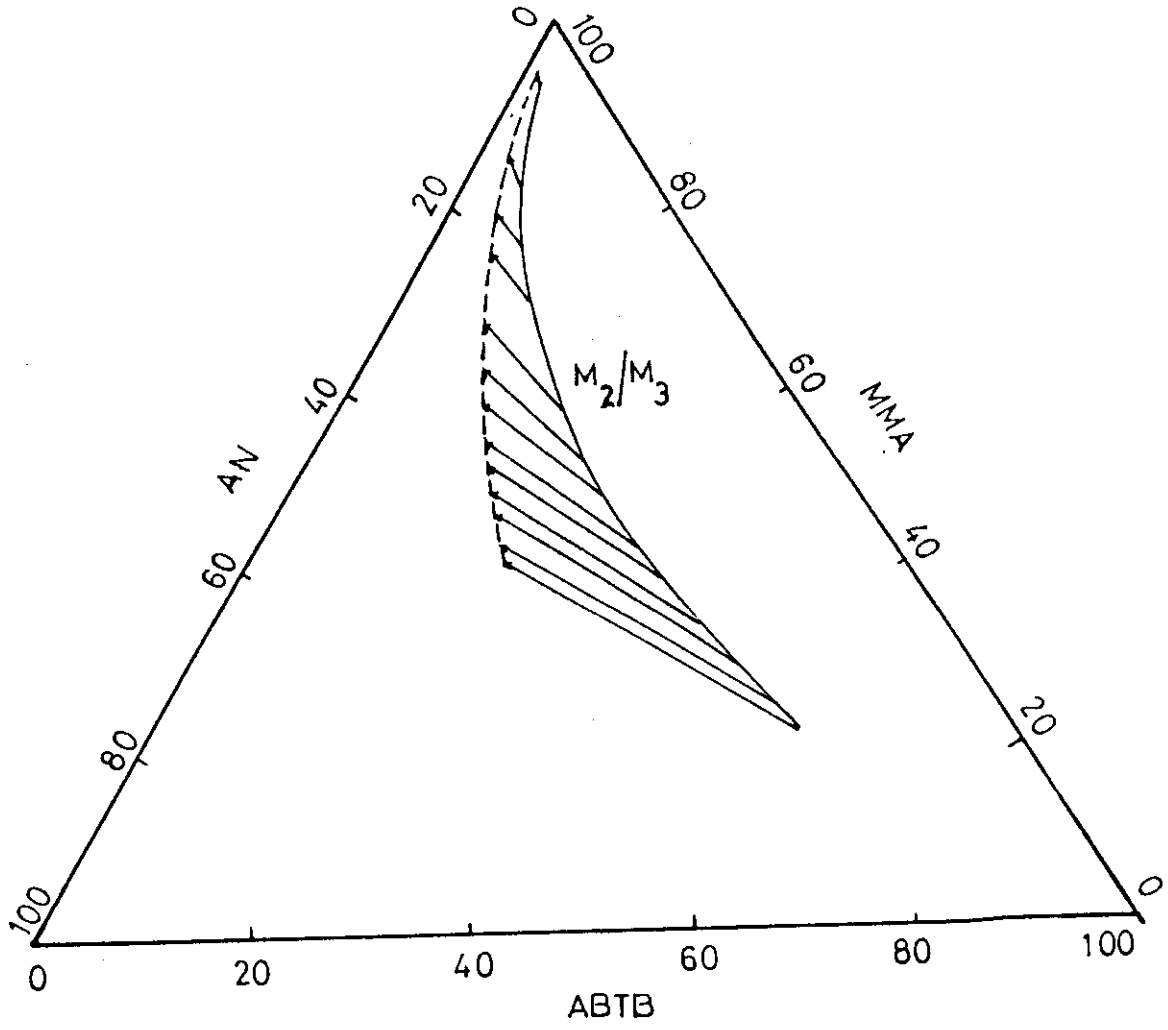

Fig. (48): The binary azeotropic lines for the system ABTB-MMA-AN: (——) monomer composition and (– – –) terpolymer composition .

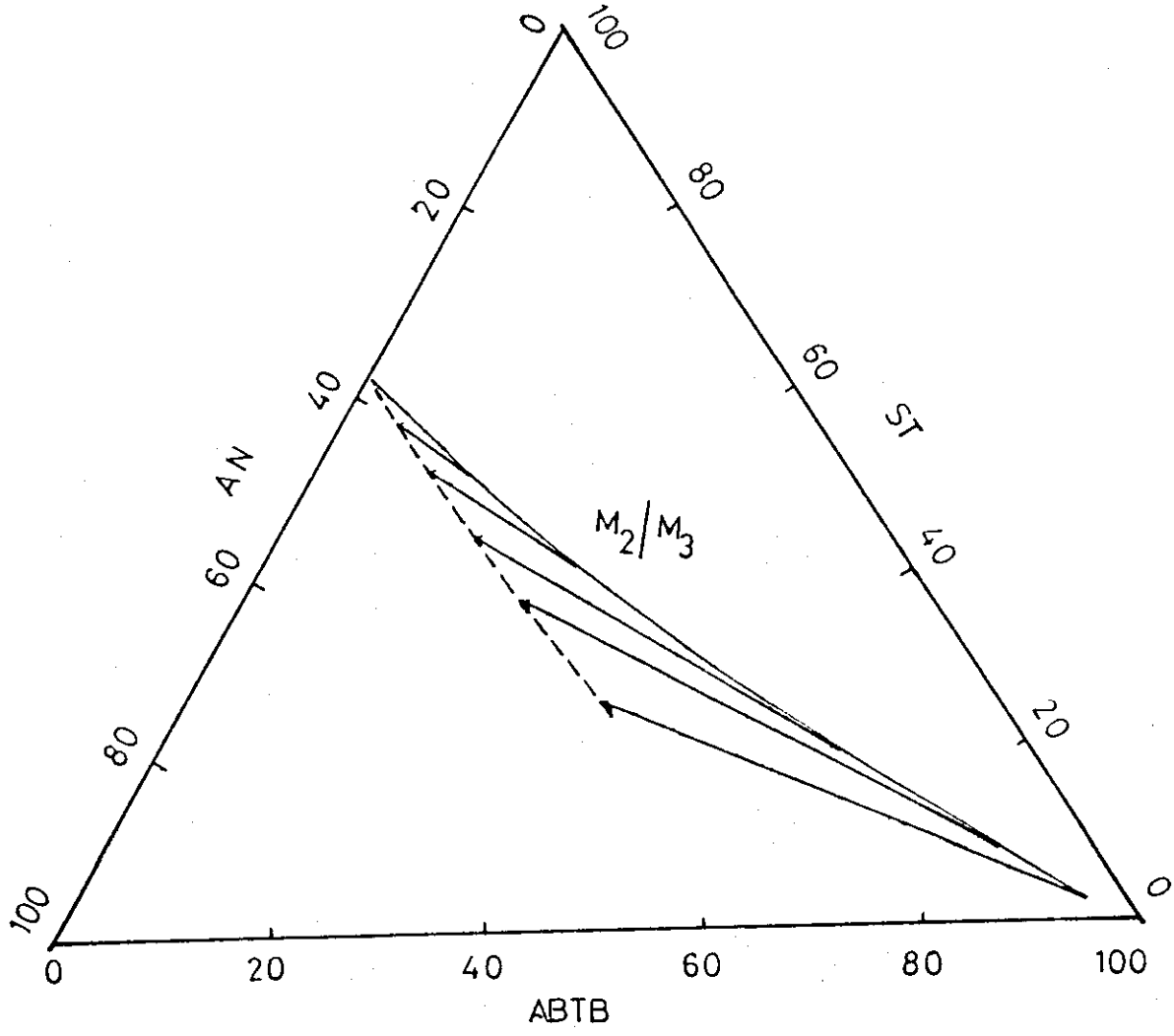

Fig. (49): The binary azeotropic lines for the system ABTB-ST-AN: (——) monomer composition and (- - -) terpolymer composition .

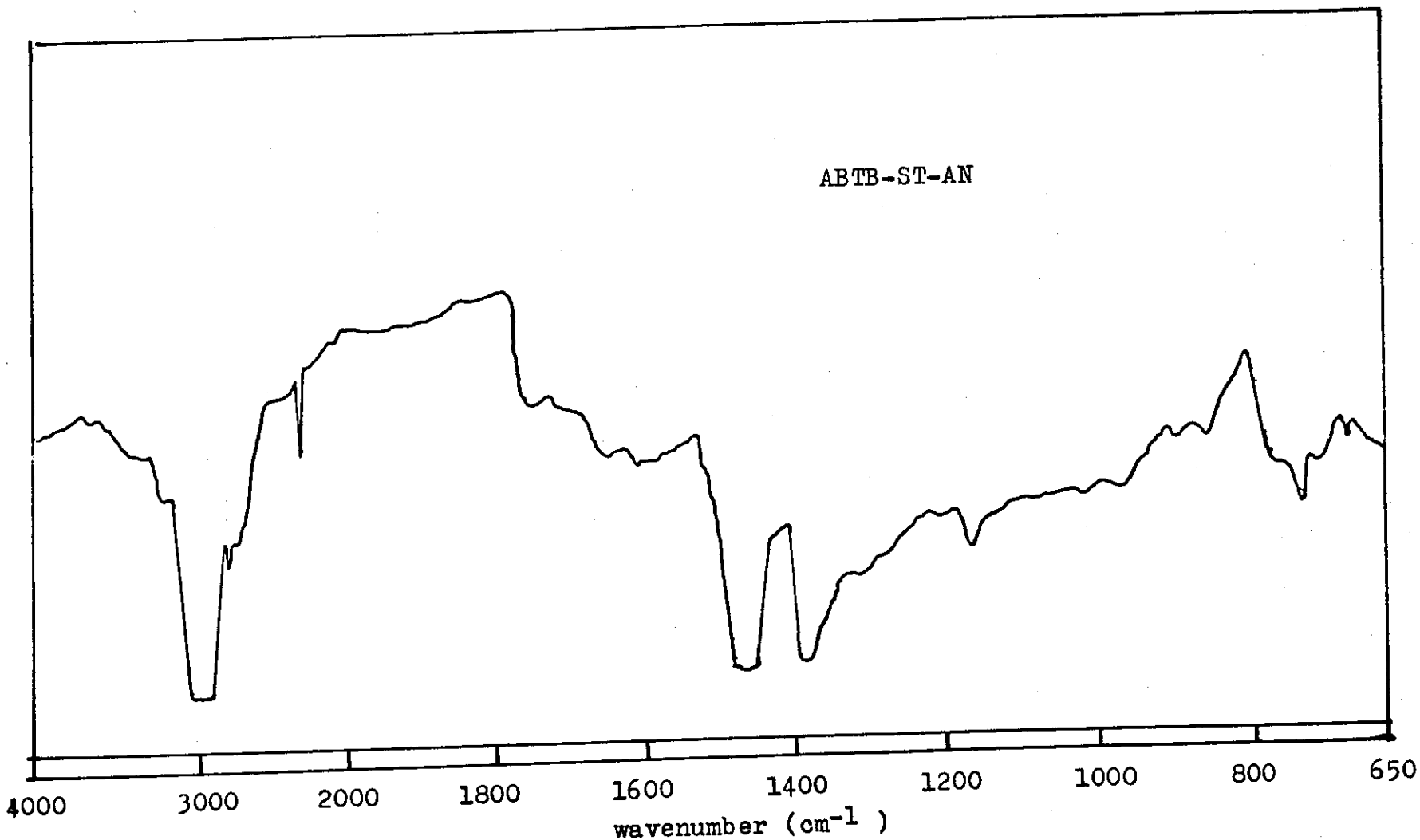

Fig. (50) : The IR spectrum of ABTB-ST-AN terpolymers .